

## **INFORMATION TO USERS**

**This manuscript has been reproduced from the microfilm master. UMI films the text directly from the original or copy submitted. Thus, some thesis and dissertation copies are in typewriter face, while others may be from any type of computer printer.**

**The quality of this reproduction is dependent upon the quality of the copy submitted. Broken or indistinct print, colored or poor quality illustrations and photographs, print bleedthrough, substandard margins, and improper alignment can adversely affect reproduction.**

**In the unlikely event that the author did not send UMI a complete manuscript and there are missing pages, these will be noted. Also, if unauthorized copyright material had to be removed, a note will indicate the deletion.**

**Oversize materials (e.g., maps, drawings, charts) are reproduced by sectioning the original, beginning at the upper left-hand corner and continuing from left to right in equal sections with small overlaps.**

**Photographs included in the original manuscript have been reproduced xerographically in this copy. Higher quality 6" x 9" black and white photographic prints are available for any photographs or illustrations appearing in this copy for an additional charge. Contact UMI directly to order.**

**ProQuest Information and Learning  
300 North Zeeb Road, Ann Arbor, MI 48106-1346 USA  
800-521-0600**

**UMI<sup>®</sup>**



***The hydrology and dissolved organic carbon (DOC)  
biogeochemistry in a boreal peatland***

*Colin J.D. Fraser  
Department of Geography  
McGill University  
Montréal, Québec  
August 1999*

*A thesis submitted to the Faculty of Graduate Studies and Research in  
partial fulfillment of the requirements of the degree of Masters of  
Science*

© Colin Fraser 1999



**National Library  
of Canada**

**Acquisitions and  
Bibliographic Services**

**395 Wellington Street  
Ottawa ON K1A 0N4  
Canada**

**Bibliothèque nationale  
du Canada**

**Acquisitions et  
services bibliographiques**

**395, rue Wellington  
Ottawa ON K1A 0N4  
Canada**

*Your file Votre référence*

*Our file Notre référence*

**The author has granted a non-exclusive licence allowing the National Library of Canada to reproduce, loan, distribute or sell copies of this thesis in microform, paper or electronic formats.**

**The author retains ownership of the copyright in this thesis. Neither the thesis nor substantial extracts from it may be printed or otherwise reproduced without the author's permission.**

**L'auteur a accordé une licence non exclusive permettant à la Bibliothèque nationale du Canada de reproduire, prêter, distribuer ou vendre des copies de cette thèse sous la forme de microfiche/film, de reproduction sur papier ou sur format électronique.**

**L'auteur conserve la propriété du droit d'auteur qui protège cette thèse. Ni la thèse ni des extraits substantiels de celle-ci ne doivent être imprimés ou autrement reproduits sans son autorisation.**

0-612-64358-1

**Canada**

## Table of Contents

<b>Abstract</b> .....	<b>i</b>
<b>Resumé</b> .....	<b>ii</b>
<b>Acknowledgments</b> .....	<b>iii</b>
<b>List of Figures</b> .....	<b>iv</b>
<b>List of Tables</b> .....	<b>iv</b>
<b>Chapter 1 - Literature Review and Research Objectives</b> .....	<b>1</b>
Section 1.1 Global carbon research, trace gases and climate.....	1
Section 1.2 Contemporary studies of global carbon: A biogeochemical approach..	2
Section 1.3 Contemporary C-budgets of peatlands and C inventories.....	4
Section 1.4 Dissolved organic carbon (DOC) - Peatland carbon budgets.....	5
Section 1.5 DOC - Chemical aspects.....	6
Section 1.6 Peatlands and hydrology - Processes and links to biogeochemistry.....	7
1.6.1 Water balance and wetlands.....	7
1.6.2 Physical aspects of groundwater flow and runoff.....	9
1.6.3 Recharge-discharge function of wetlands.....	11
Section 1.7 Summary and rationale.....	13
Section 1.8 Research objectives.....	13
<b>Chapter 2 - Study Site and Materials and Methods</b> .....	<b>15</b>
Section 2.1 Landscape development and site description.....	15
Section 2.1.1 Site description.....	15
Section 2.1.2 Geology, hydrology, and relevant research in the area.....	16
Section 2.2 Field instrumentation and methods.....	18
2.2.1 Peatland topography and estimate of hydraulic gradients.....	18
2.2.2 Marine deposits and external groundwater influences.....	19
2.2.3 Macro-scale surface water hydrology.....	19
2.2.4 Meso- and micro-scale groundwater and surface water hydrology.....	20
2.2.5 Measurement of meteorological parameters.....	21
2.2.6 Measurement of hydraulic conductivity.....	22
2.2.7 Sampling program, monitoring and time line.....	23

<b>Chapter 2 - Study Site and Materials and Methods (continued)</b>	
Section 2.3 Laboratory methods.....	23
2.3.1 Carbon and geochemical analyses.....	24
2.3.2 DOC characterization using a spectrofluorometer.....	25
<b>Chapter 3 - Hydrological Controls and DOC Export at the Mer Bleue bog.....</b>	<b>26</b>
Discussion.....	32
<b>Chapter 4 - Patterns of Groundwater Flow at the Mer Bleue bog.....</b>	<b>36</b>
Discussion.....	42
<b>Chapter 5 - Summary and discussion.....</b>	<b>49</b>
<b>Appendix .....</b>	<b>54</b>
Appendix 1 - Na <sup>+</sup> and electrical conductivity regression analysis.....	55
Appendix 2 - Tables of hydraulic conductivity (K <sub>n</sub> ) measurements.....	56
Appendix 3 - Interpolation methods for Na <sup>+</sup> migration during flow reversal.....	57
<b>References .....</b>	<b>58</b>

## Abstract

A hydrological and biogeochemical study was undertaken at the Mer Bleue bog, Ottawa, Ontario, Canada from May 22, 1998 to May 21, 1999. Basin runoff was generated by groundwater discharge at the peatland margin, and groundwater discharge was controlled by hydraulic gradients and horizontal hydraulic conductivities ( $K_h$ ). Flux of dissolved organic carbon (DOC) measured at the basin outflow was  $8.3 \text{ g C m}^{-2} \text{ yr}^{-1}$  and compared to within 23% of DOC flux estimated using a Dupuit approximation of seepage during the ice-free season. Annual DOC flux was 11% of the annual carbon sink.

Flownet analysis showed that seasonal patterns of groundwater flow were controlled by boundary condition changes that resulted from precipitation and evapotranspiration events. A pattern of recharge was most common over the hydrological year, but a discharge pattern was observed during a 40 day groundwater flow reversal. Evaluation of the peatland recharge-discharge function using *in situ* sodium concentrations and a diffusion model revealed that the peatland is a long-term recharge system. It is hypothesized that peatland biogeochemical function is controlled by long-term recharge despite annual occurrence of groundwater flow reversals.

## Resumé

Une étude hydrologique et biogéochimique a été effectuée à la tourbière Mer Bleue à Ottawa au Canada, entre le 22 mai 1998 et le 21 mai 1999. L'écoulement hors de ce bassin versant origine d'un débit d'eaux souterraines du bord de la tourbière, contrôlé par les gradients hydrauliques et les conductivités hydrauliques horizontales ( $K_h$ ) dans la tourbière. La mesure du flux net de carbone organique dissout (DOC) à la sortie du bassin a donné  $8,3 \text{ g C m}^{-2} \text{ yr}^{-1}$ , une différence de 23% par rapport à la valeur estimée selon l'approximation Dupuit pour l'écoulement dans la saison sans neige. Le bilan annuel du DOC représente 11% des additions annuelles de carbone.

Une analyse de type flownet confirme que le patron annuel d'écoulement des eaux souterraines est contrôlé par des changements aux conditions limites liés aux événements de précipitation et d'évapotranspiration. La recharge du système domine la majeure partie de l'année hydrologique, quoique une période de débit de 40 jours d'écoulement sortant a été observée. Une estimation du bilan rechargement-débit, selon les concentrations de sodium *in situ* et un modèle de diffusion, indique que la tourbière est un système de rechargement à long terme. Selon notre hypothèse, les caractéristiques biogéochimiques du système sont contrôlés par le rechargement à long terme, malgré les périodes annuelles d'écoulement sortant.

## **Acknowledgments**

Firstly, I would like to thank Professors Nigel Roulet and Tim Moore for their assistance over the last two years. Financial assistance for my graduate studies at McGill University came from NSERC operating and strategic grants issued to Professor Roulet. I thank him for his continued support and guidance at meetings, conferences and in the field. I thank Tim Moore for guidance and the discussions on DOC and the biogeochemistry of peatlands which would often take place during litter bag retrievals on Golden Pond. Working in their research groups was a great experience.

I am indebted to Mike Dalva for his time and patience in the soils laboratory. His trouble-shooting and maintenance of instruments, was well, instrumental in completing the groundwater chemistry measurements made at the Mer Bleue bog. I thank Sara Giffen and Kira Rich for their assistance with piezometer construction and installation of the groundwater network at the research site. I also thank them for assistance with bail tests and levelling surveys on the hottest days of summer 1998.

Lastly, I would like to thank my family, Jenny-Marie Ferone, friends at 76 Guilbault, the graduate students in the Carbon Research Group, and the Centre for Climate and Global Change Research for their assistance and support over the last two years.

## **List of Figures**

**Figure 1-1. Schematic of the global carbon cycle after Schimel (1995).**

**Figure 1-2. Schematic of the contemporary C budget of a peatland.**

**Figure 1-3. Hydrological cycle of a peatland.**

**Figure 2-1. a. Mer Bleue bog and the Ottawa region. b. The tower site and groundwater transects on the drainage basin.**

**Figure 2-2. Schematic of the study site showing the location of instruments at the Mer Bleue bog.**

**Figure 2-3. Rating curves used to calculate discharge.**

**Figure 2-4. Summary of manual measurements from observation wells.**

**Figure 3-1. Topographic gradients observed across the major hydraulic axis.**

**Figure 3-2. Estimates of horizontal hydraulic conductivity ( $K_h$ ).**

**Figure 3-3. Sample time lag tests for  $K_h$  after Hvorslev (1951).**

**Figure 3-4. Time series of hydrological variables and DOC measurements.**

**Figure 3-5. Regression models of runoff versus [DOC].**

**Figure 3-6. Groundwater flow reconstruction for August 26, 1998.**

**Figure 3-7. Comparison of measured and simulated runoff from the Mer Bleue bog.**

**Figure 3-8. DOC concentrations in peat pore waters.**

**Figure 3-9. Chemoplots of [DOC] in piezometers at the peatland margin.**

**Figure 3-10. Changes in 450 nm : 500 nm fluorescence ratio across the beaver pond margin and DOC concentrations from P1 and the beaver pond.**

**Figure 3-11. DIC concentrations from nests at the peatland margin.**

**Figure 3-12. Relationship between basin runoff and water table position measured at the tower site.**

**Figure 3-13. Comparison of DOC at the basin outflow and the beaver pond.**

**Figure 4-1. Generalized flownet depicting groundwater flow patterns across the major axis.**

**Figure 4-2. Baseline groundwater data collected August 26, 1998.**

**Figure 4-3. Elevation of maximum drive-point piezometer head with respect to mean, minimum and maximum water table position on the peatland.**

**Figure 4-4. Relationships between  $\text{Na}^+$ ,  $\text{Mg}^{2+}$ ,  $\text{Ca}^{2+}$  and depth in peat pore water at the Mer Bleue bog.**

**Figure 4-5. Predicted and observed concentration gradients for  $\text{Na}^+$  in peat pore waters.**

**Figure 4-6. Elapsed time required to obtain a 'best fit' to observed  $\text{Na}^+$  profiles at each nest plotted against maximum peat depth at nest.**

**Figure 4-7. Changes in precipitation, evapotranspiration and water table position at the tower site for the 1998 field season.**

**Figure 4-8. Plots of head change over time.**

**Figure 4-9. Summary of recharge-discharge plots over the period of the groundwater reversal as observed at P10.**

**Figure 4-10. Head changes at nests RA2, P10 and P2 over the reversal period respectively.**

**Figure 4-11. Changes in groundwater flow patterns over the course of the reversal as depicted by flownets across the major axis.**

**Figure 4-12. Changes in DOC concentrations over the period of the groundwater reversal.**

**Figure 4-13. Changes in electrical conductivity from piezometers P8, P9 and P10.**

**Figure 4-14. Changes in  $\text{Na}^+$  concentration prior to and during the reversal.**

**Figure 4-15. Representative dissolved carbon profiles for the Mer Bleue bog.**

**Figure 5-1. Conceptual diagram of the hydrological and biogeochemical linkages at the Mer Bleue bog.**

## **List of Tables**

**Table 1-1. Summary of annual runoff and DOC export from wetland and forested-wetland catchments reported in the literature from 1981 to 1998.**

**Table 2-1. Temperature and precipitation climate normals for the Ottawa International Airport, Ontario, Canada, 1938 to 1990 inclusive.**

**Table 3-1. Comparison of  $K_h$ ,  $K_m$  and  $K_v$  by depth for piezometer nests P4 and P9.**

**Table 4-1. Summary of DOC and electrical conductivity measurements from drive-point piezometers at the Mer Bleue bog.**

**Table 4-2. Correlation of head measurements by piezometer depth to water table position.**

## **Chapter 1 - Literature Review and Research Objectives**

This chapter summarizes findings from the scientific literature to provide an appropriate context for the research undertaken. The chapter is separated into sections by research domain, giving a brief overview of the topics and highlighting key references. Introductions to trace gas research, contemporary global C-budgeting, peatlands and carbon fluxes, dissolved organic carbon (DOC) chemistry, and peatland hydrology will follow. The chapter concludes with a synthesis of the research domains and summarizes the objectives of the hydrological and biogeochemical research completed at a peatland near Ottawa, Ontario, Canada.

### **Section 1.1 Global carbon research, trace gases and climate**

Due to the effects of increased greenhouse gas (GHG) emissions to the atmosphere, and the advent of global warming, the global carbon (C) cycle has received much scientific attention in the last few decades (IPCC, 1996). Present day concern stems from studies that have shown in both paleo- and contemporary frameworks, the linkages between changes in GHG concentrations (namely carbon dioxide [CO<sub>2</sub>] and methane [CH<sub>4</sub>]) to synchronous temperature fluctuations. These and other radiatively active gases absorb and delay the loss of heat to space, warming the lower troposphere by radiation and re-radiation in the infrared wavelengths. This finding is particularly troubling in light of the changes in GHG concentrations observed since the Industrial Revolution (c. 1750), where [CO<sub>2</sub>] and [CH<sub>4</sub>] have increased from 280 ppmv and 0.7 ppmv to present day levels of 365 ppmv and 1.7 ppmv respectively (Christopherson, 1998).

Paleo-environmental reconstructions from ice cores ‘unearthed’ high resolution and long duration GHG and temperature chronologies. Barnola et al. (1987) and Chapellez et al. (1990) summarize 160 ka records for CO<sub>2</sub> and CH<sub>4</sub> respectively from the Vostok ice core, Antarctica, and Chapellez et al. (1993) reported on comparable GHG and temperature chronologies from the Greenland Ice-core Project (GRIP). The paleo-environmental proxies

captured long climate records and a synchronicity between GHG forcing and inferred global temperature oscillations. Many climate change publications such as IPCC (1996) and Houghton (1997) concisely discuss ice-core GHG-temperature chronologies, and suggest that it is difficult to dismiss the active role  $\text{CO}_2$  and  $\text{CH}_4$  played in past atmospheres.

Separating the role of GHGs in climate and global change from natural phenomena such as volcanic emission and aerosols, sun spot cycles, orbital eccentricity (100 000 yr cycle), axial tilt (41 000 yr cycle) and timing of perihelion (23 000 yr cycle), has been a challenge at global scales. Thomson (1995) provided one of the most convincing accounts linking GHGs, global temperatures and the amplitude of the solar cycle into a model for the last 150 years. He showed that despite a decrease in the amplitude of the annual solar cycle, a strong correlation between GHGs and temperature can be found. Using an optimal fingerprint analysis and applying it to temperature trends, natural climate fluctuations and GHG forcing, Hegerl and Cubasch (1996) concluded that the probability is less than 0.05 that the global warming trend observed over the last thirty years was naturally induced. Overpeck et al. (1997) present paleo-climate records from 29 circum-Arctic sites showing evidence of ecosystem and climate change from 1840 to the middle of the 20<sup>th</sup> century in lake sediments, trees, glaciers and marine sediments. In this account, the authors also concluded that GHG forcing above and beyond changes in solar irradiance, decreased volcanic activity and internal feedbacks to the climate system are affecting atmospheric and terrestrial processes. Evidence is mounting that links between GHG forcing and temperature changes are occurring over shorter time periods, and global changes are a reality.

## **Section 1.2 Contemporary studies of global carbon: A biogeochemical approach**

To better understand the natural and anthropogenic (GHG) changes to the global carbon inventory, a biogeochemical budgeting approach has been employed to manage the different fluxes and reservoirs of carbon (Figure 1-1). Best estimates of global carbon fluxes suggest that changes in land use and fossil fuel emissions create an atmospheric source of carbon, whereas the biosphere and oceans are sinks for carbon. Uncertainty attached to the

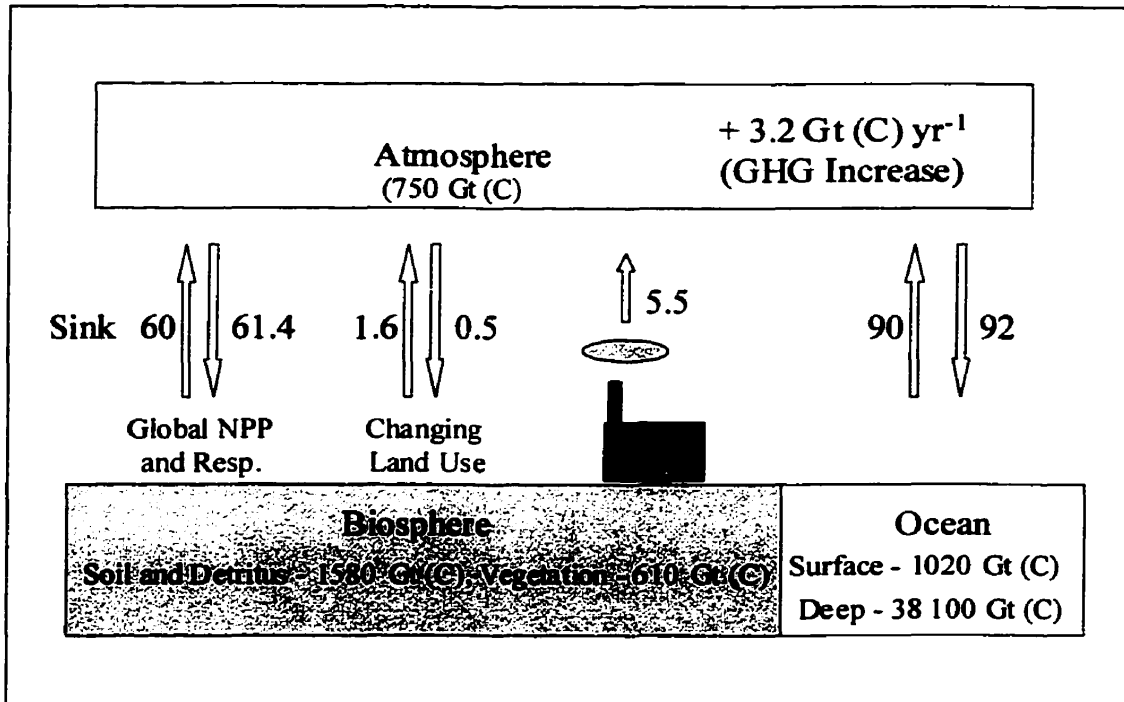


Figure 1-1. Schematic of the global carbon cycle after Schimel (1995). All fluxes of carbon are given in Gt (C) yr<sup>-1</sup> and reservoirs of carbon are given in Gt (C).

magnitude of the fluxes and reservoirs on a global scale is large.

Many research groups embarked on studies to locate global C sources and sinks. Tans et al. (1990) used atmospheric CO<sub>2</sub> data, P<sub>CO<sub>2</sub></sub> (partial pressure) for oceanic and boundary layers, and a series of calculations using transport fields from a general circulation model to quantify global carbon fluxes to and from the ocean-terrestrial-atmosphere domains. In another study, Siegenthaler and Sarmiento (1993) used records of P<sub>CO<sub>2</sub></sub> and ocean-atmosphere carbon-models to provide differential estimates of ocean-atmosphere fluxes of carbon. Ciais et al. (1995) used a <sup>13</sup>C/<sup>12</sup>C fingerprint technique based on the preferential biotic uptake of <sup>12</sup>C to give further insights into the magnitude of biosphere-atmosphere carbon fluxes. While the results of these studies differed, they all found that closure of the global carbon budget depended on a terrestrial sink. It was agreed that the terrestrial sink is 1 to 3 Gt C yr<sup>-1</sup> in magnitude and is located in the Northern hemisphere.

After the identification and location of the 'missing C sink', much speculation as to the controls on differential C uptake into the terrestrial and ocean reservoirs surfaced. Suggested reasons for carbon sequestration in terrestrial systems are: forest regrowth, nitrogen (N) - deposition, CO<sub>2</sub> fertilization of plant growth, climate variability (temperature, precipitation) or combinations thereof (Schimel, 1995). Research and discussions pertaining to increased C sequestration due to nitrogen loading are summarized in Schimel et al. (1996) and Schindler and Bayley (1993). McGuire et al. (1997) addressed potential CO<sub>2</sub> fertilization on global scales using 2 x CO<sub>2</sub> scenarios and an ecosystem model, whereas spatial and temporal changes in terrestrial C sequestration resulting from climate variability are central findings in Dai and Fung (1993), Schimel et al. (1996) and Randerson et al. (1997). These global scale studies yielded new hypotheses and data sets, and concluded that the C cycle is highly transient and poorly understood. The need then, and now, is to scale down to individual ecosystems and land classes and better understand the biogeochemical processes and controls on carbon cycling. This thesis focuses on aspects of carbon cycling in peatlands.

### **Section 1.3 Contemporary C-budgets of peatlands and C inventories**

Processes of carbon assimilation through photosynthesis and partial decomposition of biomass in saturated (low oxygen) carbon rich soils provides the potential for a large carbon sink. Many studies confirm the historical importance of organic soils in the terrestrial uptake of carbon, as well as their potential sensitivities to climate change (Schimel, 1995; Gorham, 1995; Maltby and Immirzi, 1993; and Bridgham et al., 1995). Gorham (1991) determined the global extent of northern hemisphere boreal and sub-Arctic peatlands to be  $3.46 \times 10^{12} \text{ m}^2$  and estimated the C reservoir to be 455 Gt. This C pool is one-third of the global soil C pool (Schimel, 1995), but is found on less than 3 per cent of global land surfaces (Harte, 1988). Although Gorham (1991) estimates have been robust enough to remain unchallenged for eight years, they are suggestive only (Clymo, 1996). The magnitude and uncertainty in the estimate of the C sink are dependent upon correct assumption of areal peatland extent, average peat depth, average peat density and average carbon content. Other estimates of this carbon reservoir are 600 Gt (Houghton et al., 1997) and 329-525 Gt (Maltby and Immirzi, 1993). Generally accepted estimates of average annual increment increase of peatlands are  $0.5 \text{ mm yr}^{-1}$  or  $0.096 \text{ Gt C yr}^{-1}$  after Gorham (1991) to  $0.53 \text{ mm yr}^{-1}$  or  $0.076 \text{ Gt C yr}^{-1}$  after Clymo (1984). Much like the estimates of biogeochemical reservoirs, these rates are dependent upon uncertain assumptions (including a correct estimate of the peatland soil C reservoir).

As illustrated in Figure 1-2, the  $\text{CO}_2$ ,  $\text{CH}_4$  and dissolved organic carbon (DOC) fluxes to and from a peatland must be quantified to resolve the carbon budget on a yearly basis. Net ecosystem exchange (NEE) encompasses the  $\text{CO}_2$  fluxes to and from a peatland, i.e. - the difference between gross production resulting from photosynthetic uptake during plant growth (GP) and carbon respiration from plants (RR) and soil (SR). The  $\text{CH}_4$  and DOC fluxes result from anaerobic peat metabolism and waterborne export respectively. By investigating  $\text{CO}_2$  exchange using micro-meteorological techniques Shurpali et al. (1995) found a peatland ecosystem to be a C source in 1991 of  $71 \text{ g C m}^{-2} \text{ yr}^{-1}$  and a C sink in 1992 of  $32 \text{ g C m}^{-2} \text{ yr}^{-1}$  under wetter and cooler conditions. Whiting (1994) studied  $\text{CO}_2$  exchange in the Hudson Bay lowlands and found a bog and an interior fen to be net  $\text{CO}_2$  sources of 9

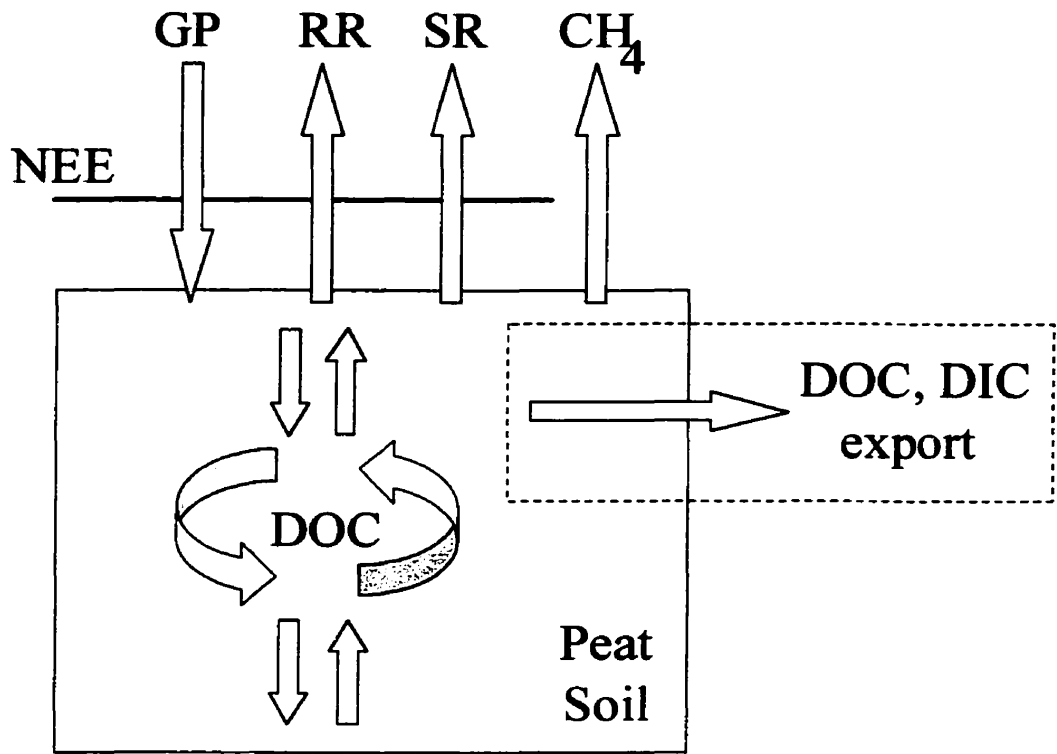


Figure 1-2. Schematic of the contemporary C budget of a peatland.

and  $21 \text{ g C m}^{-2} \text{ yr}^{-1}$  respectively. However, he found that a coastal fen was a net sink for  $\text{CO}_2$  sequestering  $6 \text{ g C m}^{-2} \text{ yr}^{-1}$ . Waddington and Roulet (1996) found that a peatland in Sweden was a  $\text{CO}_2$  sink over two years of study with estimates of storage of  $9.1$  and  $1.1 \text{ g C m}^{-2} \text{ yr}^{-1}$ , whereas Carroll and Crill (1997) found a temperate poor fen to be a source of  $145 \text{ g C m}^{-2} \text{ yr}^{-1}$  by measuring net ecosystem exchange over an unusually warm and dry year.

The few estimates of  $\text{CH}_4$  emissions from northern peatlands range from  $0$  to  $3 \text{ g C m}^{-2} \text{ yr}^{-1}$  for wetlands in the Hudson Bay Lowlands (Roulet et al., 1994) and  $3$  to  $4.5 \text{ g C m}^{-2} \text{ yr}^{-1}$  as measured across different topographic gradients and for different climate conditions (Waddington and Roulet, 1996). The annual carbon sink resulting from trace gas exchange is small compared to the magnitude of the gas fluxes and makes measurement difficult and uncertainty high. For example, Gorham (1995) estimates gross production, net respiration and methane production for a typical northern peatland to be  $296$ ,  $249$  and  $4 \text{ g C m}^{-2} \text{ yr}^{-1}$  respectively. His estimates result in a net sink of  $23 \text{ g C m}^{-2} \text{ yr}^{-1}$  once a waterborne carbon flux of  $20 \text{ g C m}^{-2} \text{ yr}^{-1}$  is exported as DOC.

#### **Section 1.4 Dissolved organic carbon (DOC) - Peatland C-budgets**

Contemporary studies typically focus on NEE and  $\text{CH}_4$  flux due to their role in greenhouse feedback and the magnitude of  $\text{CO}_2$  fluxes in peatland NEE. However, to resolve the annual C budget of a peatland, NEE,  $\text{CH}_4$ , and DOC terms must be considered (Figure 1-2). Table 1-1 summarizes estimates of DOC export from different peatland and boreal forest - peatland complexes in the open literature. Estimates range from  $1$  to  $48 \text{ g C m}^{-2} \text{ yr}^{-1}$ , thus there is evidence that DOC export can systematically affect the source-sink nature of a peatland carbon budget. Reported export ranges can be large (ie.- Urban et al. (1989)), but these ranges summarize observations from several study catchments unique in size, order, upland/wetland area and hydrogeologic setting. High water yields can be expected in peatlands with large upland to wetland area, hillslope connectivity or in coastal wetlands of Canada ( $1200 \text{ mm yr}^{-1}$ ), and in such cases export ranges similar to those reported by Urban et al., Moore (1989) and Collier et al. (1989) are very plausible. However, if relief is negligible and the catchment is dominated by peatland (ie.- Hudson Bay Lowlands), DOC

**Table 1-1. Summary of annual runoff and DOC export from wetland and forested-wetland catchments reported in the literature from 1981 to 1998.**

<b>Study</b>	<b>Type of Catchment, Location</b>	<b>Runoff (mm)</b>	<b>Export (g C m<sup>-2</sup> yr<sup>-1</sup>)</b>
Mulholland (1981)	Creeping Swamp, North Carolina, USA	485*	21
Naiman (1982)	boreal forest, Sept Iles, Quebec, CAN	570-1640**	2.5 - 48.4
McKnight et al. (1985)	Thoreau's Bog, Massachusetts, USA	240	8.4
Moore (1987)	subarctic peatland, Schefferville, Quebec, CAN	302-389	1.1 - 4.9
Collier et al. (1989)	3 wetlands, Westland, New Zealand	1120-1404	28.7 - 37.8
Moore (1989)	forested, Westland, New Zealand	1371-1755	8 - 21
Moore and Jackson (1989)	forested, Larry River, New Zealand	1023-1253	30.6 - 43.8
Urban et al. (1989)	peat, northern Minnesota and Kenora, Ont	224-1410	8 - 40
Gorham (1995)	'typical' northern peatland	not reported	20
Carroll and Crill (1997)	Sallie's fen, Barrington, New Hampshire, USA	1071 <sup>P</sup>	3.4
Scott et al.(1998)	upland peat system, North Pennines, U.K.	798-1299 <sup>P</sup>	7 - 15

\* Runoff was estimated to be ~37% of annual precipitation (1310 mm) in Mulholland (1981) study.

\*\* Runoff estimates were calculated from reported mean annual estimates of discharge and basin area estimates.

<sup>P</sup> Numbers reported are measured estimated of annual precipitation. Direct estimates of runoff were not reported.

flux may be much less than the 'typical' northern peatland estimate after Gorham (1995). For example, areas in Canada containing large percentage area of peatland (>25% per area) have mean annual runoff ranges on the order of 100-500 mm yr<sup>-1</sup> (Hare and Thomas, 1979; National Wetlands Working Group, 1988). In such instances, DOC export similar to values reported by McKnight et al. (1985) and Moore (1987) would be more plausible.

Studies such as Moore (1997); Siegel et al. (1995); Schiff et al. (1997); and Clair and Ehrman (1996) highlight potentially important changes in DOC cycling under scenarios of climate change, acid precipitation, and changing hydrology. Also, DOC has been shown to play integral roles in: the cycling of heavy metals (Thurman, 1985; Malcolm, 1993); the source of biological energy (Dahm, 1980); minimizing UV-B penetration in lakes (Schindler and Curtis, 1997; Williamson et al., 1996); and water quality and acidity transport (Urban et al., 1989; Huber et al., 1994). Dependent on the trace gas biogeochemistry and DOC regime of a peatland, conditions could result in which exported DOC may affect the contemporary C-budget of a peatland (i.e. NEE is small), the productivity of a lake, or the acidity of headwater streams. An understanding of the environmental controls on DOC export from peatlands, as well as the links between hydrology, climate and ecosystems warrants further attention.

### **Section 1.5 - DOC - Chemical aspects**

DOC consists of several large groups of organic acids, sugars, amino acids and hydrocarbons, and is typically defined as compounds that will pass through a 0.45 micron filter. A more rigorous separation of the fractions after Qualls and Haines (1991), summarizes DOC fractions into six classes: hydrophobic neutrals (hydrocarbons, chlorophyll, carotenoids, phospholipids and humic substances); weak hydrophobic acids (tannins, flavonoids and vanillin); strong hydrophobic (carboxylic) acids (fulvic and humic acids, aromatic acids and long chain fatty acids); hydrophilic acids (humic substances, oxidized carbohydrates, small carboxylic acids and sugar phosphates); hydrophilic neutrals (neutral sugars, polysaccharides and alcohols); and bases (proteins, amino acids and amino-sugar polymers). In general, DOC is composed of 55% humic substances, strong

hydrophobic acids loosely referred to as fulvic and humic acids (Malcolm, 1993), but highly coloured waters of wetlands may be as rich as 90% humic substances (Thurman, 1985). Humic substances are the products of complex degradative and polymerization processes such as leaching of plant organic matter to water; leaching through a soil profile; leaching of soil humic substances to water; lysis of algal remains and by-products of microbial activity; UV oxidation and resulting polymerization processes in waters; and polymerization reactions in natural waters (Thurman, 1985).

The DOC observed in a wetland C pool is a function of the processes and controls on DOC production, retention and export (Moore, 1997). In part, the DOC observed will be a reflection of the precipitation, evapotranspiration, and the inputs and outputs of surface and groundwaters. In this way, the physical additions and subtractions of differing DOC pools will be strongly imprinted on local DOC concentrations, as well as provide a matrix for further biochemical conversions to take place. DOC in a wetland is also a function of the biota of the system. For example, the amount of through-fall and stem-flow, type of vegetation, age and quality of the biota, and levels of microbial activity will affect the quality and quantity of DOC produced *in situ*. A pool of DOC can also be affected by retention processes in soils (Moore, 1997). Some studied mechanisms of DOC sorption include cation bonding, physical adsorption, and anion and ligand exchange (Jardine et al., 1989; Schulthess and Huang, 1991), though the nature and chemistry of the DOC will strongly influence the retention processes that may occur (Moore, 1997). Moore et al. (1992) showed that sorption of DOC by mineral soils was positively correlated with Fe and Al content, and negatively correlated with organic C. Thus, peat soils, rich in organic C but poor in Fe and Al, should have a low DOC sorption potential, with the primary controls on the DOC regime being production, transport and export.

## **Section 1.6 Peatlands and hydrology - Processes and links to biogeochemistry**

### **Section 1.6.1 Water balance and wetlands**

The water balance of a wetland as illustrated in Figure 1-3, can be simplified to:

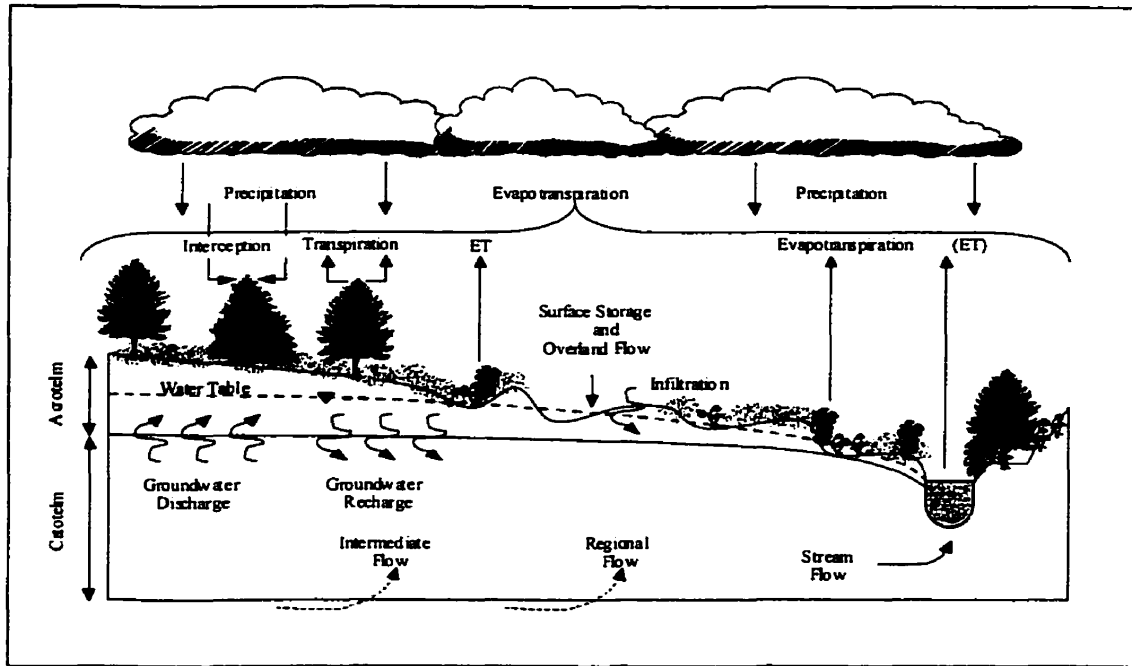


Figure 1-3. Hydrological cycle of a peatland modified after Brooks (1993).

$$R=P-ET-\Delta S+G_I-G_O \quad (1)$$

where R denotes catchment runoff, P denotes precipitation, ET denotes evapotranspiration,  $\Delta S$  denotes the change in water storage,  $G_I$  denotes groundwater inflow to the wetland and  $G_O$  denotes groundwater outflow from the system (all terms  $LT^{-1}$ ). The equation can be simplified for an ombrotrophic bog to:

$$R=P-ET-\Delta S-G_O \quad (2)$$

where  $G_O$  is seepage at wetland margins if and only if the system is completely isolated from intermediate and/or regional groundwater flow. To draw this conclusion, measurements of groundwater interaction must be made to validate the assumption, though this rarely occurs.

The water balance of wetlands and the physical principles used to estimate the components are concisely summarized in reviews by Dooge (1975), LaBaugh (1986) and Brooks (1993). If R, P, ET and G terms are quantified based on field measurements,  $\Delta S$  can be calculated both as a residual or from water table position and peat porosity measurements. This gives insight into the magnitude of uncertainty associated with measurements of the water balance components and gives confidence in runoff and load estimates if closure is obtained. Often ET or G terms are not measured, but calculated as a residual. LaBaugh (1986) found that in reviewing seven 'comprehensive water balance studies for detailed estimate of chemical yield' four of them treated groundwater exchange or evapotranspiration as a residual, and assumed the wetland under investigation to be in steady state. An assumption of steady state for dynamic systems such as wetlands was not advisable, and he showed that omission of measurements of ET or G led to uncertainty in hydrological and biogeochemical budgets.

Most studies since LaBaugh (1986) focus on the R, P and G terms of the water balance when estimating biogeochemical export (Devito et al., 1989; Hill, 1991; Devito, 1995; Branfireun et al., 1996; Waddington and Roulet, 1997), yet some of these key papers addressing chemical budgets omit direct measurements of ET as in the cases of DOC transport (Waddington and Roulet, 1997; Scott et al., 1998); nitrogen (Hill, 1991); and

methyl-mercury (Branfireun et al., 1996). Evaporation in different wetland systems has been studied rigorously (Rouse et al., 1977; Munro, 1979; Roulet and Woo, 1986; Price, 1991; Lafleur and Roulet, 1992), and the controls on ET in wetlands have been shown to be a function of energy available at the surface; the ability of the atmosphere to hold and transport vapour; and the ability of soils and plants to conduct water to the atmosphere (Roulet et al., 1997). The major hindrance in obtaining good ET estimates is that these factors can be difficult to measure and are highly variable between wetland type. This makes generalization schemes for ET a physical and financial challenge. Omission of ET does not void the importance of the studies to catchment biogeochemistry literature, rather it results in increased uncertainty if annual chemical burdens are the focus of the research.

### **Section 1.6.2 Physical aspects of groundwater flow and runoff**

Groundwater moves from areas of high hydraulic head to low hydraulic head in which:

$$h = \psi + z \quad (3)$$

where  $h$  is hydraulic head at the measurement location,  $\Psi$  is pressure head of the water and  $z$  is the elevation head of the water (all terms  $L$ ). Dependent on the height above an arbitrary datum and the pressure water is under, groundwater flow can develop in three-dimensions. The physical process of groundwater flow is governed by Darcy's Law in which discharge of water ( $Q$ ) can be estimated by:

$$Q = -K \cdot I \cdot A \quad (4)$$

where  $Q$  is measured as a volume per unit time ( $L^3T^{-1}$ ),  $K$  is a measure of hydraulic conductivity ( $LT^{-1}$ ),  $I$  is the hydraulic gradient (dimensionless) and  $A$  is the cross-sectional area through which groundwater moves ( $L^2$ ). Estimates of  $I$  are spatially variable across a heterogenous peatland, yet this variability is small when compared to the several orders of magnitude change documented for  $K$  in organic soils (Boelter, 1965; Ingram et al., 1974;

Gafni and Brooks, 1990; Letts, In press). It would appear that K largely controls discharge estimates from peatlands, but it has been shown that hydraulic gradient is equally important as a control on Q in raised dome bogs (Ingram, 1982; Gafni and Brooks, 1990). These authors agree that hydraulic gradients steepen at peatland margins and steepen over time due to groundwater mounding.

K values are typically highest at the peat surface and peatlands have highest elevation at their dome centre. Thus, Q is confined to a lens of higher flow at the peat surface as water discharges to low lying margins. Depending on the peatland, a Dupuit-Forcheimer approximation may be an adequate framework for direct estimate of discharge or hydraulic parameters at peatland margins (Ingram, 1982; Gafni and Brooks, 1990). Using this methodology, discharge from different soil lenses is determined by:

$$Q_d = -K \cdot b \cdot h(x) \cdot dh/dx \quad (5)$$

where  $Q_d$  is discharge ( $L^3T^{-1}$ ), K is the horizontal hydraulic conductivity of the lens ( $LT^{-1}$ ), b is a width in a perpendicular direction (L),  $h(x)$  is the thickness of the lens at a peatland margin (L) and  $dh/dx$  is the slope of the water table (dimensionless). It is assumed that the equipotentials are vertical and flow is horizontal, and that the hydraulic gradient is equal to the slope of the water table and to be invariant with depth. Further, discharge and loads calculated using a Dupuit approximation compare favourably with more mathematically intensive methods if the gradient of the water table is small and that the depth of the unconfined flow field is shallow (see Bear (1972) and Freeze and Cherry (1979) for further details).

Other approaches to estimate discharge have focused on basin connectivity in which peatland response to precipitation and evapotranspiration was explained using measurements of water table position and basin discharge (Bay, 1969; Verry et al., 1978; and Verry et al., 1988). The authors found that ombrotrophic bogs and peatlands were not effective at storing water or regulating flow throughout dry periods since P and ET events rapidly raised or drew-down water tables to increase or decrease discharge respectively. This 'tight' water table to discharge relationship forwarded the hypothesis that basin discharge could be

estimated from continuous measurements of water table. Discharge from bogs and peatlands was shown to mimic streamflow patterns generated from a level reservoir following the empirical relation:

$$Q_s = a \cdot (WT)^{b+c} \quad (6)$$

where WT is measured continuously (L), and a, b, and c are generated coefficients from a best fit regression of  $Q_s$  ( $L^3T^{-1}$ ) against WT (Verry et al., 1988).

### **Section 1.6.3 Recharge-discharge function of wetlands**

The acrotelm-catotelm model (Ingram and Bragg, 1984) holds that discharge from peatlands occurs along a high K lens near the surface, and that deep patterns of groundwater flow are non-existent or unimportant for discharge considerations. From a water yield perspective this is largely the case, but studies such as Siegel (1987), McNamara et al. (1992), Siegel (1993) and Romanowicz et al. (1993) have shown that the recharge-discharge function of peatlands can be significantly altered by regional patterns of groundwater flow. These changes in groundwater flow patterns have been shown to produce episodic  $CH_4$  emissions from peatlands (Romanowicz et al., 1993; Siegel et al., 1995) and transport solutes and alkalinity to discharge areas, effectively altering local pH and chemical balances (McNamara, 1992; Siegel, 1993). It has been speculated that evaporative draw-down and climate change play active roles in altering groundwater flow patterns and inducing head reversals (Romanowicz et al., 1993; Siegel et al., 1995, Devito et al., 1997).

Peatland development often occurs on sediments such as glacial tills or marine clays. A physical connection to these chemical rich boundaries can result in steep concentration gradients of salts, nutrients, dissolved gases or metals as peat accumulates and groundwater flow patterns develop. The concentrations of chemical constituents are predominantly a function of net recharge and flushing of the soil profile with chemically 'inert' precipitation. Yet, a change from recharge to discharge in deeper peats, even for a short duration, can result

in the transport of chemical species at higher concentrations to the acrotelm where physical export or *in situ* transformations may occur. Thus, changes in deep groundwater flow patterns can play a more important role in controlling biogeochemical cycling than was once thought. Uncertainty in assessing the role of flow patterns on biogeochemical cycling stems from an inadequate knowledge of horizontal and vertical hydraulic conductivities for organic soils, and the frequency and duration in which flow reversals occur.

Observed concentrations of solutes in a soil profile can be compared to predictions from a diffusion-model to evaluate peatland recharge-discharge function. An equation governing the diffusion process as summarized by Crank (1975) is:

$$C=C_0/2[erfc\cdot z/\sqrt{(D^*\cdot t)}] \quad (7)$$

where C is the calculated concentration using  $C_0$  as the concentration at the base of the profile, z is a depth (L),  $D^*$  is the effective coefficient of molecular diffusion ( $L^2/T$ ), t is time in seconds and *erfc* is the complementary error function.  $D^*$  for cations in groundwater typically range from  $1.0-2.0 \times 10^{-9} \text{ m}^2 \text{ s}^{-1}$  (Freeze and Cherry, 1979). Siegel (1988) found that wetland sites with well defined recharge functions near Juneau, Alaska, had observed concentrations lower than those predicted by the diffusion model. This suggested that a horizontal and downward flushing mechanism dominates the soil profile. In contrast, sites of dominant discharge had observed concentrations higher than those predicted by diffusion, indicating an upward flux of water and solute. This approach provided a chemical means of reconstructing patterns and changes of groundwater flow, chemical transformations and ecological transitions. Coupling this chemical information with head measurements and flow-nets could allow for estimates of chemical transformation, timing of reversal events and  $\text{CO}_2$  -  $\text{CH}_4$  degassing, or the location of 'hot-spots' for solute transport and *in situ* methylation ( $\text{CH}_4$  or methyl-mercury).

## **Section 1.7 Summary and rationale**

Global carbon research in the early 1990's showed that the global carbon cycle is perturbed by fossil fuel emissions and changes in land use, and to balance the global carbon cycle a northern hemisphere terrestrial sink is required. These findings led to investigations probing the specific locations and controls governing increased carbon sequestration in the boreal and sub-arctic regions over the last decade.

In the case of peatlands, trace gas biogeochemistry received scientific attention due to the role of CO<sub>2</sub> and CH<sub>4</sub> as radiatively active species and the importance of CO<sub>2</sub> in NEE and annual carbon sequestration. However, to accurately assess the source-sink nature of peatlands, hydrology and DOC biogeochemistry must be considered. In spite of the fact that most discharge from peatlands occurs through a zone of high K at the peat surface, changes in groundwater flow patterns appear to play a much more active role in biogeochemical cycling than once thought. Thus, research reported in this thesis seeks to build on the literature by quantifying the DOC term of the contemporary carbon budget and assessing the importance of groundwater flow at a peatland where continuous measurements of NEE and micro-meteorological parameters were made.

## **Section 1.8 Research objectives**

*Objective 1 - Monitor the groundwater and surface water hydrology of the Mer Bleue bog in attempt to isolate the hydrological controls of the peatland at several spatial and temporal scales;*

*Objective 2 - Compute the water balance of the peatland for one hydrological year;*

*Objective 3 - Determine the spatial and temporal variability of DOC in the Mer Bleue bog;*

***Objective 4 - Using data obtained to address objectives 1 and 3; determine the net DOC export and the relative importance of DOC export in the contemporary carbon budget of the peatland; and***

***Objective 5 - Determine the importance of groundwater flow patterns in maintaining and/or controlling carbon cycling and pore water chemistry at the Mer Bleue bog.***

Chapter 2 of this thesis provides background on the study site and outlines the materials and methods used for this research. Chapter 3 summarizes the biogeochemical and hydrological findings used to determine net DOC export from the Mer Bleue bog. Chapter 4 summarizes an analysis of groundwater flow patterns and geochemical findings at the Mer Bleue bog. The thesis concludes with Chapter 5 where major findings of Chapters 3 and 4 are considered jointly to advance discussion and questions for future research.

## **Chapter 2 - Study Site and Methodologies**

### **Section 2.1 Landscape development and site description**

#### **Section 2.1.1 Site description**

The Mer Bleue bog, located 45° 05' to 45° 30' N and 75° 30' to 76° 00' W, is a raised *Sphagnum* bog, characterized by numerous peat domes that are ombrotrophic in nature (National Capital Commission, 1997). The bog is 2800 ha in size, of which the northern most finger of the peatland (this study) is 480 ha and has a perimeter of 11, 000 m (Figure 2-1). Upland areas are well drained by ditches and thus most of the contributing area is the peatland itself, but an areal estimate encompassing uplands and peatland was 580 ha. Ground and surface water leaving the peatland enters a network of 15 different beaver ponds with well-aged beaver dams along the perimeter of the peatland. Discharge leaves through a single outflow at the western extent of the drainage basin. Dependent upon point of discharge on the peatland, horizontal path-length from the upper-most pond reaches to the basin outflow may be as great as 4, 900 m.

The drainage basin slopes from 70 to 66 m above sea level from east to west, yielding a basin gradient of 0.0008. Upland and hillslope contributing areas are dystic and eutric brunisols (Tim Moore, personal communication) underlain by marine clay at shallow depth. Measurements made along a piezometer transect on a hillslope near the study site yielded a gradient of 0.06 and was in agreement with gradients calculated from an NCC GPS survey of the same area. Upland slopes exist with gradients as high as 0.4 - i.e. the north facing hillslopes on the sand spits near the main outflow. *Sphagnum spp.* (*orders - angustifolium, cuspidatum, fallax, fuscum, magellanicum, majus, rubellum*) are the dominant moss species found on the bog surface, and several heath and grass species such as labrador tea (*Ledum groenlandicum*), leatherleaf (*Chamaedaphne calyculata*), blueberry (*Vaccinium spp.*), sheep-laurel (*Kalmia augustifolia*), cotton grass (*Eriophorum spp.*) and sedges (*Carex spp.*) dominate the micro-canopy (Birgit Isernhagen, pers. comm.). The bog margins exhibit a

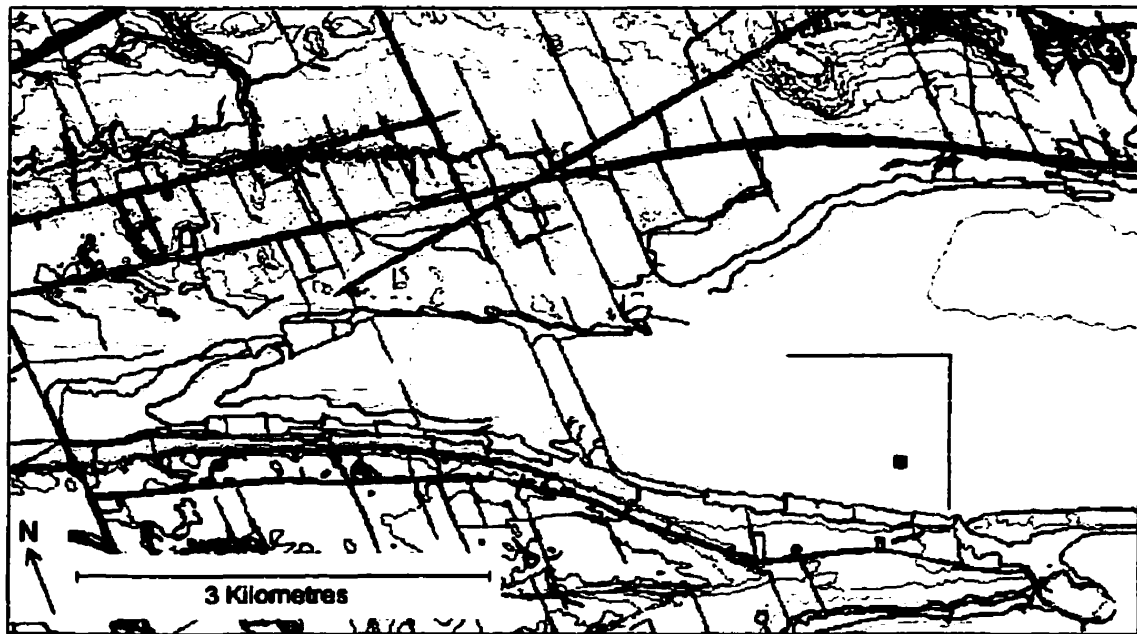
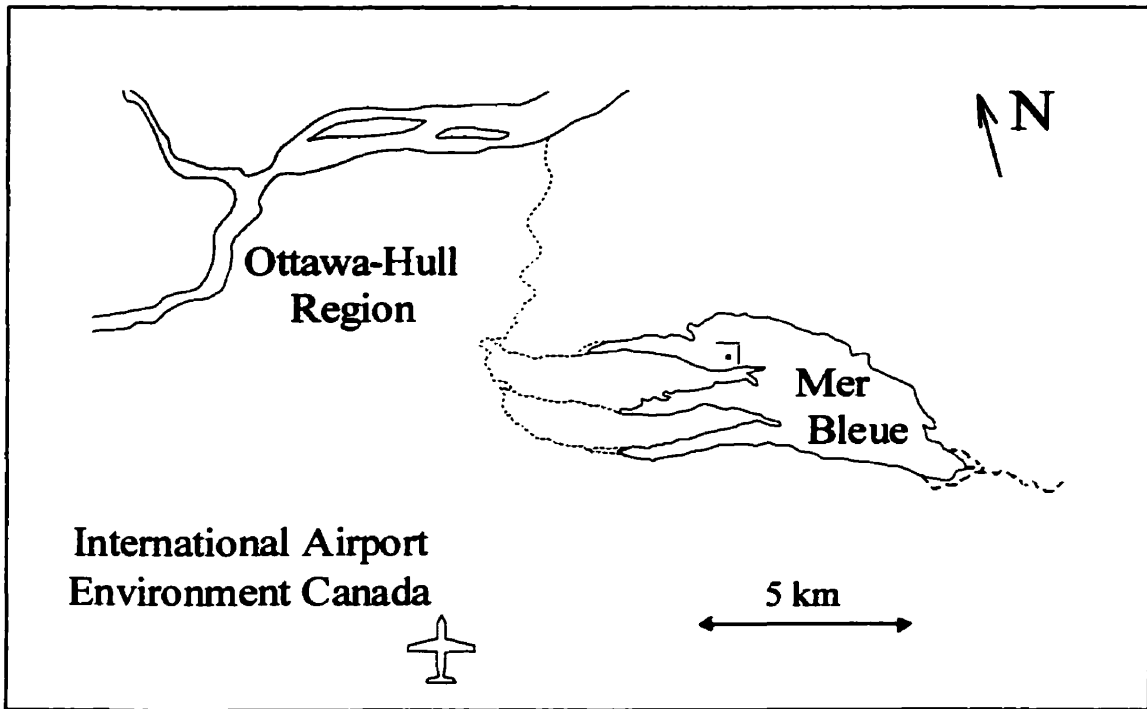


Figure 2-1. a. Mer Bleue bog and the Ottawa region. b. The tower site and groundwater transects on the drainage basin. Spatial data was provided by the National Capital Commission.

transition to *Carex spp.*, *Eriophorum spp.* and cattail (*Typha latifolia*) vegetation types, with the dominant over-story species of black spruce (*Picea mariana*), tamarack (*Larix laricina*) and white paper birch (*Betula papyrifera*) found in highest density towards these edges. Classified as a cold humid continental climate, the Mer Bleue bog is characterized by a mean annual temperature of 5.8°C, mean annual precipitation of 910 mm, and a mean annual growing season of 193 days. Table 2-1 summarizes 50 year temperature and precipitation normals for monthly and annual observations recorded at the Ottawa International Airport 10 km to the south of the Mer Bleue bog (Figure 2-1).

### **Section 2.1.2 Geology, hydrology and past research in the Ottawa area**

A majority of the Mer Bleue area is underlain by shale bedrock of the Carlsbad, Billings and Queenston Formations of the late Ordovician Age, and blanketed by a clay lining considered to be marine deposits of the Pleistocene Champlain Sea (Hobson, 1969). A seismic survey of the Mer Bleue area by Hobson indicated drift thickness to range between 12-30 m and seismic estimates were in agreement with bore hole measurements made on the survey area. The results of Hobson (1969) also correlate with Geological Survey of Canada drilling surveys where they found the area to be underlain by Billings Formation (black shale with some brown shale) and Carlsbad Formation (grey shale and sandy shale with some dolomite layers) of depth up to 180 m, with drift thickness highly variable (18-45 m) in the Ottawa Hull area (Belanger and Harrison, 1977). Bedrock topography ranges in height between 38 and 60 m a.s.l. (Belanger and Harrison, 1977; Hobson 1969), and the bog surface is approximately 70 m a.s.l. Maximum peat depth reported at the Mer Bleue bog is 5.5 m after (Mott and Camfield, 1969)

The Mer Bleue bog is situated in the central part of the St. Lawrence Lowlands, which is a major fault-generated depression situated between the Appalachian and Adirondack highlands to the south and the Laurentian highlands to the north (Richard et al., 1987). At the time of the last glaciation, great masses of ice from the Wisconsinan Event induced crust flexion and the development of a depression lying below sea level which filled

**Table 2-1. Temperature and precipitation climate normals for the Ottawa International Airport, Ontario, Canada, 1938 to 1990 inclusive. Station location is 45°19' N 75°40' W and station elevation is 116 m.**

	<i>Jan</i>	<i>Feb</i>	<i>Mar</i>	<i>Apr</i>	<i>May</i>	<i>Jun</i>	<i>Jul</i>	<i>Aug</i>	<i>Sep</i>	<i>Oct</i>	<i>Nov</i>	<i>Dec</i>	<i>Mean</i>
<b><i>Temperature</i></b>													
Daily Maximum (°C)	-6.3	-4.6	1.8	10.8	18.6	23.6	26.4	24.6	19.6	12.8	4.7	-3.7	10.7
Daily Minimum (°C)	-15.5	-14	-7.3	0.3	7.1	12.2	15.1	13.7	8.9	3	-2.8	-11.7	0.8
Daily Mean (°C)	-10.8	-9.2	-2.7	5.6	12.8	17.9	20.8	19.2	14.3	7.9	1	-7.6	5.8
<b><i>Precipitation</i></b>													
Rainfall (mm)	15.3	16.4	32	58	74.8	76.9	88.1	92	82.9	70.3	62.5	32.6	701.8
Snowfall (cm)	49.6	45.2	32.3	9.1	1.2	0	0	0	0	4.1	24.2	55.8	221.5
Precipitation (mm)	58	58.6	64.8	69	76.4	76.9	88.1	92	82.9	74.8	86.4	82.5	910.5

**Data Source - Environment Canada - Canadian Climate Normals - Copyright 1998**

with waters from the Atlantic Ocean and glacial meltwaters to yield the Champlain Sea 12,000 yr BP (Mott and Camfield, 1969). The sea persisted until 9,500 yr BP after which isostatic rebound forced sea waters eastward to the Atlantic Ocean. The production of rock powder from glacial scouring and sedimentation processes in the glacial Champlain Sea yielded the fine marine clay deposits found in the Ottawa-Hull Area (Richard et al., 1987).

The three fingers of the Mer Bleue bog (Figure 2-1) were once meltwater channels en route to the Ottawa River that eroded into the local marine clay deposits to depths of 9 m (Mott and Camfield, 1969; Richard et al., 1987). The mineral soils surrounding the peatland are mostly silt and silty clay soils, however, the three fingers of the Mer Bleue bog are separated by sand that in places has been reworked into dunes that cap the ridges between the ancient channels (Mott and Camfield, 1969; Richard et al., 1987). Processes of terrestrialization and subsequent bog formation likely started about 8,000 yr BP based on carbon dating and the marine to marsh transition in peat cores (Pierre Richard, pers. comm.). Presently, the entire lowland is a basin triangular in shape which is drained by the St Lawrence and lower Ottawa Rivers and their many tributaries, such as Green Creek which drains the eastern portions of the Mer Bleue bog to the Ottawa River.

The Mer Bleue bog is designated as a conservation zone within the National Capital Commission (NCC) Greenbelt. In 1950, the concept of a Greenbelt in the Ottawa area was forwarded, and land not publicly owned was acquired around the reserve by 1956. After another acquisition in 1974, a Greenbelt area of 20,350 ha existed with the mandate to conserve the natural environment for the preservation and maintenance of the open and rural character of the landscape. Since the Greenbelt creation, the peatland has been the focus of many regional forestry, ecology, palynology, and geology research programs. Relevant studies yielding baseline hydrological information are few, yet it was found that: from seven piezometer nests around the Mer Bleue bog inserted to depths of 40-60 m yielded salinity levels of 10,000 ppm (Bik et al., 1971); the slow recovery rate of piezometers in marine clay imply low permeability and a negligible rate of upward flow despite the occurrence of salt accumulation in subsoils found in many regions of the Central Research Forest (Bik et al., 1971); and the upper 20 m of marine clay were deposited in a Champlain Sea that had lost

much salinity, presumably from dilution by meltwaters at the time of glacial retreat more than 10, 000 yr BP (Gadd, 1962; Bik et al., 1971).

The Mer Bleue bog has survived disturbances such as the encroachment of farming; peat utilisation for fuel and horticulture; ditch-digging as a means of generating employment during the Depression; and as a range for bomb and track vehicle testing during World War II (Baldwin and Mosquin, 1969). More recently, the Mer Bleue bog was sited as a Canadian RAMSAR wetland as it is the largest of its kind remaining in the St. Lawrence Lowlands and is an example of a wetland typically found in other biogeographical areas of Canada. The site is also hosting the Peatland Carbon Study (PCARS) project until 2001 and beyond, a multi-disciplinary carbon-climate-ecosystem study involving investigators from McGill University, Mount Holyoke, Trent University, Université de Montréal, Université de Québec a Montréal and the University of New Hampshire.

## **Section 2.2 Field instrumentation and methods**

### **Section 2.2.1 Peatland topography and estimate of gradients**

During the winter of 1998, a topographic survey of the Mer Bleue bog was completed after a major ice storm left a 100 mm thick ice lens on the bog surface which conformed to the macro-topographic features of the peatland. Using a Nikon<sup>o</sup> Total Station, 380 points on the peat dome were surveyed to arbitrary X, Y, and Z co-ordinates. The results from the survey allowed for the identification of the major and minor topographic axes, and the 14 piezometer nests on the peatland were inserted (Figure 2-2a). Transect distances and elevations were measured and referenced to the beaver pond (for the major axis), the major axis (for the minor axis) and to a local benchmark. Two theodolite surveys of the piezometer nests, wells and estimated surface elevation showed excellent agreement with the winter survey. A database of roads, rivers, vegetation and 1400 spot heights from a GPS survey of the peatland was provided by the National Capital Commission. The resolution of the GPS was too crude to estimate small hydraulic gradients, but the database proved to be useful for estimating drainage direction, drainage basin areas, and the peatland perimeter.

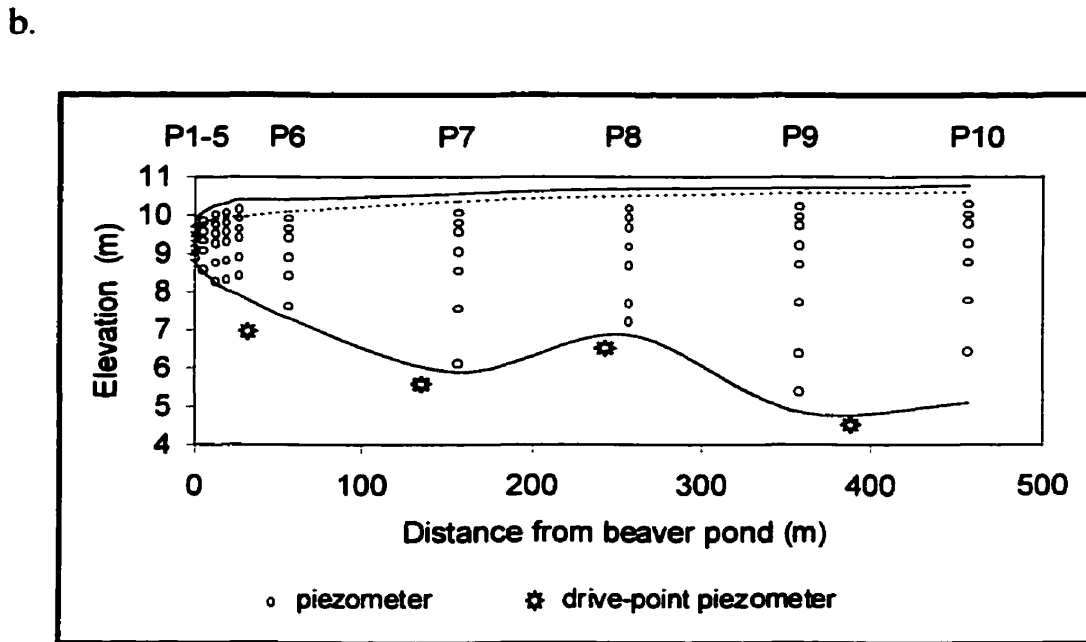
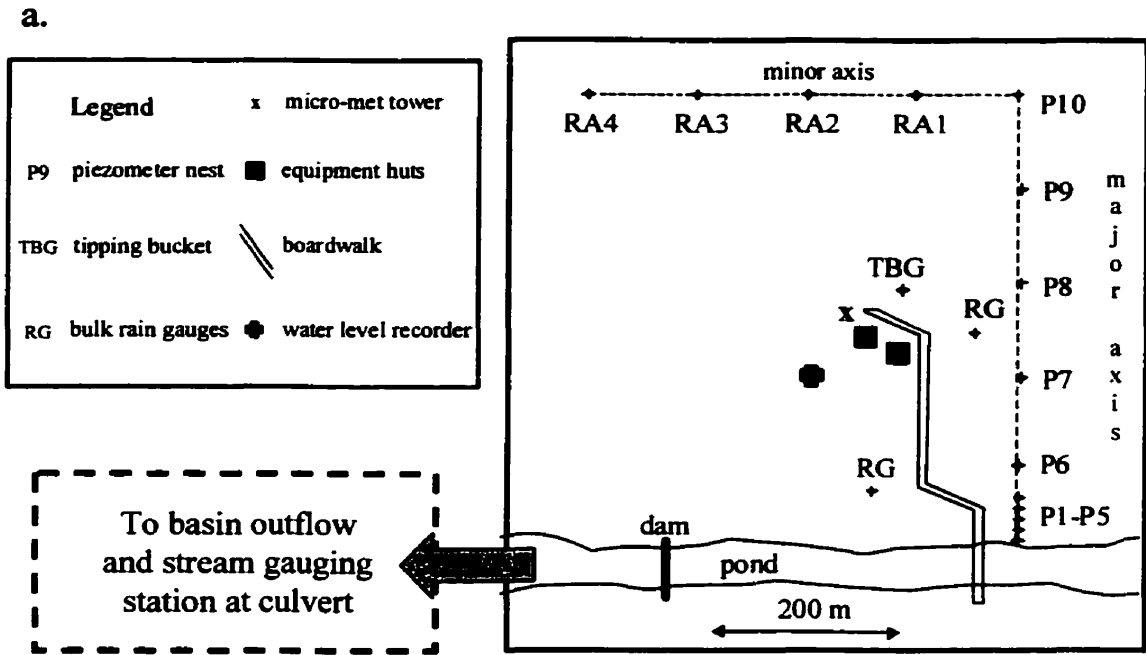


Figure 2-2. Schematic of the study site showing the location of instruments at the Mer Bleue bog. a. Plan view of instrumentation on the drainage basin. b. Cross-section of the major axis showing the location of piezometers and changes in surface and peat-clay interface topography.

### **Section 2.2.2 Underlying marine clay and external groundwater influences**

A 6.5 m PVC probe constructed from 12.5 mm ID Schedule 80 pipe was used to determine peat and marine clay depth along the major and minor axes. A total of 30 insertions were made - 18 evenly spaced along the major axis and 12 along the minor axis. A best estimate of the peat-marine clay interface was recorded based on probing results and the bottom features were mapped (Figure 2-2b). A ground penetrating radar (GPR) survey was completed to map in three dimensions the bottom topography of the major axis and isolate changes in bulk density and peat properties through the profile. However, due to the high electrical conductivity of peat pore waters at the Mer Bleue bog, the GPR survey yielded no information about changes in bulk properties below 2 m depth as the radar signal was dampened due to heat transfer to the ionic waters in the profile (Stephen Robinson, pers. comm.).

Using information from the probing survey, four Solinst drive point piezometers were inserted along the major axis to evaluate the patterns and magnitude of groundwater exchange across the base of the peatland (Figure 2-2b). Standard 30 cm Waterloo Drive Point Piezometers with 180  $\mu\text{m}$  shields were coupled to 19 mm galvanized pipe and inserted through the peat to the underlying marine clay using a sledge hammer and a standard coupler to by-pass apparatus. Attached to a nipple on the drive point piezometer and extending to the peatland surface was 9.5 mm LDPE tubing suitable for recording measurements of head or sampling groundwater chemistry.

### **Section 2.2.3 Macro-scale surface water hydrology**

All outflow waters from the study basin flow through a single 0.70 m radius culvert at the western boundary of the catchment. Discharge was calculated from downstream velocity measurements, continuous measurements of stage and estimates of cross-sectional area. Stream gauging observations were used to develop three rating curves for discharge observations as summarized in Figure 2-3. Downstream velocities were measured using a Model 625 Pygmy Current Meter and a Teledyne Gurley Flow Velocity Indicator at 0.6

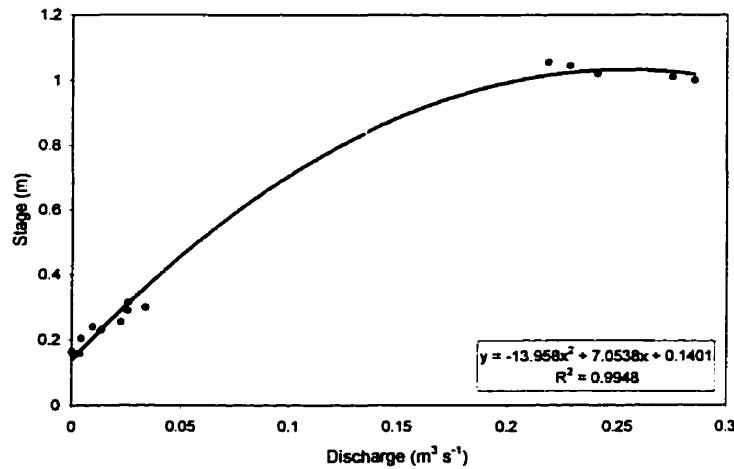
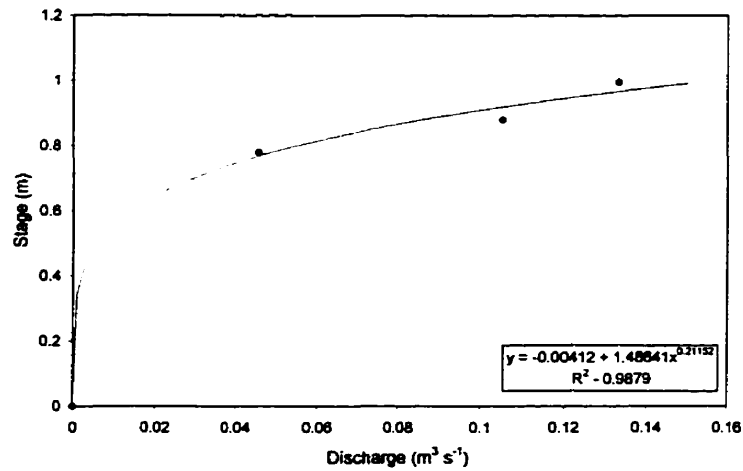
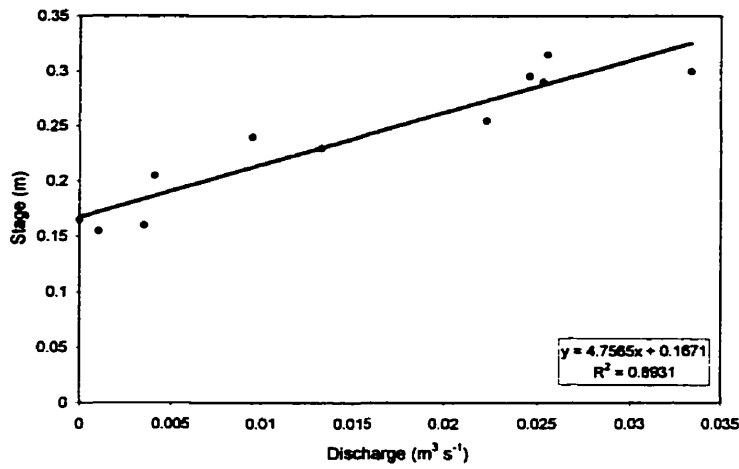


Figure 2-3. a. Rating curve used for spring, summer and autumn 1998 discharge observations. b. Rating curve used for high stage - low discharge observations under ice cover during winter 1999. c. Rating curve used for discharge observations during spring melt 1999.

observed discharge depth. Continuous measurements of stage were made using a Campbell Scientific CR-10 datalogger every thirty seconds and averaged into half hour and mean daily values for final storage.

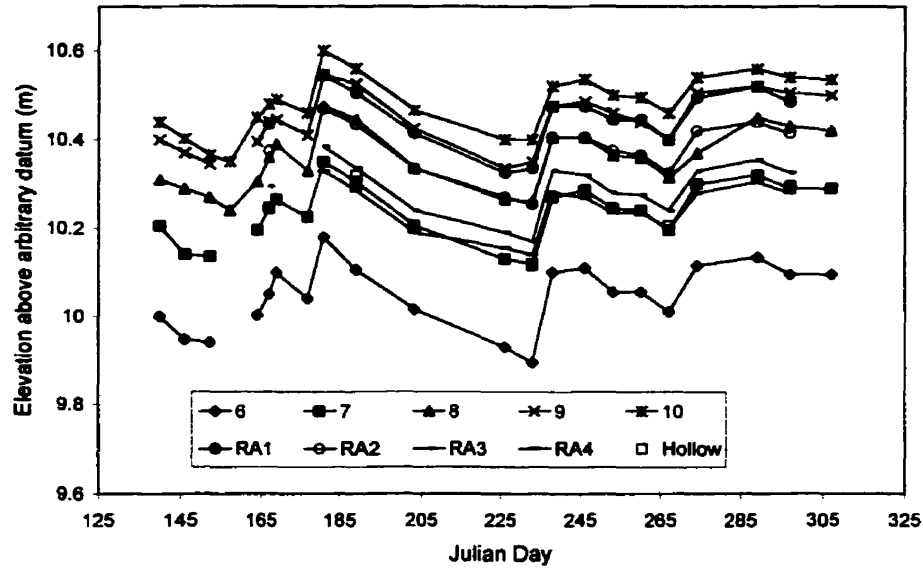
A ten point rating curve with an adjusted r-square of 0.89 was found to be satisfactory in estimating discharge for ~75% of total stages, those observed from spring to autumn 1998. A four point rating curve was used to estimate discharge from the peatland during a mid-winter melt event where high stage and low velocities persisted beneath ice cover at the outflow for a fifty day period. A 15 point rating curve was used to estimate high discharges during snow melt in early April 1999. Runoff was calculated from discharge estimates assuming catchment area to be 4 800 000 m<sup>2</sup>.

#### **Section 2.2.4 Meso- and micro-scale groundwater and surface water hydrology**

Nests of piezometers were inserted at 14 stations on the major and minor axes of the peatland for measurement of head and chemical sampling of pore waters. Piezometers were constructed from 12.5 mm inside diameter (ID) Schedule 80 PVC pipe attached to 20 cm perforated heads covered with 40  $\mu$ m Nitex meshing. All nests had spatial coverage with depth to or near the underlying marine clay of the peatland and manual wells were inserted for measuring water table at each station. Stations P1 to P5 had piezometer installations of 0.25, 0.5, 0.75, 1.0 m and 1.5 and 2.0 m where depth to clay permitted. These five stations were closely spaced at the perimeter of the peatland where the steepest hydraulic gradients were found to occur based on topographic surveys. At this area, stations were equipped with 15 cm ID wells and water level recorders connected to a datalogger. Water table was measured every 30 seconds and stored as half hourly and daily mean water tables. The 9 nests on the peatland were instrumented with piezometers at 0.5, 0.75, 1.0, 1.5, 2.0, 3.0 and 4.75 m depths and 5 cm ID manual observation wells. Correlations between manual wells and two continuous records of water table from wells at the main tower (hummock and hollow wells) approached unity and allowed for transformation of the continuous records of water table from the tower to all piezometer nest on the peatland (Figure 2-4).

A 15 m transect of four piezometer nests and manual wells were inserted in the

a.



b.

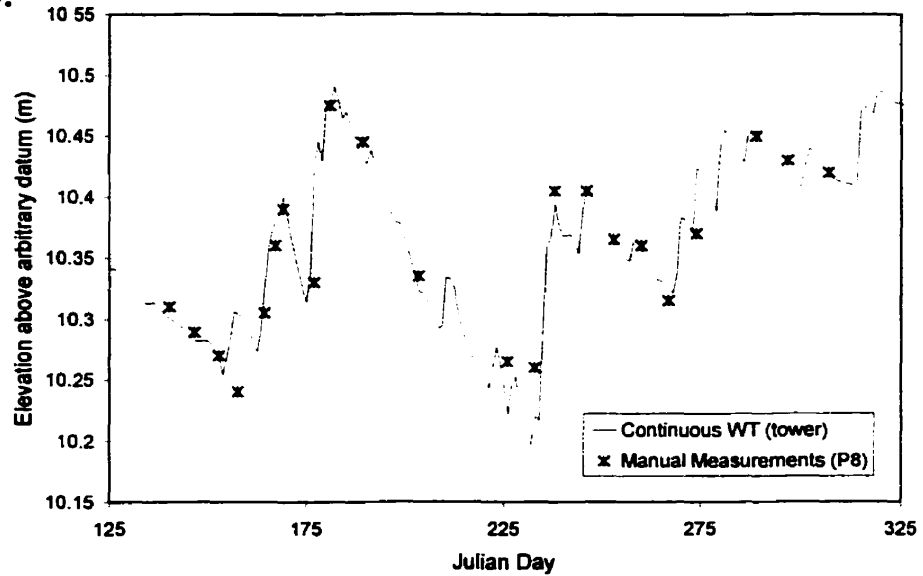


Figure 2-4. a. Summary of manual measurements from observation wells P6 to P10 on the major axis and RA1 to RA4 on the minor axis. Correlations between records ranged from 0.95 to 0.99. b. Continuous record of water table position from the tower site transformed to manual observations at nest P8. Similar graphs could be produced for stations on the peatland (P6-P10, RA1-RA4).

mineral soil hillslope (Figure 2-2a) opposite the peatland to estimate water and chemical input to the pond from the mineral soil. Marine clay was found under the mineral soil at depths ranging from 1.0 to 1.5 m. Thus, piezometers of 0.25, 0.5, 0.75 and 1.0 m were inserted to the hillslope. Chemical sampling from all piezometers (major, minor, hillslope) was performed using Tygon tubing and a peralstaltic pump, and head measurements were made using a Solinst electric tape. Prior to sampling pore water chemistry, all piezometers were first bailed and left to recharge with 'fresh' water.

A 0.4 m wide rectangular flume box was installed in a beaver dam downstream of the major axis (Figure 2-2a). A stilling well with a water level recorder was connected to a datalogger to establish continuous records of pond stage and estimate discharge through the flume box. Monitoring at this station was stopped when it was determined that the well-aged beaver dam was unsuitable for controlling pond water levels and the measured stage-discharge relationships were meaningless.

### **Section 2.2.5 Measurement of meteorological parameters**

Precipitation, energy balance partitioning, air temperature and evapotranspiration were measured at the main tower site or calculated from the tower data as part of the PCARS project. Precipitation (P) was measured using a tipping bucket rain gauge, and evapotranspiration (ET) was calculated using continuous eddy covariance measurements of  $Q_E$  and surface temperature (data provided by P. Lafleur and S. Admiral, Trent University). From Oke (1987):

$$ET = Q_E / L_v \rho_w \quad (8)$$

where  $Q_E$  is the latent heat flux, and  $L_v$  and  $\rho_w$  are the latent heat of vaporization and density of water respectively. For elaboration on the methods and calibrations for measurement of micro-meteorological and eddy covariance variables at the Mer Bleue bog refer to Lafleur and Admiral (In prep.). On-site estimates of precipitation were calibrated against measurements made from bulk precipitation gauges on the peatland and data provided by an Atmosphere Environment Service station at the Ottawa International Airport.

A ten point snow course was established along the major axis and snow water equivalent (SWE), snow depth, and snow density estimates were made on four sample dates through the winter dependent upon timing of snowfall, above-zero temperatures and snowpack ablation. A snow gauge with a Nipher shield was installed near the tower site to measure precipitation, and a sonic snow sensor capable of measuring changes in pack ablation and mean pack depth was connected to the tower site datalogger.

### **Section 2.2.6 Measurements of hydraulic conductivity**

Surveys of hydraulic conductivity (K) were conducted for piezometers inserted in the peatland and mineral hillslope. Measurements of horizontal hydraulic conductivity were estimated using methodologies for slotted head cylindrical piezometers after Hvorslev (1951) and Freeze and Cherry (1979):

$$K_h = (r^2 \cdot \ln(L/R)) / (2 \cdot L \cdot T_0) \quad (9)$$

where r is the piezometer radius (L), R is the piezometer head radius (L), L is the piezometer head length (L), and T<sub>0</sub> is the time required for the complete equalization of the initial head if the first rate of recovery was maintained until recovery was complete (T). Using an electric tape and peralstaltic pump, piezometers were bailed and water level recoveries over several time intervals were recorded until equilibrium head was again achieved. Head recovery versus time plots were later used to graphically solve for T<sub>0</sub> giving estimates of K<sub>h</sub>.

Two additional piezometer nests were inserted at P4 and P9 to assess mean hydraulic conductivity (K<sub>m</sub>). Piezometers were of length 0.5, 0.75, 1.0, 1.5 and 2.0 m at P4 and 0.5, 0.75, 1.0, 1.5, 2.0, 3.0 and 4.5 m at P9. The nine piezometers for estimate of K<sub>m</sub> were screened with 40 μm Nitex at the lower end, yielding an integrated measure of both K<sub>h</sub> and vertical hydraulic conductivity, K<sub>v</sub>. Bail tests were performed as were those tests for estimates of K<sub>h</sub>, however, K<sub>m</sub> was determined following the relationship:

$$K_m = (\pi \cdot D) / (11 \cdot T_0) \quad (10)$$

where  $D$  is the diameter of the piezometer cavity and  $T_0$  is the basic time lag after Hvorslev (1951). Making direct measurements of  $K_v$  in peatlands would be desirable, but this requires large diameter casings and heavy equipment for installation (Chason and Siegel, 1986). Instead,  $K_v$  was calculated from measurements of  $K_m$  and  $K_h$  using the relationship:

$$K_m = \sqrt{K_h \cdot K_v} \quad (11)$$

### **Section 2.2.7 Sampling program, monitoring and time line**

Manual measurements of discharge against a permanent staff gauge began at the basin outflow April 8, 1999 and continuous measurements of stage at the outflow stilling well were operational May 22, 1998. Meteorological parameters and precipitation measurements were continuous after May 20, 1998. The hydrological year for this study was from May 22, 1998 to May 21, 1999. Data collected prior to the start date were not discarded, rather used as reference data for snowmelt observations in the spring of 1999. The hydrology was completed as part of the Peatland Carbon Study (PCARS) research project and limited to a year for the purpose of annual export calculations, however, baseline hydrology and hydro-chemical measurements are to continue for three more years.

Grab samples for DOC analysis were taken from the main outflow and from the beaver pond near piezometer station P1 weekly over the hydrological year, and precipitation samples from a collector covered with a 40 um screen were analyzed when available. Grab samples were collected in clean Nalgene bottles and kept cool on transport from the field to the laboratory at McGill University, Montréal, Québec.

Piezometer nests were inserted May 22, May 26, and June 13, 1998 on the major axis, mineral hillslope and minor axis respectively. Head measurements were made bi-monthly for most of the study period, but more frequently during an evaporative draw-down in July and August 1998. In summary, head measurements were made on 17, 15, and 13 occasions for the major axis, minor axis and mineral hillslope respectively. Sampling of pore waters

for chemical analysis was performed using a peralstaltic pump and Tygon tubing to clean Nalgene bottles on 10, 7 and 8 sample dates for the major, minor and hillslope axes over the study period. DOC samples were filtered with 0.45  $\mu\text{m}$  membrane filters in the field or transported in coolers for filtration at McGill University. DIC samples were drawn from recharging piezometers to a 60 cc syringe, filtered with a 0.45  $\mu\text{m}$  membrane to a second syringe sealed by a stopcock while in the field. Water temperature of samples was measured and recorded in the field.

Snow course work commenced December 19, 1998 and ended March 17, 1999. Sampling was governed by patterns of mid-winter melts and timing of precipitation events. SWE, pack depth, and profile characteristics were surveyed on January 6, January 20, February 19, and March 17, 1999. After March 17, 1999 snow course work was stopped and the main outflow was re-instrumented for spring melt. Stream gauging and grab sampling continued at the outflow until the close of the hydrological year. Head measurements were made across the piezometer network for three dates in the spring of 1999 and groundwater chemistry was analysed at a subset of piezometers four times prior to the conclusion of the study.

## **Section 2.3 Laboratory methods**

### **Section 2.3.1 Carbon and geochemical analyses**

Water samples taken in the field for analysis of DOC were kept cool while transported to McGill University. Some of the sample was filtered with 0.45  $\mu\text{m}$  membrane filter paper to a clean 8 mL auto-analyser sample vial sized for a Shimadzu 5050 TOC Analyzer. The remaining sample was filtered to clean 28 mL scintillation vials or 60 mL Nalgene bottles, acidified to pH 2 by addition of 2 N hydrochloric acid and refrigerated at 4 °C for later geochemical analyses.

Samples for analysis of DOC were acidified with 2 N hydrochloric acid to pH 2 and sparged by an inert carrier gas to bubble off dissolved inorganic forms of carbon as carbon dioxide ( $\text{CO}_2$ ) prior to measurement. Injected samples in the Shimadzu 5050 TOC Analyzer

were then combusted in a catalyst at 680 °C to CO<sub>2</sub> gas and passed through a halogen scrubber to a non-dispersive infrared detector (NDIR). The NDIR outputs an analog detection signal which generates a peak based on the amount of carbon dioxide in the gas samples which can then be measured by a data processor. To measure DIC, sample vials were filled to capacity from the original sample syringe, and simultaneously covered with paraffin wax such that zero head space remained. The unacidified DIC samples were injected into a reaction vessel where carrier gas and sample are sparged with 25% phosphoric acid. The sparging process releases inorganic carbon species as CO<sub>2</sub> which can then be detected by the NDIR to give a measurement of dissolved carbon dioxide and hydrogen carbonate in solution. Whether measurements for DOC or DIC were performed, averages of 6 injections per sample were made, and standard deviations (SD) and coefficient of variation (CV) were recorded for each sample. Extra injections were performed by default until coefficients of variance were below 1% and 2% for DOC and DIC respectively.

Measurements of electrical conductivity (EC) were performed on surface water, groundwater and precipitation samples for the study period. Temperatures were recorded in the field at the time of sampling for calculation of environmental EC, but samples were transported to Montreal and analysed on a Consort K220 Microcomputer Conductometer at room temperature (~21 °C). Prior to measurement, the meter was calibrated for temperature and EC using standard solutions of 0.01 M potassium chloride. Measurement of Ca<sup>2+</sup>, Mg<sup>2+</sup> and Na<sup>+</sup> in ground and surface water samples was performed at the Earth and Planetary Sciences Geochemistry Laboratory, McGill University using Flame Atomic Adsorption Analysis for 85 samples taken August 26, 1998. All dilutions, standard solutions and analyses were performed by a research technician at the laboratory. Detection limits for Ca<sup>2+</sup>, Mg<sup>2+</sup> and Na<sup>+</sup> were 0.04, 0.01 and 0.02 parts per million respectively. A regression of Na<sup>+</sup> and electrical conductivity was used to predict Na<sup>+</sup> concentrations from electrical conductivity measurements made over the study period (see Appendix 1 for more details).

### **Section 2.3.2 DOC characterization using a spectrofluorometer**

Fluorescence scans were performed on 70 DOC samples with a Shimadzu RF-1501

scanning spectrofluorometer (Biological Sciences Wet Lab, University of Alberta) equipped with a xenon lamp and using optically clear quartz cuvettes with path length 1.000 cm. Excitation radiation was fixed at 370 nm and scans of emissions were performed from 370 to 650 nm where variations in spectral intensity were corrected for using scans of a standard 1 ug/L quinine sulfate solution in 0.1 N H<sub>2</sub>SO<sub>4</sub> (Donahue et al., 1998). Scans of sample blanks (distilled de-ionized water) were used to find and remove scattering by subtracting the blank fluorescence values from the emission scans obtained from samples acidified to pH 2 with hydrochloric acid. The values of the 450 nm and the 500 nm emission intensity were isolated from the emission scans and the ratios of 450 : 500 wavelength emission intensity were calculated. Low magnitude ratios (~1.4) have been shown to qualitatively typify terrestrially derived, allochthonous organic carbon, whereas high ratios (~1.9) have been typified as microbially derived, autochthonous organic matter (Dianne McKnight, pers. comm.; Donahue et al., 1998). Further, a high ratio denotes high aromaticity and low ratio denotes low aromaticity.

## **Chapter 3 - Hydrological controls and DOC export at the Mer Bleue Bog**

### **Section 3.1 Hydrological controls at the Mer Bleue Bog**

#### **Section 3.1.1 Peatland topography and hydraulic gradients**

The winter survey of the peat dome encompassed the main tower site and yielded X (major axis), Y (minor axis) and Z (elevation) co-ordinates. This allowed for the interpolation of a plane through the data points and the isolation of the major and minor gradients of the bog. As illustrated in Figure 3-1, the major axes of the peatland had two distinct gradients. The steeper gradient was  $\sim 0.03$  for the bog margin, whereas the lesser gradient was  $\sim 0.001$  and extended a distance of 450 m from P3 to the bog centre. There was excellent agreement between the results of the total station winter survey and two theodolite surveys in the summer in which average surface, wells and piezometers were leveled with respect to an arbitrary datum.

#### **Section 3.1.2 Patterns of peatland hydraulic conductivity (K)**

$K_h$  decreased in magnitude with depth following the acrotelm-catotelm model of Ingram and Bragg (1984). As illustrated in Figure 3-2a (see Appendix 2 (a-d) for actual values), a high  $K_h$  lens was confined to the upper 0.5 m of the peatland. High  $K_h$  values were also found near the surface at the peatland margin (Figure 3-2b), coinciding with steepest gradients and where highest water tables were most common. Beneath the high K lens and extending to the underlying clay,  $K_h$  values across the peatland were variable and ranged from  $10^{-9}$  to  $10^{-4}$   $\text{m s}^{-1}$ . These  $K_h$  values suggest that the peatland is heterogenous between depths of 0.5 and 4.75 m. Two examples of time lag tests to determine  $K_h$  are shown in Figure 3-3.

Estimates of mean and vertical hydraulic conductivity ( $K_m$  and  $K_v$ ) were calculated

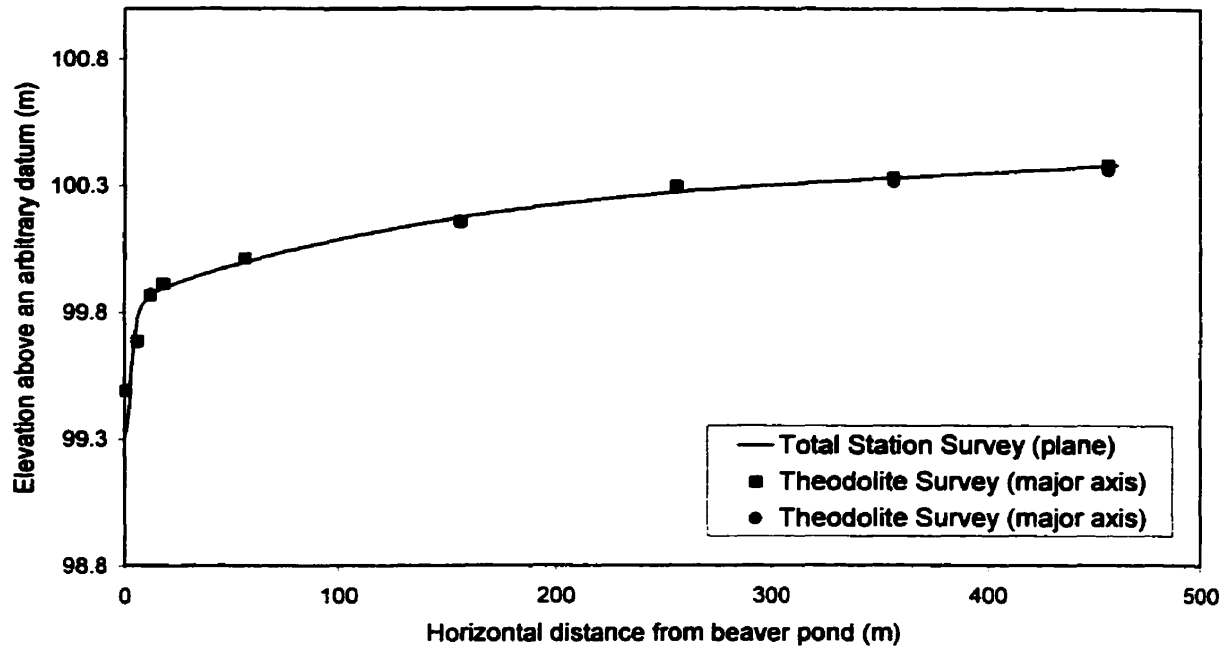


Figure 3-1. Topographic gradients observed across the major hydrologic axis after surveys with a Total Station and a Theodolite Level. Greatest elevation change occurs at the beaver pond margin (gradient = 0.022).

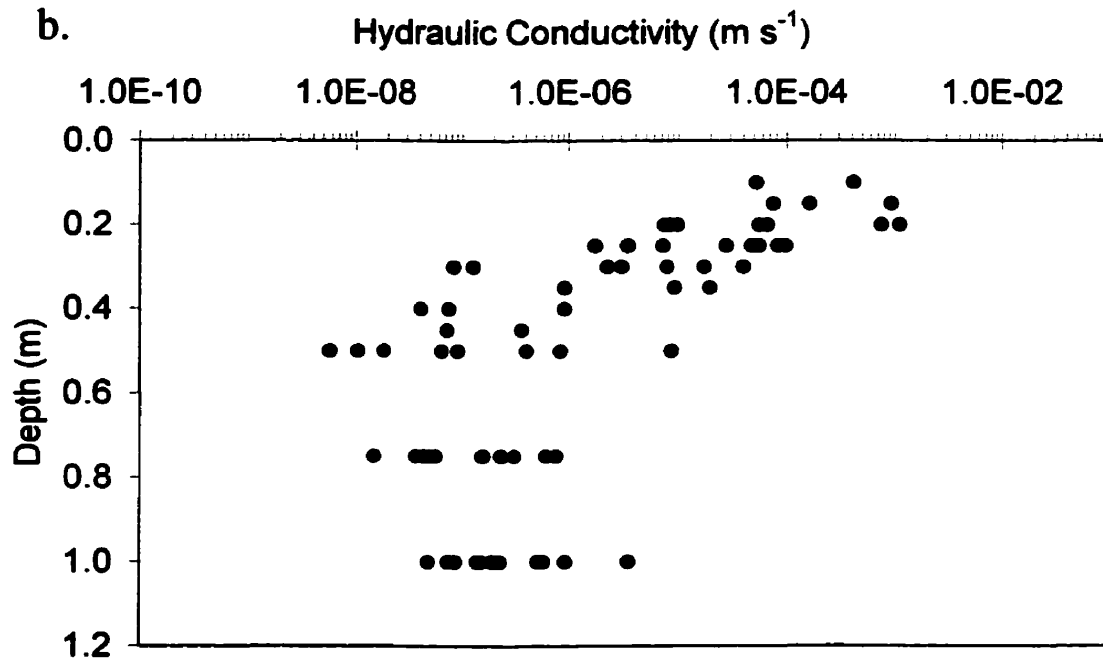
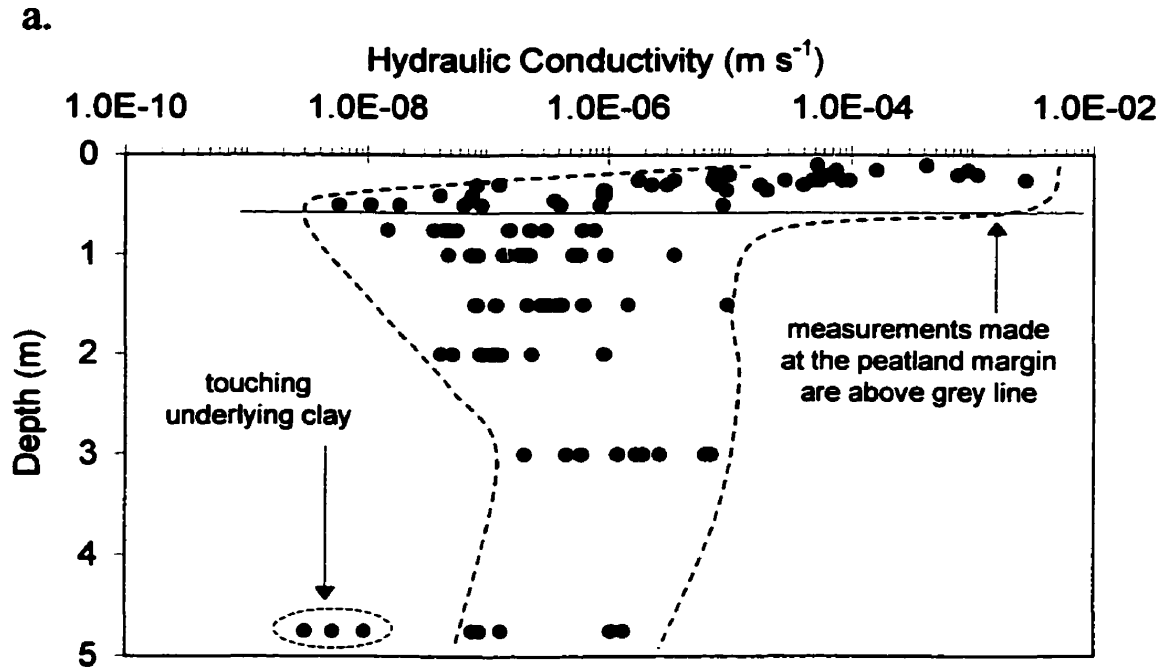


Figure 3-2a. Estimates of horizontal hydraulic conductivity ( $K_h$ ) from bail tests performed at piezometers inserted to peat after Hvorslev (1951). b.  $K_h$  values from piezometers inserted to peat at the peatland margin. All  $K_h$  values reported in  $\text{m s}^{-1}$ .

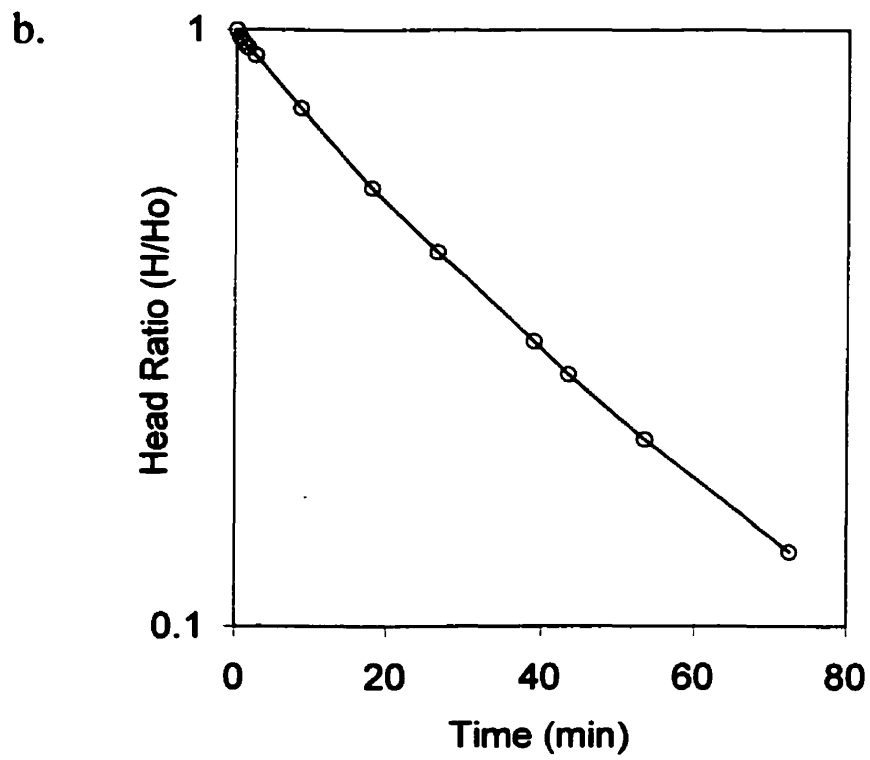
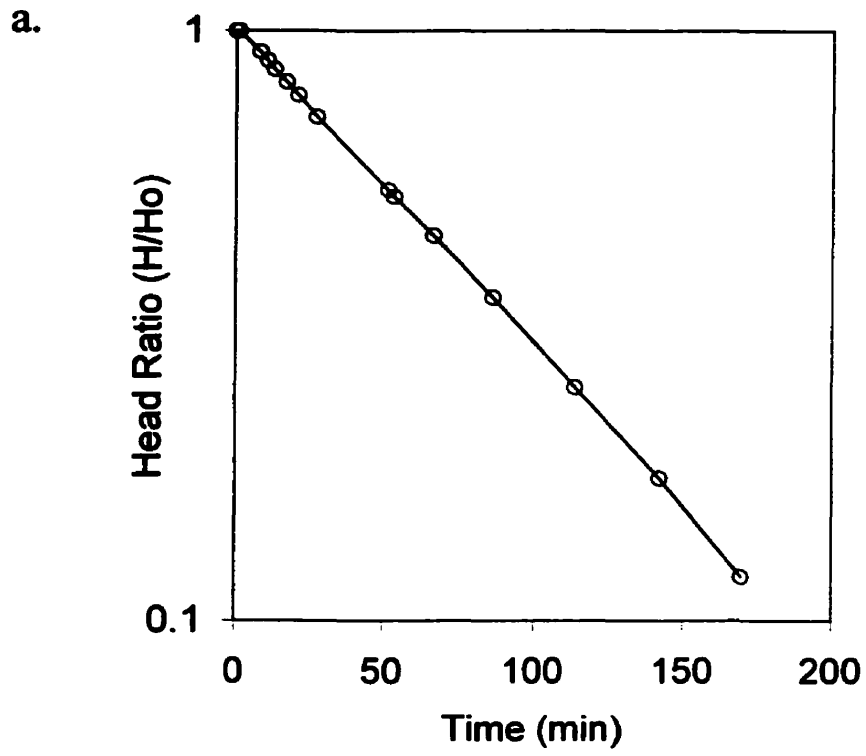


Figure 3-3. Sample time lag tests for piezometers P5 1.5 m (a) and P8 3.0 m (b) at the Mer Bleue bog.

from piezometers at two nests and results are summarized in Table 3-1. With the exception of one test,  $K_m$  values were one or more orders of magnitude lower than  $K_h$  estimates for corresponding depths, and  $K_v$  values were one or more orders of magnitude lower than  $K_m$  estimates. Thus, measurements suggest that the Mer Bleue bog is a heterogenous and anisotropic system.

The marine clay under the peatland had low  $K_h$  values. Tests on four drive-point piezometers inserted into the marine clay underlying the peatland varied between  $4.3 \times 10^{-11}$  to  $7.7 \times 10^{-10} \text{ m s}^{-1}$ . These estimates agree with  $K_h$  estimates of  $10^{-12}$  to  $10^{-9} \text{ m s}^{-1}$  for unweathered marine clay (Freeze and Cherry, 1979) and  $10^{-13}$  to  $10^{-9} \text{ m s}^{-1}$  for unweathered clay after Bear (1972). Since the underlying clay at the Mer Bleue bog is as thick as 40 m (see Chapter 2), the peat-clay interface was considered to be a no flow boundary for the purposes of this study.

Bail tests were also performed on three piezometer nests on the mineral hillslope as summarized in Appendix 2d. In general, the  $K_h$  values in the mineral soils were similar to deep peat  $K_h$  values, and  $K_h$  values in the mineral hillslope were variable with depth.  $K_h$  values do not increase near the surface as do  $K_h$  values on the peatland. Thus, groundwater contributions from the mineral hillslope are constrained by  $K$  values and were small in magnitude.

### **Section 3.2 Macro-scale hydrology and DOC export**

The runoff record for the hydrological year May 22, 1998 to May 21, 1999 as measured at the basin outflow is illustrated in Figure 3-4a. Concentrations of DOC reported in  $\text{mg C L}^{-1}$  are plotted on the same figure. The runoff record is dominated by a large snow melt event where 84 mm of runoff was measured between March 16 and April 20, 1999, and by a mid-winter melt where 34 mm of runoff was measured between January 7 and February 19, 1999. The temperature record from the tower site highlights these two melt periods (Figure 3-4b). They accounted for over 53 % of the annual runoff measured at the outflow.

Spring, summer and autumn runoff were controlled by precipitation and evaporation

Table 3-1. Comparison of  $K_h$ ,  $K_m$  and  $K_v$  estimates by depth for a piezometer nest at the peatland margin (P4) and at the peatland centre (P9). Estimates of  $K_h$  were derived using Hvorslev (1951) methods for slotted head piezometers, whereas  $K_m$  estimates were determined using methods for piezometers without slotted heads.  $K_v$  was determined from estimates of  $K_h$  and  $K_m$  (see Chapter 2.2.6).

Piezometer Depth (m)	P4			P9		
	$K_h$	$K_m$	$K_v$	$K_h$	$K_m$	$K_v$
0.5	9.13E-08	---	---	4.80E-05	---	---
0.75	6.24E-07	1.26E-08	2.54E-10	1.54E-07	3.36E-07	7.33E-07
1	1.39E-07	1.30E-07	1.21E-07	1.52E-07	6.45E-08	2.74E-08
1.5	3.29E-07	1.07E-08	3.48E-10	4.30E-07	1.24E-06	3.58E-06
2	1.34E-07	8.51E-09	5.40E-10	9.50E-08	1.95E-08	4.00E-09
3	---	---	---	1.18E-06	5.26E-08	2.34E-09
4.5	---	---	---	1.31E-06	---	---

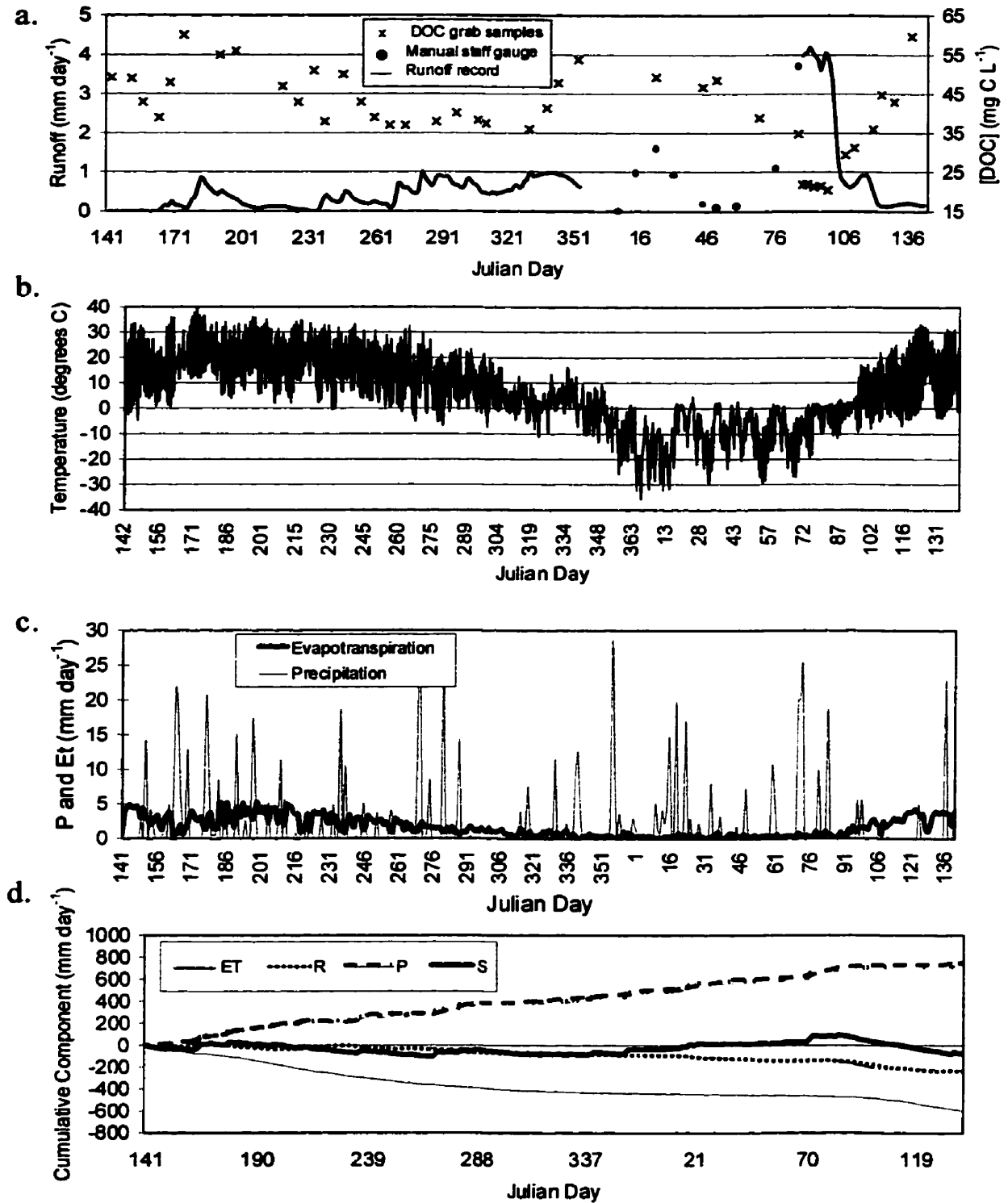


Figure 3-4. a. Runoff and DOC record as measured at the basin outflow. b. Air temperature measured at the tower site. c. Daily estimates of precipitation and evapotranspiration for the hydrological year measured at the tower site. d. Mer Bleue bog water balance plotted as cumulative functions where P is positive and R and ET are negative values. S was calculated as a residual where:  $S = P - ET - R$ .

events, and the resulting changes in basin storage. A large summer runoff peak was observed from June 14 to July 19 1998 which coincided with unusually high precipitation recorded for this period (Figure 3-4c). Climate normals for the Ottawa International Airport (Table 2-1) predict 76.9 and 88.1 mm of precipitation for the months of June and July respectively. Measured precipitation at the tower site was 119 and 85 mm for June and July 1998, where a majority of the July precipitation was recorded in the first 12 days of the month. The evaporative draw-down that occurred from July 19 (JD 200) to August 23 (235), 1998 depleted basin storage such that runoff was negligible. These records also show that the highest runoff not influenced by snowmelt occurs with normal precipitation and decreased evapotranspiration in the autumn.

Lowest DOC concentrations in runoff coincide with spring melt where the mixing of DOC rich water with low DOC melt water yields concentrations between 20 and 23 mg C L<sup>-1</sup>. Highest concentrations of DOC in runoff were observed in mid-June and in late December 1998, and ranged from 55 and 60 mg C L<sup>-1</sup>. A statistically significant inverse relationship between DOC concentrations and basin runoff was documented based on observations recorded over the hydrological year (Figure 3-5a). However, the relationship was not statistically significant after removing spring melt 1999 observations (Figure 3-5b).

By combining the discharge record, the DOC concentrations and integrating for loss of DOC over time, it was estimated that 8.3 g C m<sup>-2</sup> yr<sup>-1</sup> was exported from the Mer Bleue bog between May 22, 1998 and May 21, 1999. To assess the quality of the discharge record, Figure 3-4d plots annual estimates of the three measured hydrological components of the water balance at the Mer Bleue bog for the hydrological year. The change in storage ( $\Delta S$ ) was calculated as a residual of -66 mm based on measurements of P, ET and R of 754, 598 and 222 mm respectively. The water balance closure observed in Figure 3-4d is well within the error associated with the methods used to quantify the components ( $\leq 30\%$ ). Greatest margin of error is associated with measurements of R. Highest confidence resides in estimates of P and ET for the Mer Bleue bog based on station to station comparison of precipitation data sets and low measurement error associated with eddy-covariance techniques. Near closure of the water balance at the Mer Bleue bog based on independent measurement of the components provides assurance in the 8.3 g C m<sup>-2</sup> yr<sup>-1</sup> DOC export

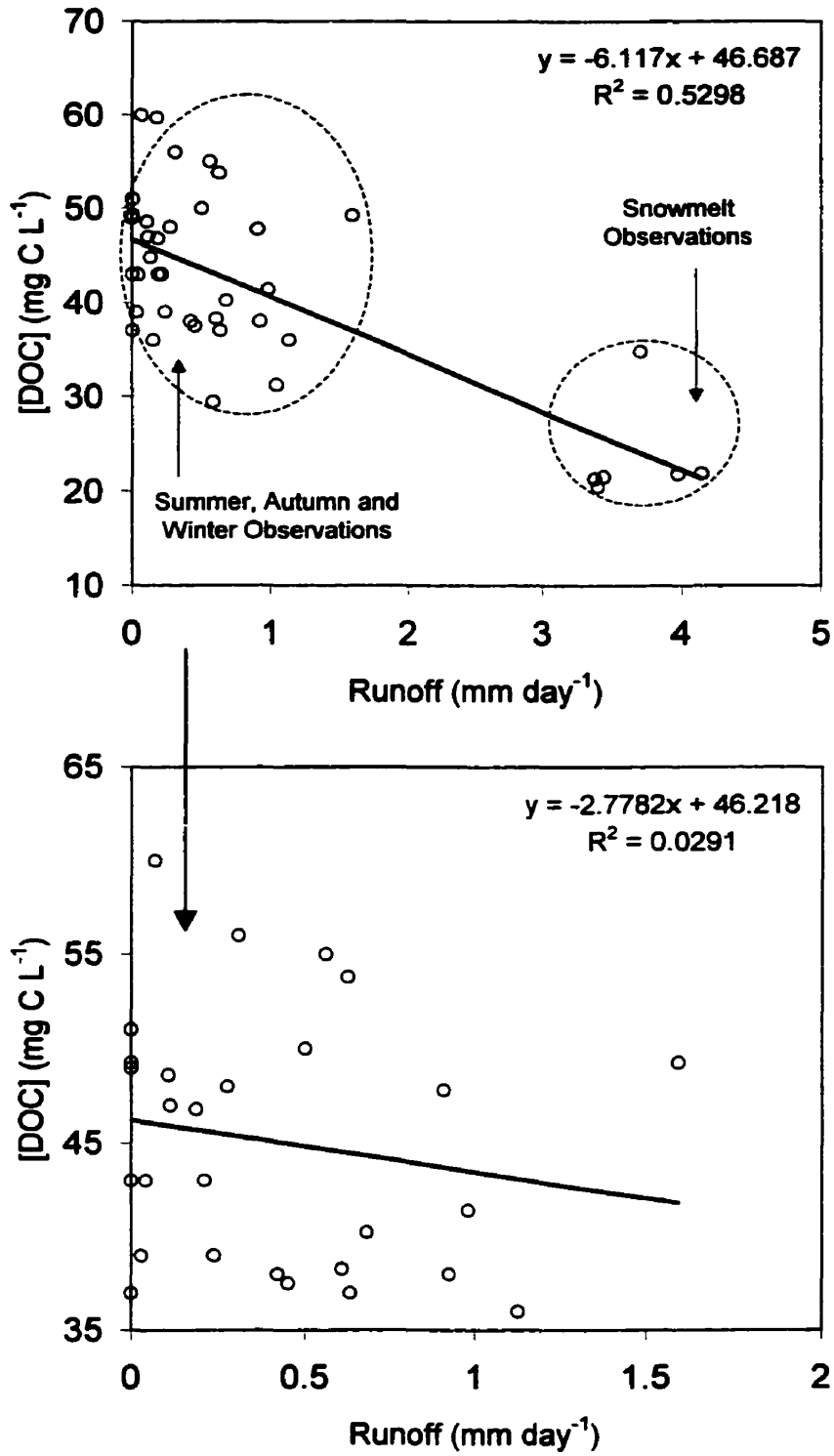


Figure 3-5a. [DOC] versus runoff regression model for 40 observations over the hydrological year. b. [DOC] versus runoff regression model for 28 observations measured during the summer, autumn and winter 1998-9 (spring melt 1999 removed).

measured at the basin outflow, but a true estimate of uncertainty is difficult to quantify.

### **Section 3.3 Groundwater hydrology and DOC export**

#### *Hydrology*

Figure 3-6a illustrates patterns of groundwater flow across the major axis of the study site (see Chapter 4 for more details). Flow reconstructions for several groundwater sampling dates and field measurements suggested a seepage face at the pond edge was likely to exist. Figure 3-6b shows a plot of hydraulic head values for all piezometers at P2 in the seepage area for the summer 1998. There is a negligible difference in heads between the depths 0.25, 0.5, 0.75, 1.0 and 1.25 m, implying that horizontal flow occurred at the seep over the sample period. The plots for stations P1, P3, P4 and P5 were the same. Figure 3-6c shows changes in water table with respect to the peat surface for the five piezometer stations at the seep for summer 1998. The gradient of the water table was determined to be less than the gradient of the peat surface, where average water table and surface gradient at the seepage face were 0.022 and 0.03 respectively.

Based on the above observations, a Dupuit-Forcheimer approximation of groundwater discharge was applied at the peatland perimeter assuming that flowlines are horizontal and equipotentials vertical, and that the slope of the hydraulic gradient was equal to the slope of the water table and invariant with depth. From a 1.0 m deep peat profile, water flux was computed for each 0.01 m layer. Discharge from each lens was quantified using hydraulic conductivity tests for seep peats, continuous records of water table and constant water table gradient.

Figure 3-7a illustrates the results of the Dupuit approximated flow scaled by a wetted perimeter estimate of the bog. A regression model and summary statistics illustrate the relationship between measured and approximated groundwater flow (Figure 3-7b). The Dupuit approximated flow was in good agreement with water yield from the runoff record, and regression statistics suggest that a seepage process adequately accounts for total amount

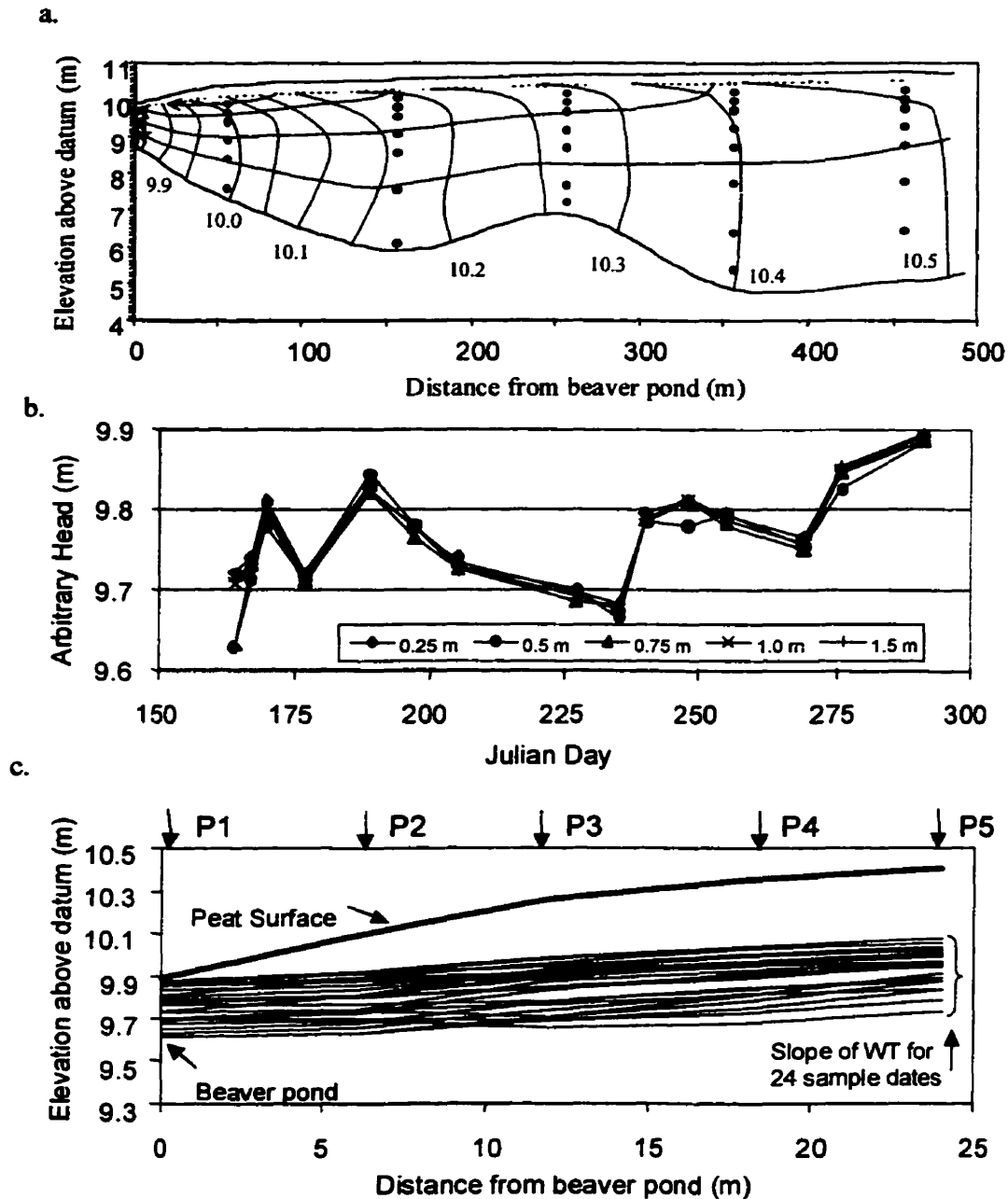


Figure 3-6. a. Cross-section of the major axis showing a groundwater flow reconstruction for August 26, 1998. Black dots denote the location of piezometers. b. Change in head for five piezometers at P2 for the 1998 spring-summer-fall period. Negligible difference in head with depth illustrates horizontal flow at the beaver pond margin. c. Water table position at the peatland margin for 24 dates over the study period.

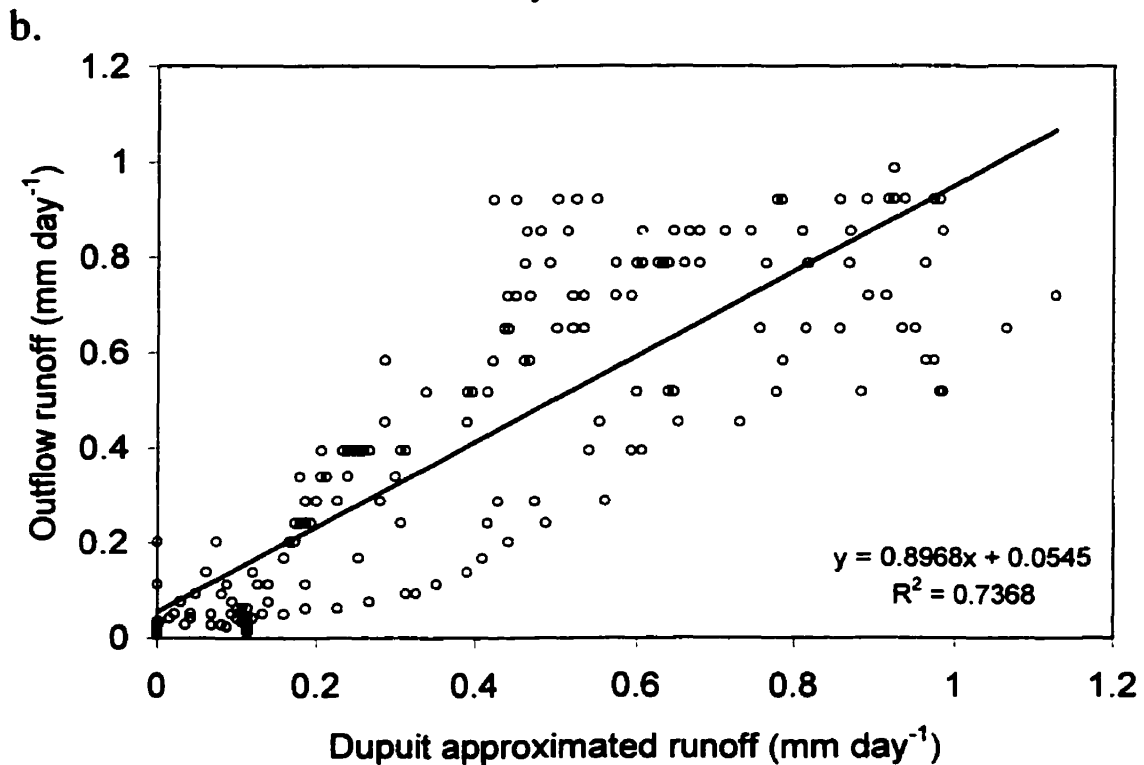
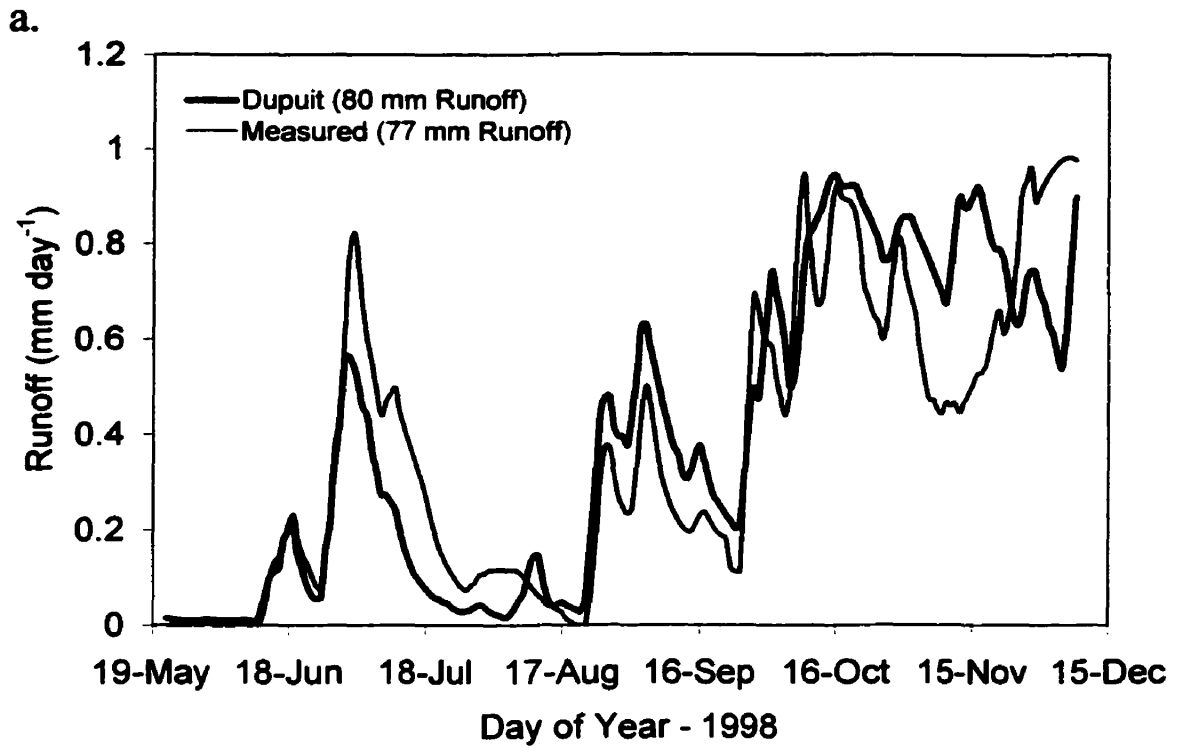


Figure 3-7a. Comparison of measured and simulated runoff from the Mer Bleue bog. The measured record runs from May 21, to December 9, 1998 at the main outflow. The simulated record was obtained using a Dupuit approximation for discharge at the peatland margin and then scaled to the same area and time interval as the outflow b. Regression model of measured vs. Dupuit approximated runoff ( $r^2=0.74$ , F-Stat = 562.6, Sg < 0.00001).

and temporal changes in discharge at the basin outflow. A best fit line through the highest  $K_n$  values by depth was used for the approximation, assuming groundwater would find the path of least resistance through the peat profile despite heterogeneity.

### *DOC Chemistry*

DOC chemistry at the peatland margin is shown in Figures 3-8 and 3-9. In general, deeper water showed less temporal variation in DOC concentration range as compared to upper profile concentration ranges over the study period (Figure 3-8). High and variable DOC concentrations near the surface are presumably the result of differential flushing, DOC production and DOC consumption. DOC concentrations of exportable water (0 to 0.45 m) decreased on some sample dates by as much as  $40 \text{ mg C L}^{-1}$  (i.e. - 90 to  $50 \text{ mg C L}^{-1}$ ) between P5 and P1 (Figure 3-9). A comparison of DOC concentrations from nest P1 and the pond near P1 illustrate the convergence of DOC concentrations at the pond-peatland interface (Figure 3-10a), thus pond concentrations were assumed to be an adequate approximation of the exported DOC from the peatland. Fluorescence ratios showed that the decrease in DOC concentration with depth occurred as the fulvic fraction of the DOC decreased (Figure 3-10b).

DOC export was calculated using the runoff record for the Dupuit approximation (Figure 3-7) and an interpolated record of DOC for the peatland margin. DOC concentrations for missing dates were interpolated based on curve fitting through the actual points measured over the simulation period. Calculations showed that a 203 day Dupuit simulation resulted in a DOC export of  $4.3 \text{ g C m}^{-2} \text{ t}^{-1}$ . As a comparison, the DOC export measured at the outflow for the same time period was  $3.3 \text{ g C m}^{-2} \text{ t}^{-1}$ .

### *DIC Export*

High concentrations of DIC were found at depth in seep peats based on measurements in spring-summer 1999 (Figure 3-11a). The presence of DIC in interstitial water presumably results from diffusion of carbonate species from the underlying marine clay sediments (see

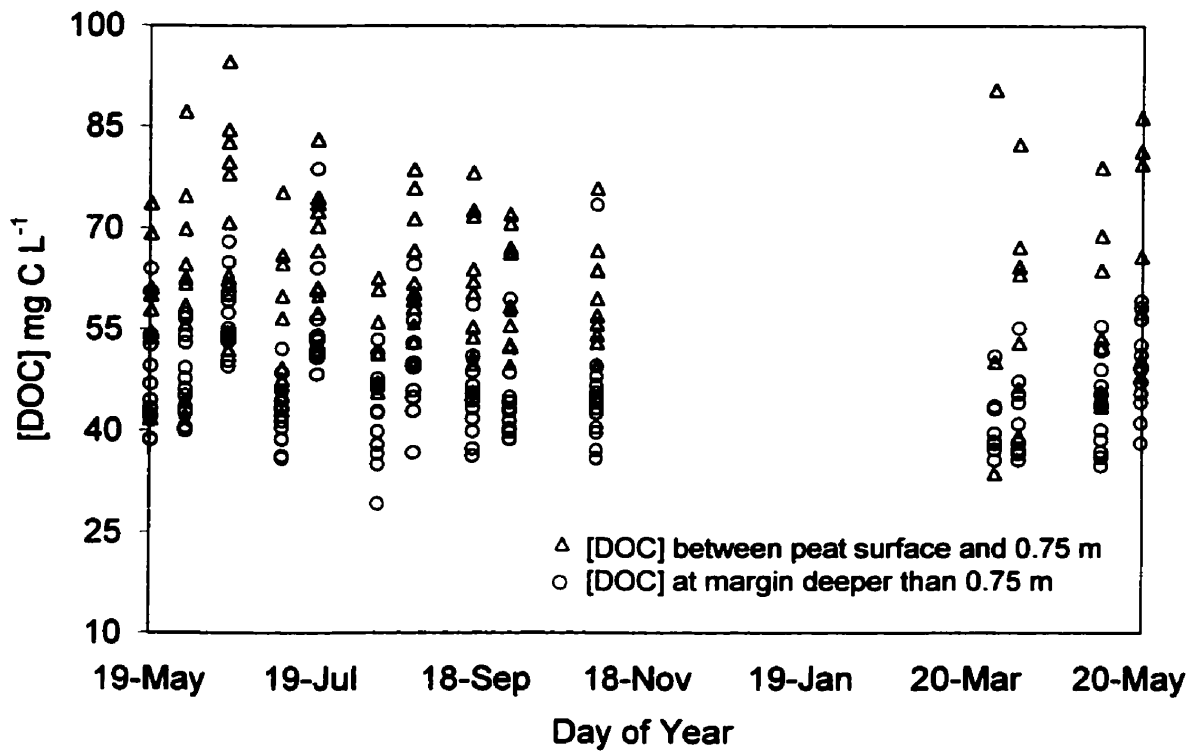


Figure 3-8. Plot of DOC concentrations in peat pore waters from piezometers at the peatland margin. Samples from the peat surface to 0.75 m are plotted with a triangle and deeper samples with a circle.

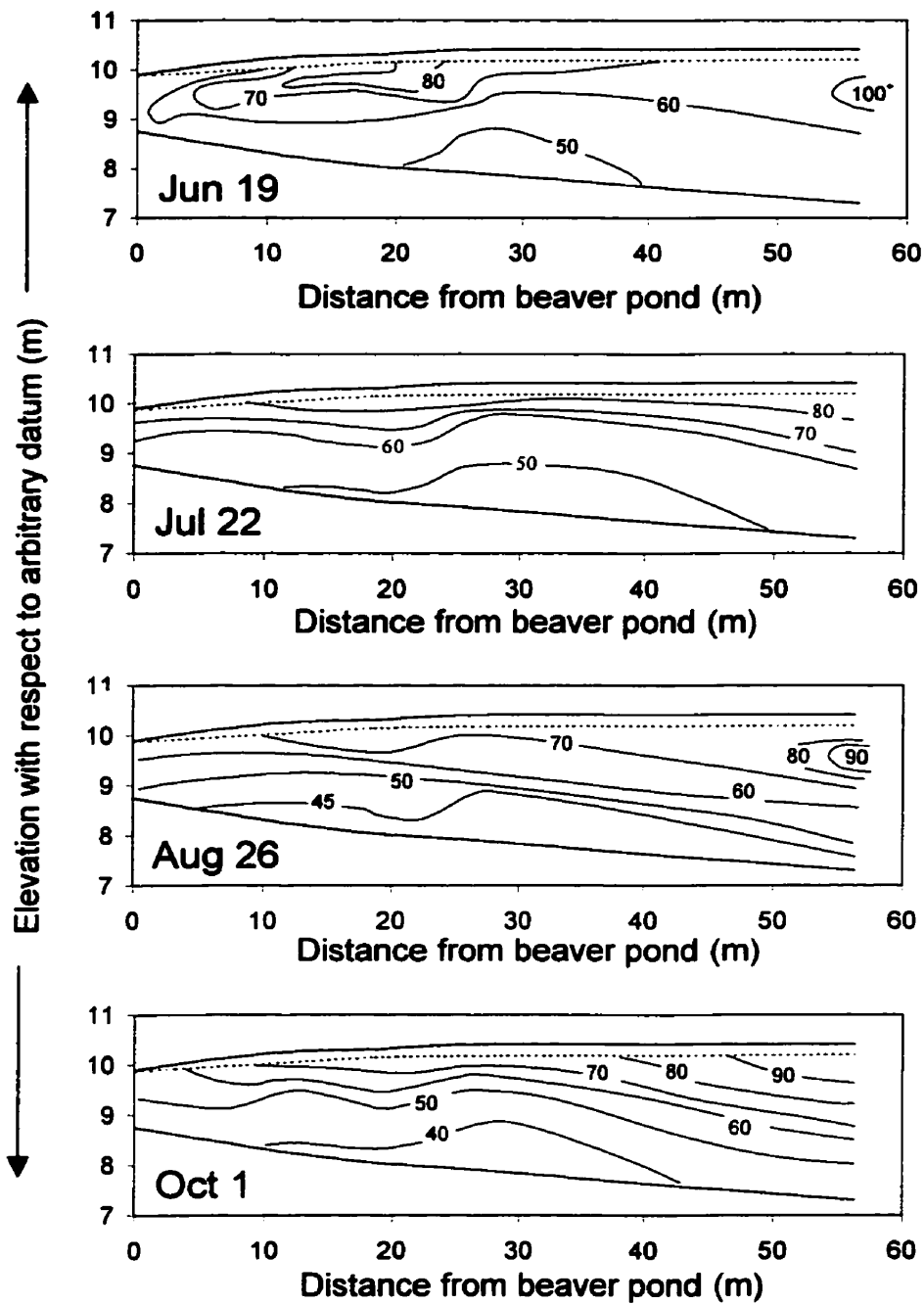
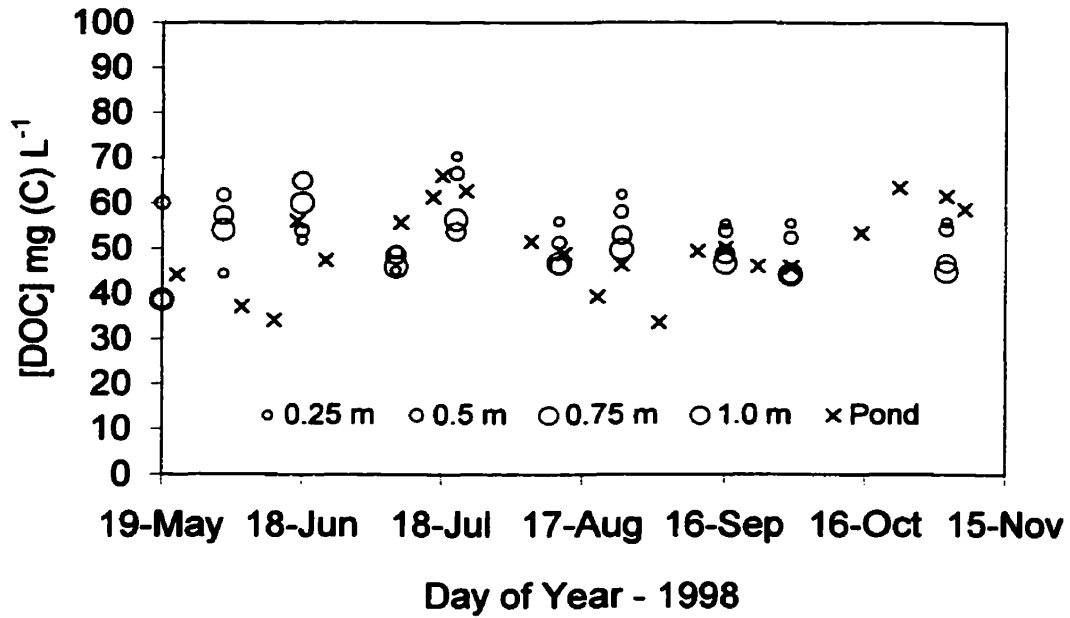


Figure 3-9. Chemoplots of [DOC] from piezometers at the peatland margin on June 19, July 22, Aug 26 and Oct 1, 1998.

a.



b.

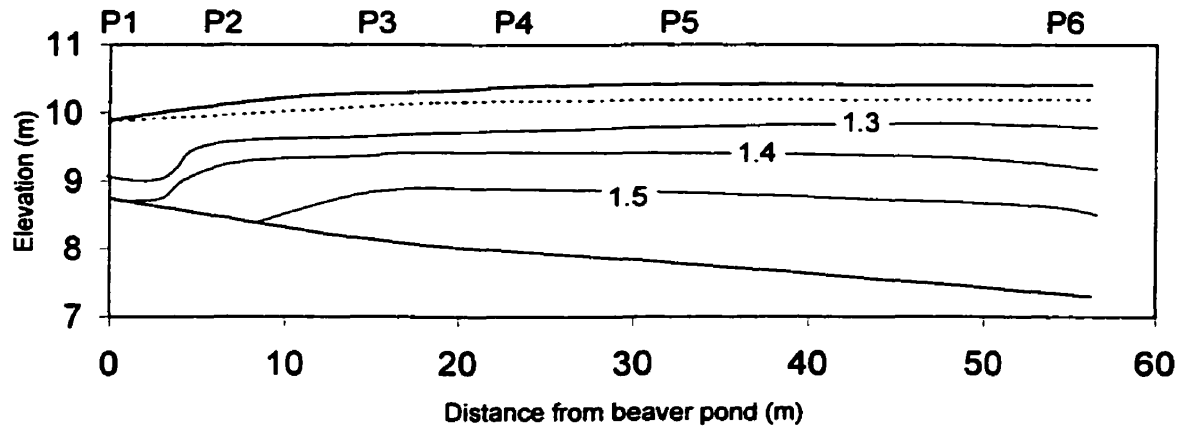


Figure 3-10. a. DOC concentrations from P1 and the pond near P1. b. Changes in the 450 nm to 500 nm fluorescence ratio across the beaver pond margin. The ratio increases with depth and decreases toward the beaver pond.

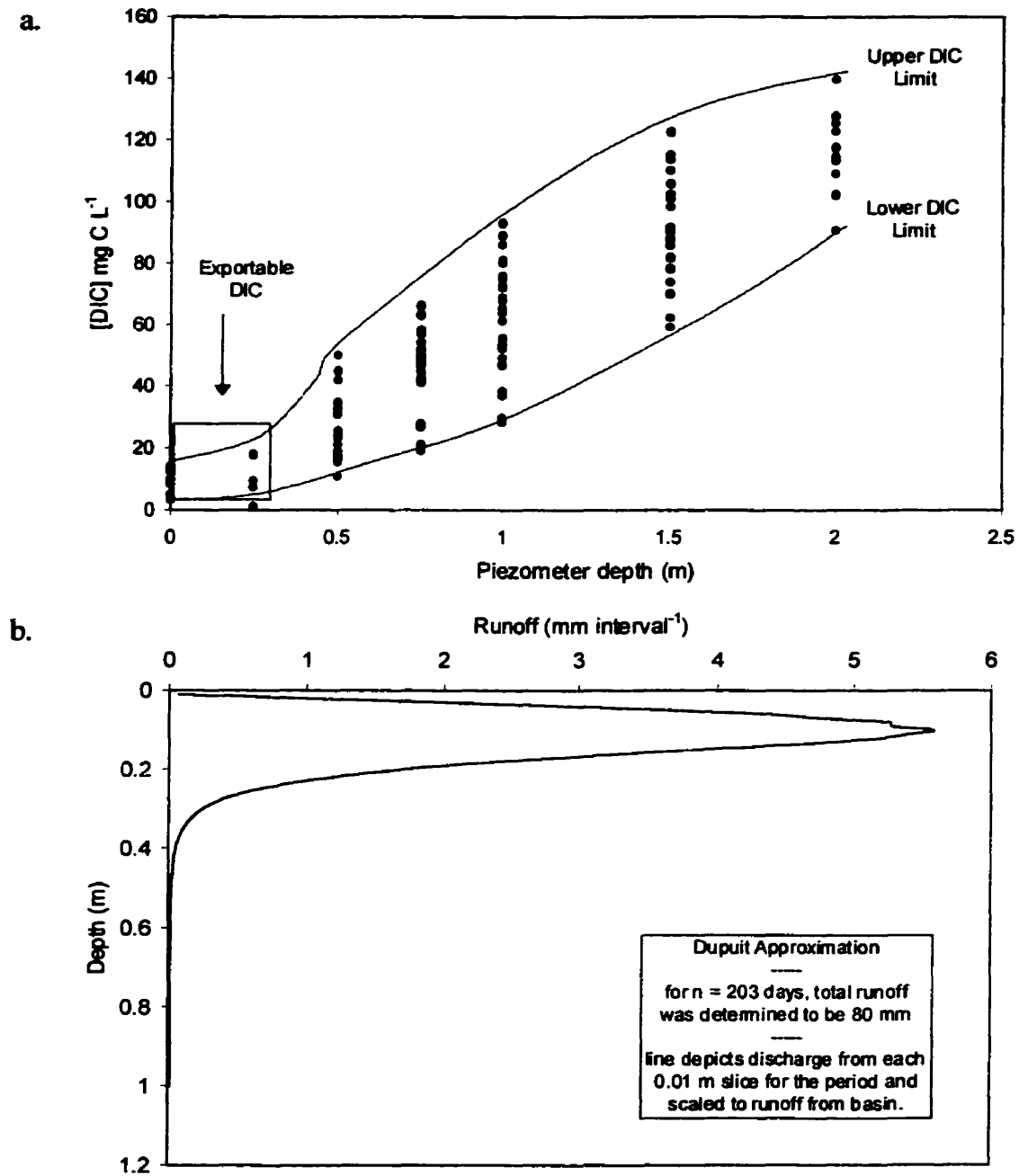


Figure 3-11. a. DIC concentrations from nests at the peatland margin. DIC concentrations decrease from depth to the surface and toward the pond margins. Exportable DIC highlighted by the box was delineated from the Dupuit approximation at the peatland margin (see Figure 3-8b). b. Summary of cumulative runoff by 0.01 m layer as estimated by Dupuit approximated groundwater discharge. Highest discharge occurs between 0 and 0.3 m depths.

Chapter 4 for more details). Concentrations of DIC decrease from  $\sim 140 \text{ mg L}^{-1}$  at depths of 2.0 m to  $\sim 10 \text{ mg L}^{-1}$  between 0.25 m and the peat surface. Dupuit simulations showed that almost all discharge occurs from 0 and 0.3 m depths (Figure 3-11b), and therefore transports the DIC store shown in Figure 3-11a. Assuming these seven sample dates adequately describe the variability of DIC with depth, a ratio of exportable DIC : DOC was calculated. Base on DIC concentrations marked by the 'Upper DIC Limit' line (Figure 3-11a), and the changes in pond DOC concentrations for the hydrological year, DIC : DOC is estimated to be 0.28-0.45. Assuming hydrological transport of DIC to be negligible during winter and snowmelt, this DIC : DOC ratio and a Dupuit approximation of runoff yields an estimated 1.5 to  $2.3 \text{ g C m}^{-2} \text{ yr}^{-1}$  loss of carbon as DIC from the Mer Bleue bog.

### **Section 3.4 Empirical modelling and DOC export**

A third approach was employed to estimate basin runoff using continuous records of water table on the peatland and exploring an outflow runoff - water table relationship for the basin. Figure 3-12 shows a regression of measured basin runoff and the water table from the tower site on the bog for the same time period as the Dupuit approximation. The adjusted  $r^2$  is 0.81 and F-Stat is 429.85 ( $p = 0.0000$ ). This is remarkable given that basin runoff was recorded more than 4 km away from the measurement of water table. Using this relationship and DOC concentrations in outflow waters,  $3.1 \text{ g C m}^{-2} \text{ t}^{-1}$  was exported as DOC, compared to  $3.3 \text{ g C m}^{-2} \text{ yr}^{-1}$  measured at the outflow. Caution should be used in interpreting this result, since the simulated runoff is a dependent function of measured runoff.

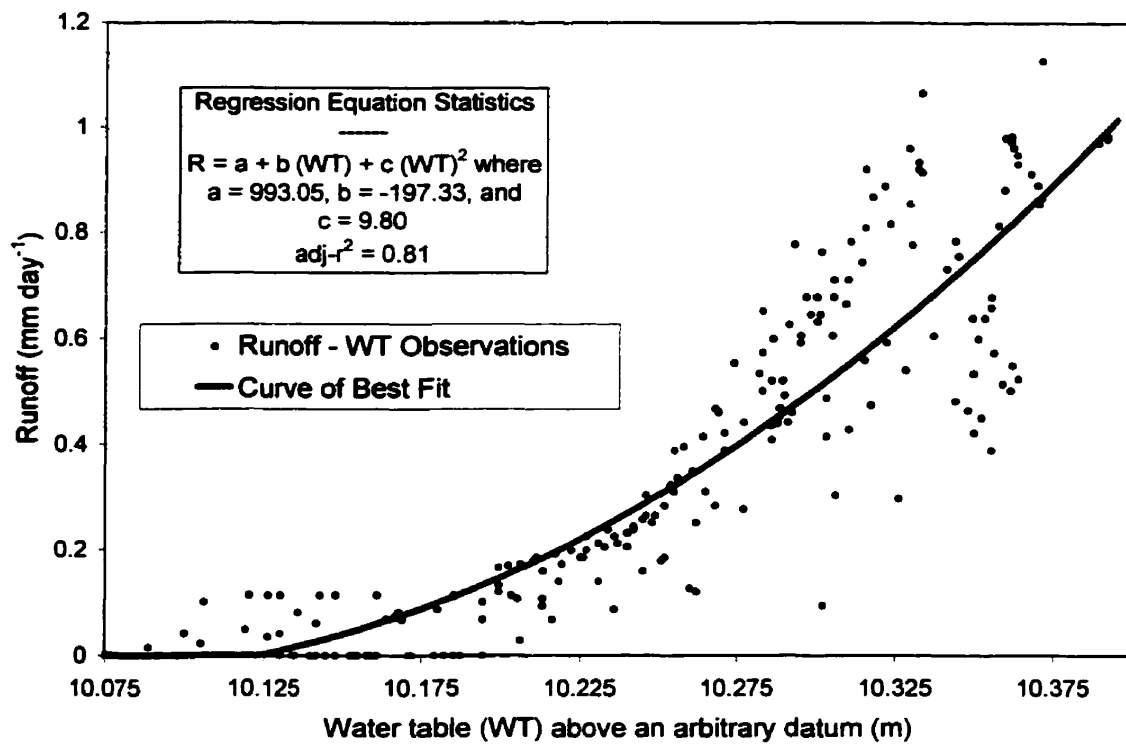


Figure 3-12. Regression of basin runoff and water table position measured at the tower site.

## **Section 3.5 Discussion of DOC export**

### **Runoff and water balance**

222 mm of runoff was measured at the basin outflow of the Mer Bleue bog, corresponding to a DOC export of  $8.3 \text{ g C m}^{-2} \text{ yr}^{-1}$ . From the agreement between runoff and load comparisons from the outflow record and the Dupuit approximation, it is concluded that seepage of groundwater can account for the production of runoff at the basin outflow. During the winter and spring seasons, runoff and load estimates can be generated from measurements at the basin outflow only, since the ground is frozen and water table cannot be measured. Closure of the water balance for the hydrological year provides added confidence in discharge and DOC export estimates.

Of the 222 mm of total runoff, over half of this water volume was associated with snow related melt processes. Measurement of this melt runoff is restricted to the basin outflow. The steep rise and fall of the hydrograph for the melt (Figure 3-4a) illustrates the likelihood of fast flow over a surface of frozen peat during the winter melt events or overland flow through inter-connected pools to the peatland margins. This was visually observed in the field and resulted in the reduction in DOC concentrations during the spring melt event from 60 to near  $20 \text{ mg L}^{-1}$  as the DOC stored in the beaver pond mixed with low DOC snowmelt water. Snowmelt water had a DOC concentration of 3 to  $8 \text{ mg L}^{-1}$ . A pond at the peatland margin being 1 m deep and 10 m wide, provides a 15 mm water reservoir that mixes with 84 mm of melt waters. This dilution can account for the decrease in DOC concentrations observed during the snowmelt period, and emphasizes the importance of winter measurements in estimating biogeochemical budgets.

### **DOC export**

The measured export of DOC from the Mer Bleue bog is similar to export estimates from other studies (refer to Table 1-1 in Chapter 1). The  $8.3 \text{ g C m}^{-2} \text{ yr}^{-1}$  is slightly larger than estimates from subarctic peatlands (Moore, 1987) and a mid-latitude fen (Carroll and Crill,

1997), but similar to estimates from a forested wetland (Moore, 1989), and upland peat complex (Scott et al., 1998). However, the DOC export estimate from the Mer Bleue bog is smaller than estimates from a swamp (Mulholland, 1981), boreal catchments (Naiman, 1982), New Zealand wetlands (Collier et al., 1989; Moore and Jackson, 1989), mid-latitude wetlands (Urban et al., 1989; Dalva and Moore, 1991) and a 'typical' northern peatland (Gorham, 1995). DOC export estimates from these latter 7 studies are as high as  $48.4 \text{ g C m}^{-2} \text{ yr}^{-1}$ .

The comparisons above are based on the assumption that the single year observations obtained in the present study are representative of the runoff and DOC export at the Mer Bleue bog. Climate normals tabulated from the Ottawa International Airport predict normal rainfall and snowfall for the region to be 702 and 208 mm respectively. In this study, 780 mm of precipitation was measured in which 254 mm of the sum was measured as snowfall and rainfall through the winter. Thus, the study period had 130 mm less precipitation than normal. Assuming the catchment is in steady state with respect to  $\Delta S$ , what range of DOC export values might this precipitation difference account for? If 130 mm of precipitation contributed solely to discharge from large storms in the summer or fall when DOC concentrations can be as high as  $55 \text{ mg L}^{-1}$ , 130 mm could translate into an additional  $7 \text{ g C m}^{-2} \text{ yr}^{-1}$ . However, if the precipitation was stored as snow and exported under fast flow conditions in which concentrations of DOC were as low as  $20 \text{ mg L}^{-1}$ , an additional  $2.5 \text{ g C m}^{-2} \text{ yr}^{-1}$  of DOC could be exported. This range illustrates that the timing of precipitation relative to the supply of DOC is a critical control on DOC export, and that the difference between precipitation and evapotranspiration constrains DOC export. This would suggest that DOC export in a 'normal' year at the Mer Bleue could range from 11 to  $16 \text{ g C m}^{-2} \text{ yr}^{-1}$ . Even when considering 100 mm of precipitation in excess of normal and high concentrations of DOC ( $55 \text{ mg L}^{-1}$ ) for an entire year, export of DOC at the Mer Bleue bog would not exceed that of a 'typical' peatland ( $20 \text{ g C m}^{-2} \text{ yr}^{-1}$ ) after Gorham (1991). Uncertainty associated with the magnitude of ET for different precipitation/export scenarios at the Mer Bleue bog makes the export estimates conjectural only.

## **Seepage and discharge comparison**

Assuming the discharge and DOC load predicted by the Dupuit approximation is correct, there is a slight discrepancy between measurements at the basin outflow and at the seepage face. Whether the approximation is correct depends strongly on K values and profile heterogeneity, but the Dupuit approximation appears to produce plausible discharge results based on the high correlation between measured and simulated records ( $r = 0.86$ ) and similar total discharge (measured = 77 mm; simulated = 80 mm). However, the difference between DOC export estimated at the outflow and seepage is 25 %. Given the variability of K, this difference is not surprising, but it is also possible that DOC is transformed over the 4, 900 m path of the beaver ponds along the margin of the peatland.

Figure 3-13 illustrates the similarities and differences in DOC concentrations observed at the outflow and from the pond near piezometer nest P1. For measurements made in the spring and during snowmelt there is good agreement between the two grab sample records. However, from July 9 (JD 190), to December 16 (350), 1998, concentrations of DOC measured in the pond were typically 5 to 20 mg L<sup>-1</sup> higher than those at the outflow. The dates where pond concentrations were found to be higher than outflow concentrations accounted for 150 of the 203 days in which the Dupuit approximation was employed. Using higher DOC concentrations with similar runoff values explains the 1.0 g C m<sup>-2</sup> r<sup>-1</sup> discrepancy between Dupuit and outflow DOC yields.

Assuming the discrepancy in DOC concentrations is real, processes of photo-degradation, methanogenesis, consumption and sedimentation along the pond network could account for the decrease in DOC concentrations along the path-length to the outflow. Alternatively, hillslope contributions from upland areas may dilute the pond margins by contributing low concentration DOC water. The upland mineral soils have low K values and small area (< 18 % of area), but this cannot exclude the role of uplands in contributing DOC to the pond system. The decrease in DOC concentrations could also occur where the peatland changes to fen-like and marsh-like wetland features closer to the basin outflow, and impact exportable DOC concentrations. If the outflow record under-estimates the export of DOC due

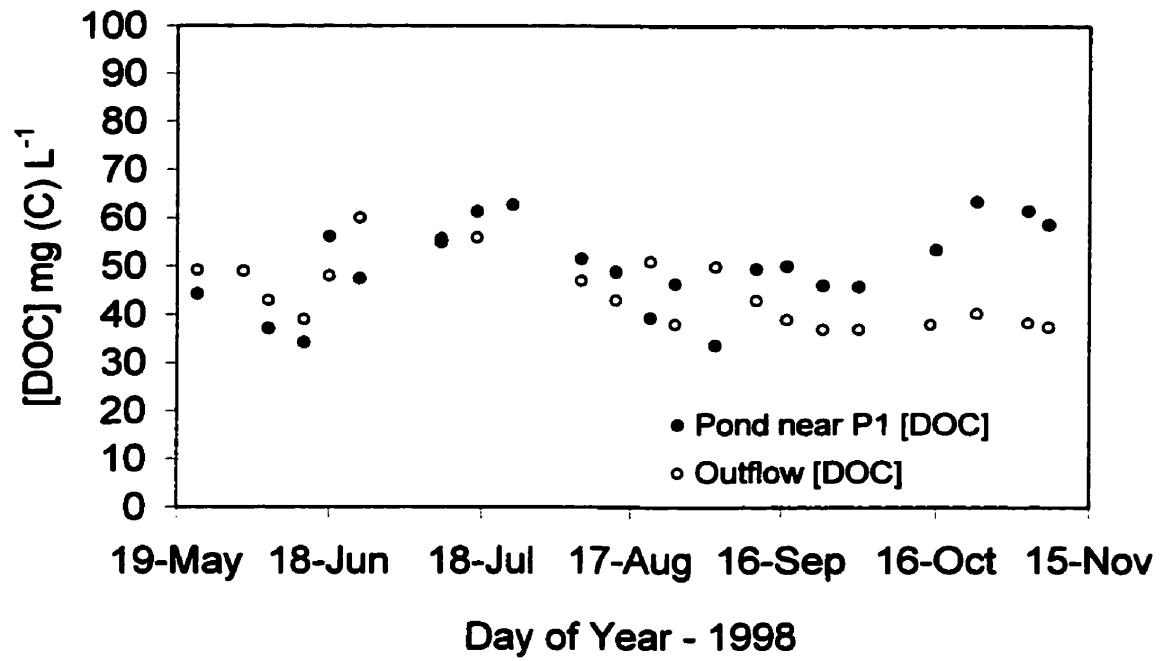


Figure 3-13. Comparison of DOC grab samples taken at the basin outflow and from the beaver pond near piezometer nest P1.

to a transformation of DOC over path-length, the under-estimate is small. At the very most, DOC export from the Mer Bleue bog for this study period would be 9-10 g C m<sup>-2</sup> yr<sup>-1</sup>.

### **Role of DOC export in the peatland C budget**

NEE measured at the Mer Bleue bog (Jun 1, 1998 to May 31, 1999) was 82 g C m<sup>-2</sup> yr<sup>-1</sup> (Roulet et al., in prep). Thus, DOC export (8.3 g C m<sup>-2</sup> yr<sup>-1</sup>) was 10% of the NEE sink. Reported values for [DOC] in precipitation are 1-3 mg L<sup>-1</sup> (Thurman, 1985; Moore, 1997). Using measured annual precipitation (754 mm), it was estimated that DOC flux to the peatland as precipitation was 1-2 g C m<sup>-2</sup> yr<sup>-1</sup>. Tallying annual NEE (+82), DOC export (-8), DOC in precipitation (+2) and DIC export (-2), the resultant carbon sink (74 g C m<sup>-2</sup> yr<sup>-1</sup>) is large compared to paleo- and contemporary studies of carbon sequestration in peatlands (see Chapter 1 for a summary). Long term carbon sequestration at the Mer Bleue bog determined from peat cores has been estimated to be 20 to 30 g C m<sup>-2</sup> yr<sup>-1</sup> (Pierre Richard, pers. comm.). Therefore, the carbon sink was 2 to 3 times larger than rates of long term sequestration. The measured DOC export was 28 to 42% of the long term sink.

## **Chapter 4 - Groundwater flow patterns and geochemistry**

Concurrent with the measurements made to quantify dissolved carbon export from the Mer Bleue bog, the spatial and temporal patterns of groundwater flow and chemistry were evaluated. Using head measurements and pore water chemistry from piezometer nests on the major and minor axes, the main objectives were to isolate the controls on groundwater flow patterns and determine the role of groundwater flow patterns in the maintenance of peatland chemistry. This chapter is divided into five sections. The sections are: groundwater flow patterns and chemistry (Section 4.1); geochemistry and peatland recharge-discharge function (Section 4.2); P and ET controls on groundwater flow patterns (Section 4.3); the characterization of a groundwater flow reversal (Section 4.4); and changes in peatland chemistry linked to the flow reversal (Section 4.5). The chapter concludes with a discussion of the major findings.

General patterns of groundwater flow and chemistry are discussed using data from August 26, 1998 (Figures 4-1 and 4-2). Groundwater chemistry for this date (Figure 4-2) was typical of chemistry for all sampling dates. The recharge pattern of groundwater flow (Figure 4-1) was the most common pattern of groundwater flow at the Mer Bleue bog, but variations to the flow patterns were observed. Construction of 12 flownets from head measurements made over the hydrological year revealed that discharge flow patterns occurred during a 40 day groundwater reversal. Emphasis is on recharge conditions in Sections 4.1 to 4.3, whereas discharge patterns are the emphasized in Section 4.4.

### **Section 4.1 Groundwater flow patterns at the Mer Bleue bog**

A flownet across the major axis at the Mer Bleue bog is shown in Figure 4-1. Head decreased from the centre of the peat dome to the pond margin. Vertical hydraulic gradients showed recharge conditions on the peatland (P6 to P10, RA1 to RA4) and values ranged from 0.01 to 0.017. Horizontal gradients on this main portion of the peatland ranged from 0.0012 to 0.0016, yielding a ratio of vertical to horizontal gradients of 10:1. Vertical

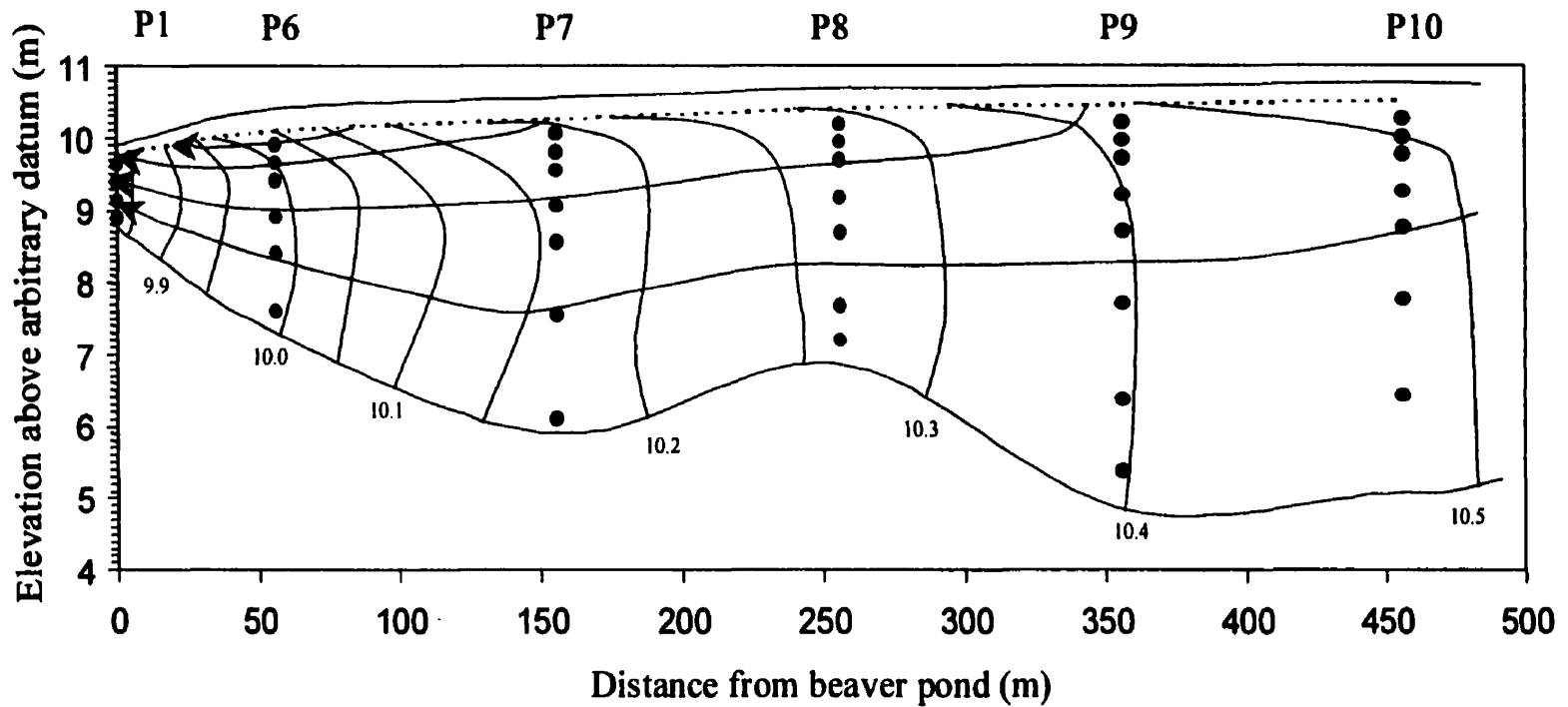


Figure 4-1. Generalized flownet depicting groundwater flow patterns across the major axis. The flownet was constructed from head measurements made August 26, 1998 and illustrates recharge conditions across the axis.

Figure 4-2. Baseline groundwater data collected August 26, 1998. a. Spatial changes in DOC concentrations. b. Spatial changes in carbon specific fluorescence (CSF) ratio. c. Patterns of pore water temperature across the major axis. d. Changes in electrical conductivity across the major axis. All isopleths were drawn based on measurements made at the piezometers illustrated in Figure 4-1.

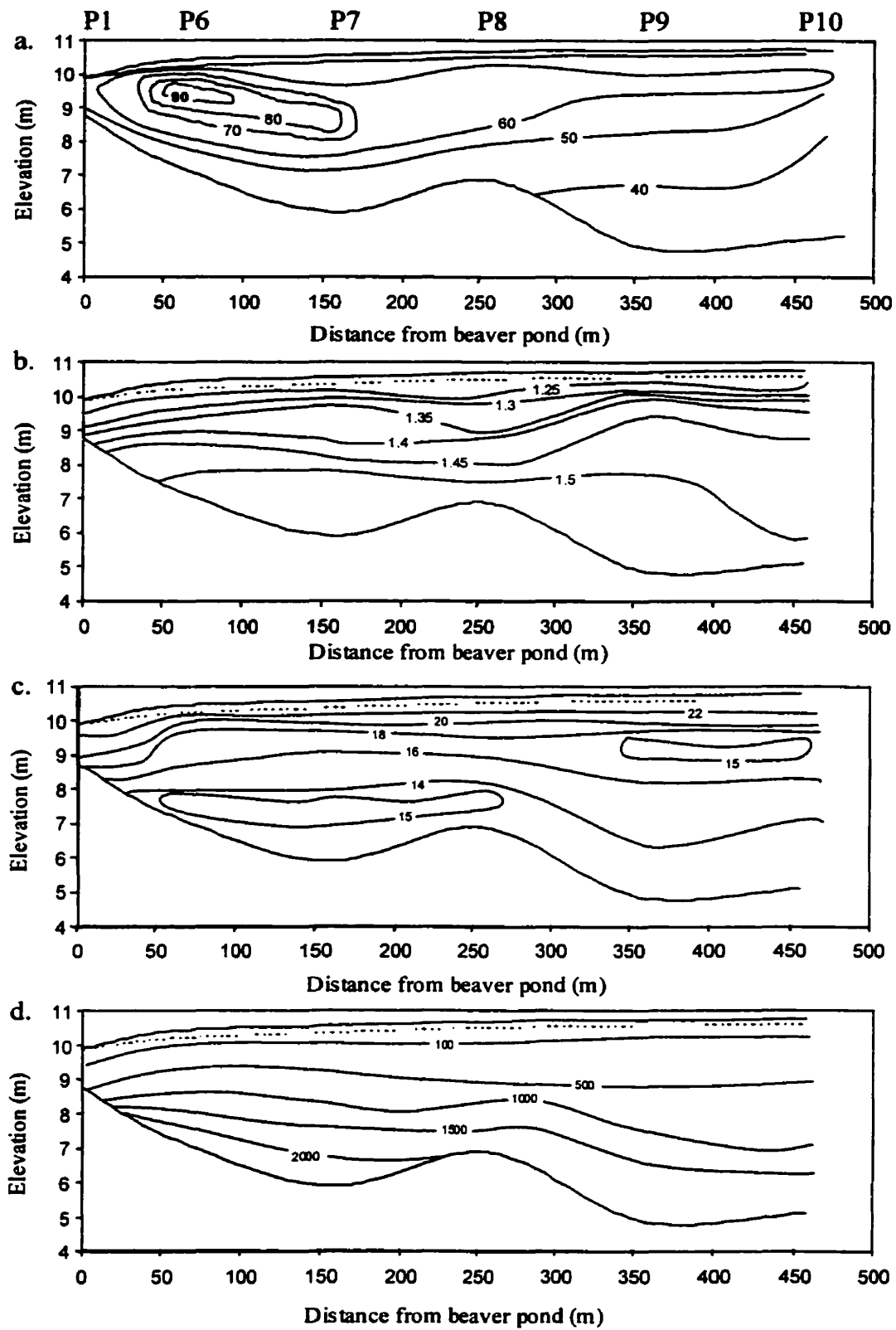


Figure 4-2. See figure caption on Figure 4-1 following p. 36.

gradients at the peatland margin were negligible, but the horizontal gradients were greater than those on the peatland. Therefore discharge at the margin was always horizontal (see Chapter 3 for details). Hydraulic conductivity calculations showed that  $K_v$  estimates were 1-2 orders of magnitude less than  $K_h$  estimates (see Chapter 3 for details). Thus, system anisotropy affects groundwater flow at the Mer Bleue bog. Flownets were plotted with vertical exaggeration of 23 (Figures 4-1 and 4-11), and were scaled as such to account for the difference in  $K_v$  versus  $K_h$  for the Mer Bleue bog.

Spatial patterns of DOC concentration, DOC quality, groundwater temperature and electrical conductivity for August 26, 1998 are illustrated in Figure 4-2 (a-d). In general, DOC concentrations are greatest at the surface and decrease with depth (Figure 4-2a). However, highest DOC concentrations were observed at shallow depths near P6, where groundwater convergence occurs in Figure 4-1. Fluorescence ratio increased with peat depth (Figure 4-2b) suggesting that the fulvic fraction of DOC decreased with depth. Temperature (Figure 4-2c) and electrical conductivity measurements (Figure 4-2d) did not reveal a source of deep groundwater to the peatland.

Maximum head observations from drive-point piezometers in the clay substrate beneath the peatland are compared to average, minimum and maximum water table position in Figure 4-3. With the exception of DP4, water table position and head measurements from piezometers across the peatland were greater in the peat than in the underlying marine clay. Maximum head measurement at DP4 was equal to the average water table position in the peatland, and suggests that discharge from the marine clay to the peatland is possible under certain hydrological conditions. However, the  $K$  values of the clay are  $10^{-10}$  to  $10^{-11}$   $\text{m s}^{-1}$ , and groundwater contribution to the peatland through the marine clay would be negligible. DOC and electrical conductivity samples taken from drive-point piezometers ranged from 31-77  $\text{mg L}^{-1}$  and 3657-4527  $\mu\text{S}$  respectively (Table 4-1). The dramatic differences between electrical conductivities and DOC concentrations across the peat-marine clay interface (see Figure 4-2 and Table 4-1) suggest the exchange of regional groundwater is negligible.

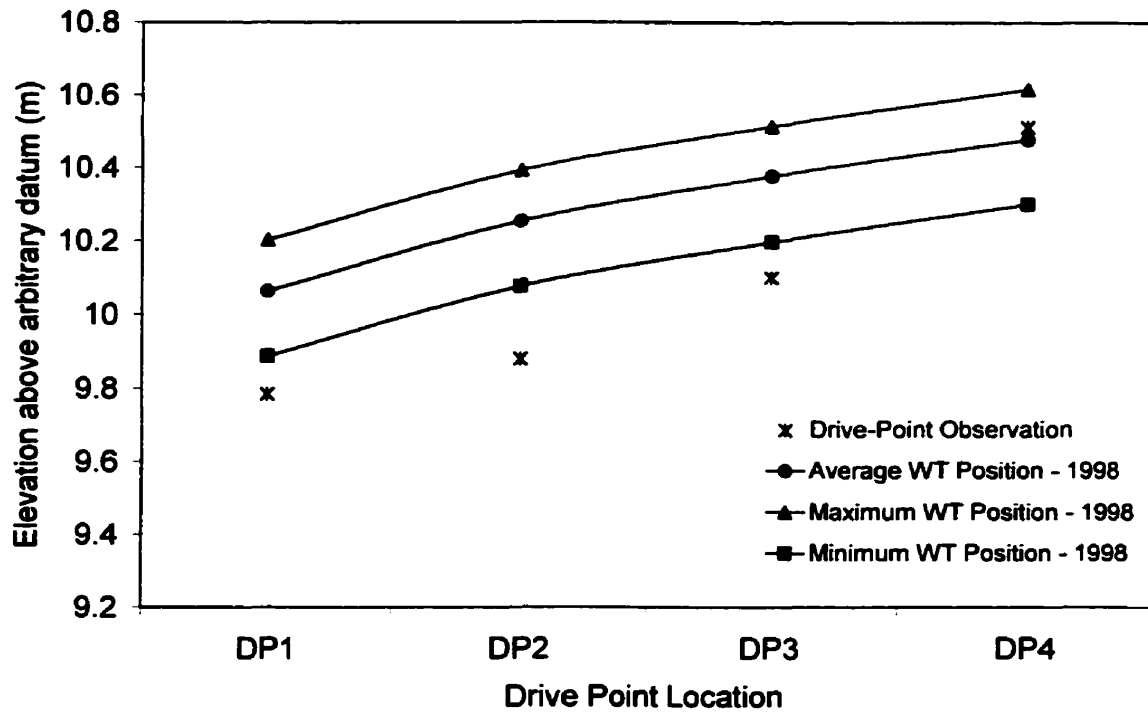


Figure 4-3. Elevation of maximum drive-point piezometer head with respect to mean, minimum and maximum water table position in the peatland. Head values in the marine clay were lower than all water table observations at nests DP1, DP2 and DP3. Head at DP4 recharged near mean water position of the peatland (refer to Figure 2-2 for drive-point piezometer location).

**Table 4-1. Summary of DOC and electrical conductivity measurements from drive-point piezometers at the Mer Bleue bog. DOC values are reported in mg C L<sup>-1</sup> and electrical conductivity values are reported in  $\mu\text{S cm}^{-1}$ .**

a)		[DOC] mg C L <sup>-1</sup>			
Sample Date	DP1	DP2	DP3	DP4	
10-Jul	57	68.7	—	35.2	
24-Jul	60.3	68.6	87.7	30.1	
14-Aug	45.1	86.5	74.4	23.8	
3-Sep	—	70.6	57.2	34.4	
3-Nov	36.8	—	—	43.7	
Mean	44.6	73.6	73.1	33.4	
Standard Deviation	10.9	8.6	15.3	7.3	
CV (%)	24.3	11.7	4.1	16.9	

b)		Conductivity ( $\mu\text{S cm}^{-1}$ )			
Sample Date	DP1	DP2	DP3	DP4	
24-Jul	4335	3595	3055	—	
14-Aug	4804	3814	3644	3284	
3-Sep	4470	4090	3760	3650	
3-Nov	4501	4171	4171	4501	
Mean	4527.5	3917.5	3657.5	3811.7	
Standard Deviation	197.9	263.8	460.9	624.4	
CV (%)	4.4	6.7	12.6	16.4	

## Section 4.2 Geochemistry and the recharge-discharge function of the Mer Bleue bog

Geochemistry of pore water samples from August 26, 1998, was used to evaluate the recharge-discharge function of the Mer Bleue bog. End member mixing was illustrated by concentration-depth profiles (Figure 4-4a). The marine clay was a source of cations to the peatland, which then mixed with precipitation to yield the concentration-depth profiles. Regressing Na and Mg yielded a high  $r^2$  (0.97) and showed that the species were conservative (Figure 4-4b). However, the lower  $r^2$  (0.85) calculated by regressing Na and Ca (Figure 4-4b), and the scatter of Ca observations near the peat surface (Figure 4-4a) suggested that Ca was not conservative. Output scenarios from a simple diffusion model were compared to observed concentrations at piezometer nests (see Section 1.6 for model details) assuming that the spatial patterns of peatland salinity are controlled by a diffusion process from the underlying marine clay. Scenarios in which the observed concentration profile was less than that predicted by the model for a given time interval, indicate flushing of the profile by a precipitation-recharge processes. In contrast, profiles with concentrations that are greater than those predicted by the diffusion model imply an upward discharge of solutes in excess of the rate of natural diffusion - i.e. groundwater discharge.

Recharge-discharge scenarios for nest RA2 are illustrated in Figure 4-5. Observed  $\text{Na}^+$  concentrations were lower than predicted concentrations for 1000, 2000 and 5000 year simulations using an effective coefficient of molecular diffusion ( $D^*$ ) of  $2.0 \times 10^{-9} \text{ m}^2 \text{ s}^{-1}$  (Figure 4-5a). Therefore, over time scales that rule out seasonal or decadal variations in chemistry, geochemical indicators show that a recharge process by low concentration precipitation yields a flushing of peat pore waters from the expected to the observed concentrations. The effect of changing  $D^*$  by  $\pm 30\%$  in diffusion scenarios is illustrated in Figure 4-5b for 2000 year diffusion runs. Output scenarios for all nests at the Mer Bleue bog showed a long-term recharge signal in diffusion scenarios.

The elapsed time required to obtain a best fit diffusion solution to the observed  $\text{Na}^+$  observations was also calculated. Regression of the elapsed time and peat depth (Figure 4-6) had an  $r^2$  value of 0.98. This result should be interpreted with caution as depth is not

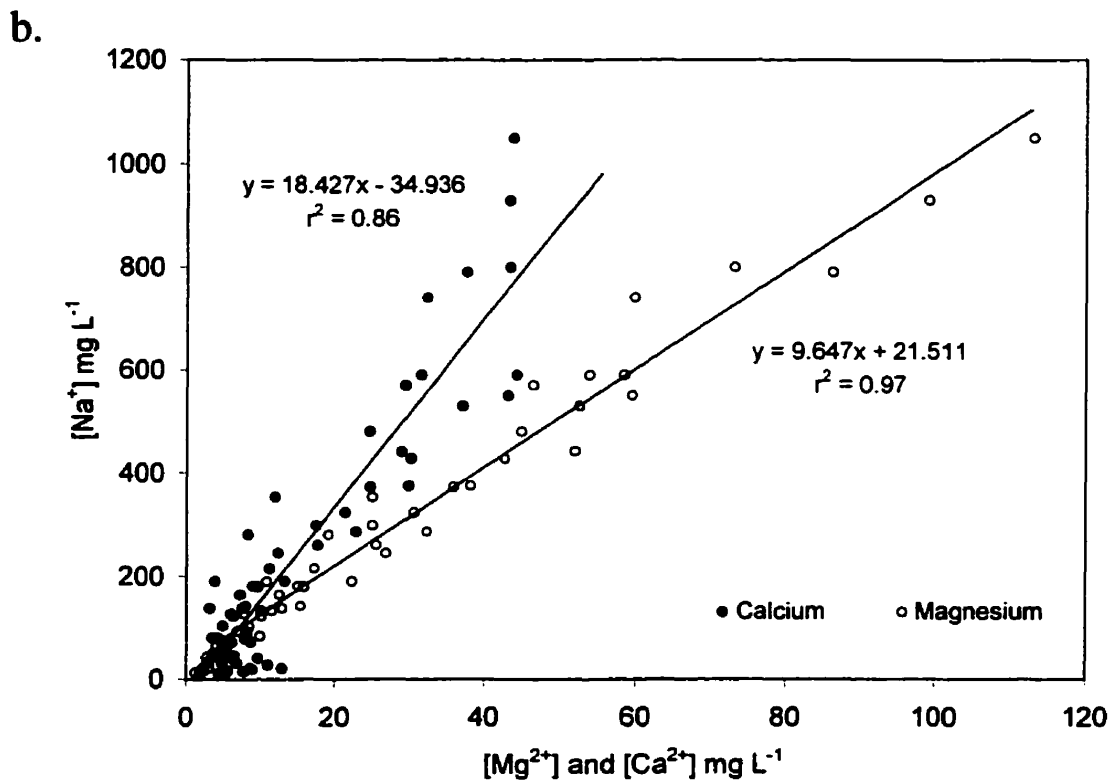
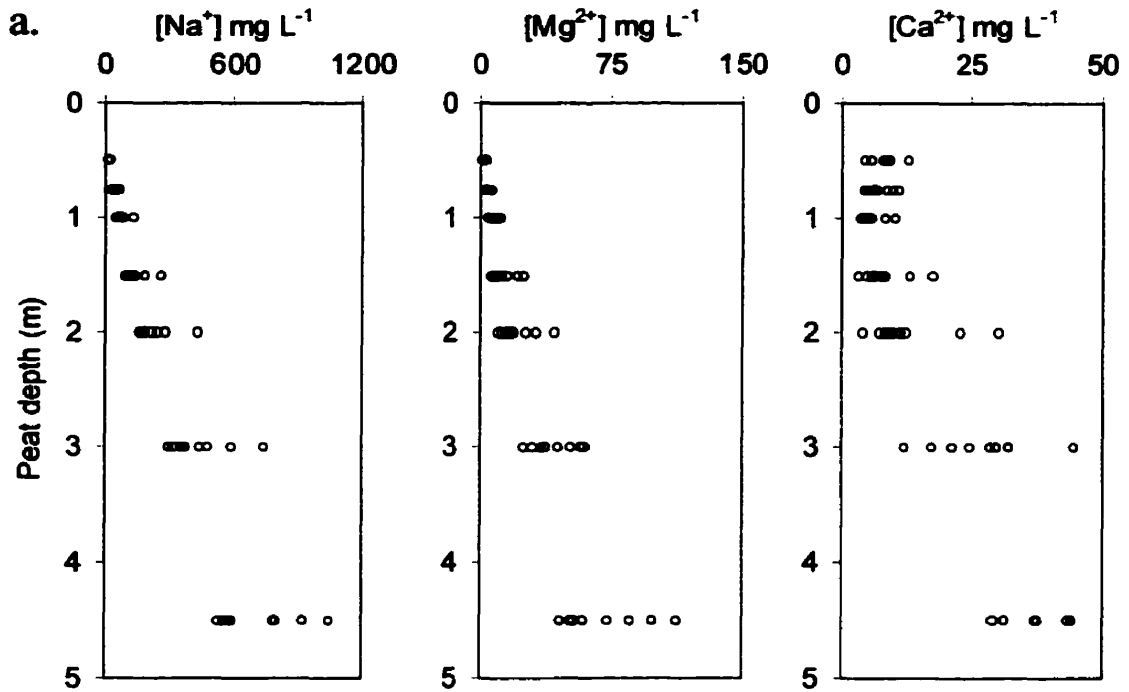


Figure 4-4a. Concentration-depth profiles for  $\text{Na}^+$ ,  $\text{Mg}^{2+}$  and  $\text{Ca}^{2+}$  for piezometers at nests P6-10 and RA1-4. b. Regression analysis of Na-Mg and Na-Ca. Both relationships were statistically significant ( $p < 0.00001$ ).

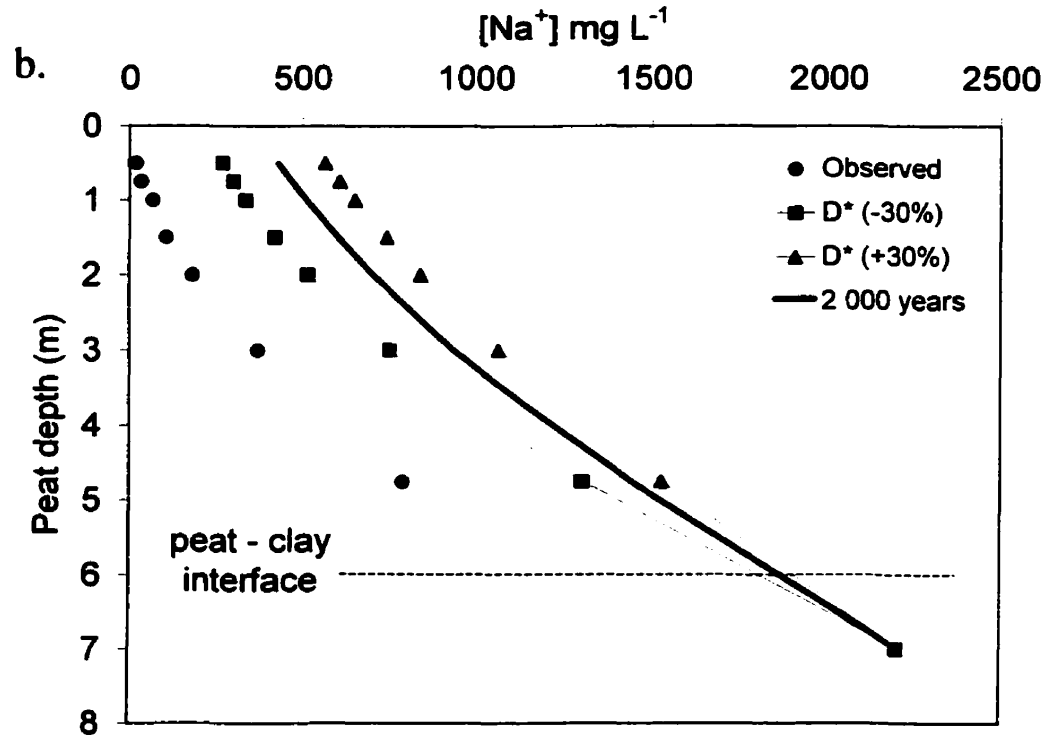
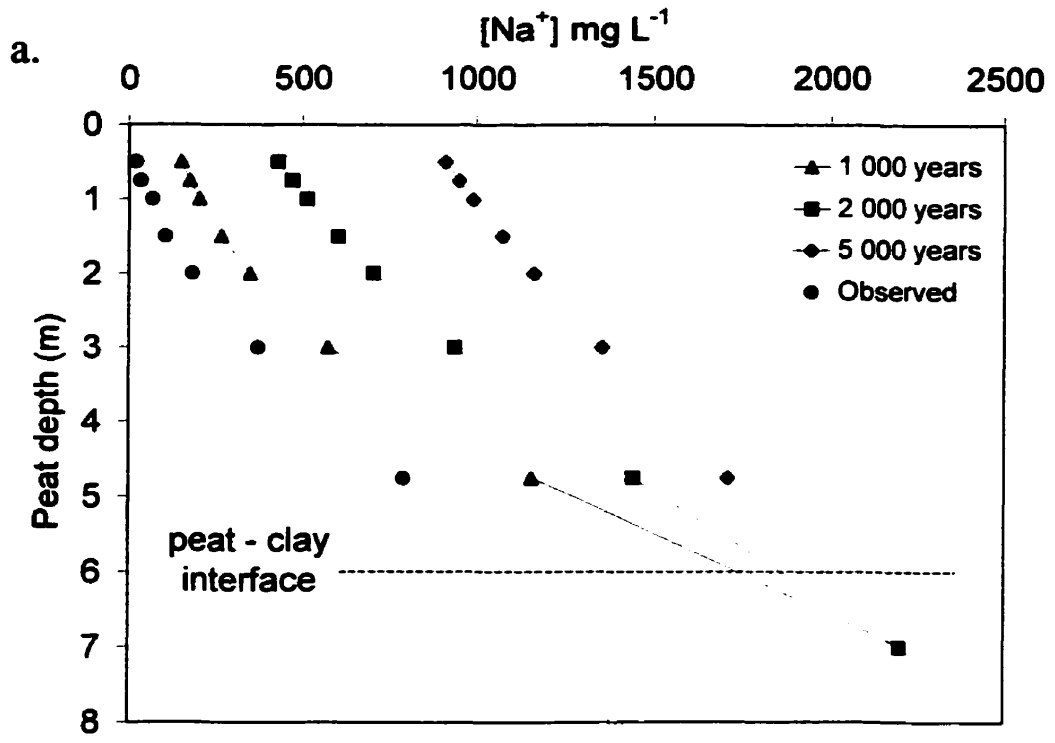


Figure 4-5a. Predicted Na<sup>+</sup> profiles for 1000, 2000 and 5000 year simulations compared to observed Na<sup>+</sup> concentrations at nest RA2 ( $D^* = 2.0 \times 10^{-9} \text{ m}^2 \text{ s}^{-1}$ ). b. Sensitivity of a 2000 year simulation to a  $\pm 30\%$  change to  $D^*$ .

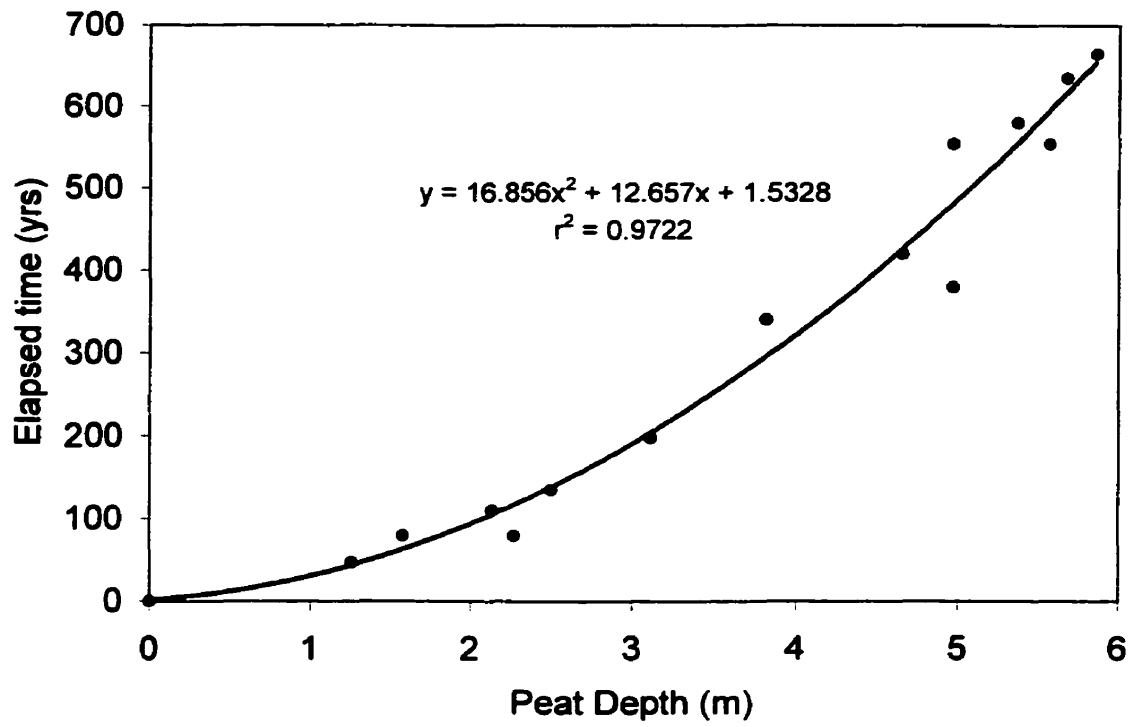


Figure 4-6. Regression of the elapsed time required for a best-fit curve to observed  $\text{Na}^+$  observations at each nest versus peat depth.

independent of concentration based on the diffusion model used. However, the regression analysis does illustrate that a complete mixing of diffused species ( $\text{Na}^+$ ) and atmospheric water occurs at all points of measurement in the peatland, regardless of peat depth. A point falling above the regression line would indicate differential discharge or weakened recharge due to anomalously low K in certain areas of the peatland, whereas a point below the line would indicate increased recharge or greater flushing due to high K. These situations do not appear to occur based on the points of measurement in the groundwater network. Complete mixing of groundwater as inferred from the high  $r^2$  values in Figures 4-4 (Na-Mg) and 4-6, may also suggest that the hydraulic properties peat are much more homogenous than hydraulic conductivities indicated.

#### **Section 4.3 P and ET controls on groundwater flow patterns at the Mer Bleue bog**

Figure 4-7 shows records of water table, precipitation and evapotranspiration from the tower site from June 13 to November 3, 1998. The water table record was separated into three periods: high position resulting from excess precipitation over runoff and evapotranspiration during June and early July 1998 (Julian days 160 to 190); a period of water table draw-down from mid-July through August 1998 (Julian days 190 to 238) due to evapotranspiration greatly exceeding precipitation; and a period of high water tables in the autumn due to excess precipitation over reduced evapotranspiration (Julian days 238 to 307).

Head data for piezometers at depths of 0.5, 1.0, 2.0 and 4.5 m for the period June 13 to November 3, 1998 are shown in Figure 4-8. Changes in water table and head due to precipitation and evapotranspiration can be compared using Figures 4-7 and 4-8. In general, shallowest piezometer best reflect the P and ET changes of the water table over the sample period, showing the greatest change in head over (Figure 4-8 (a-b)). Piezometers at the peatland margin show greater change in total head as compared to piezometers at the same depth on the peatland (Figure 4-8 (a-c)). Head changes of 0.2 m were recorded for piezometers of 0.5 m depth, as compared to 0.1 m head changes in deeper peats. Despite the smaller changes in total head recorded for deepest piezometers, the gross features of the P-

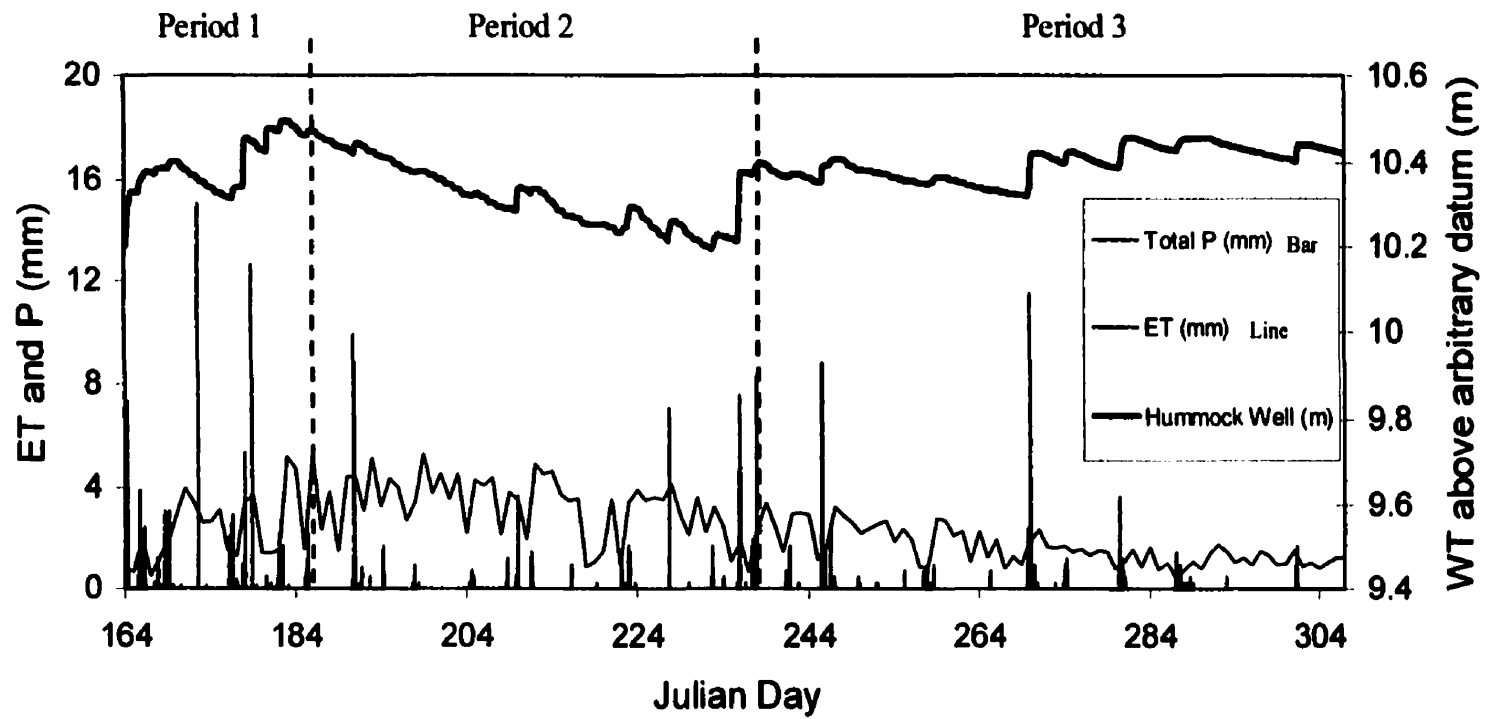


Figure 4-7. Changes in precipitation, evapotranspiration and water table position at the tower site for the 1998 field season.

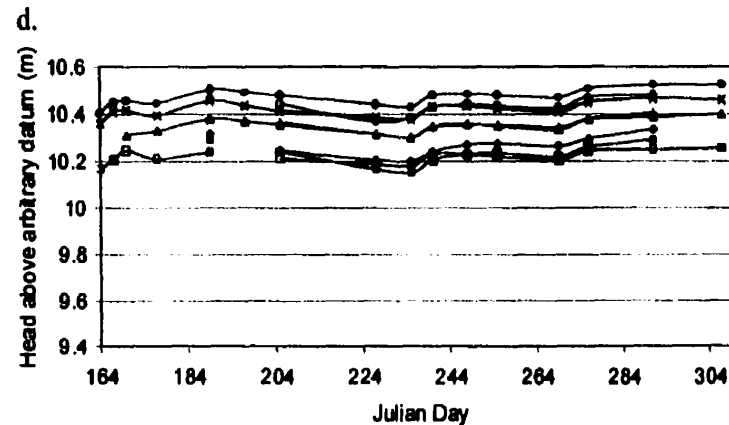
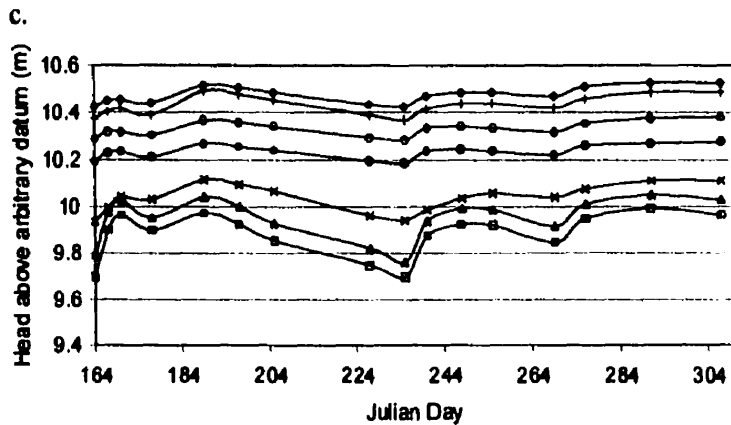
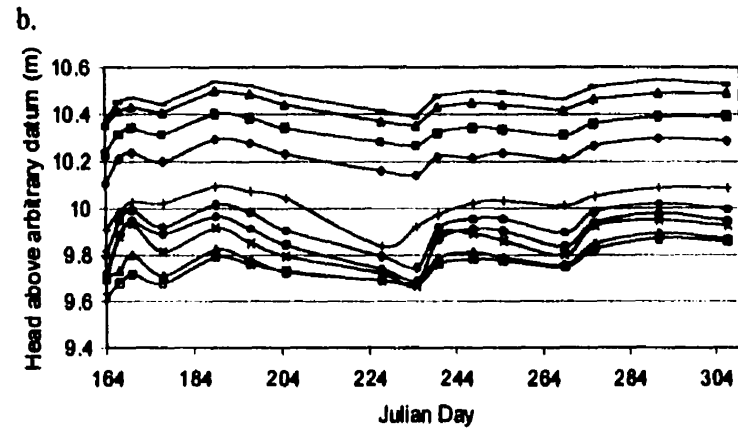
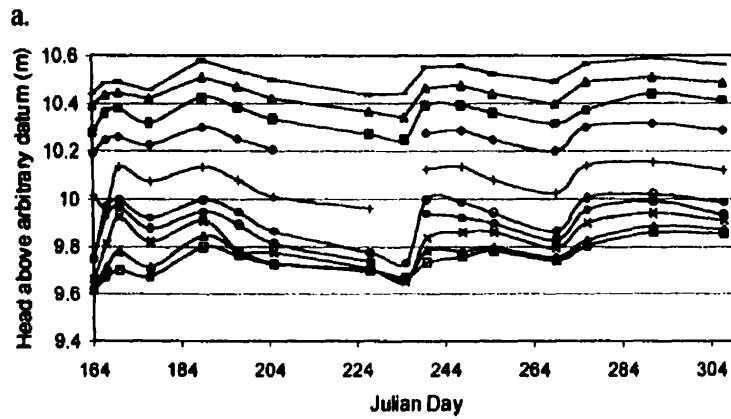


Figure 4-8. Plots of head change over time for piezometers of the same length. a. Head change for 0.5 m piezometers (P1 (lowest head values) to P10 (highest head values)) for June 13, to November 3, 1998. b. Head change for 1.0 m piezometers from P1 to P10. c. Head change for 2.0 m piezometers at nests P4 to P10. d. Head change for 4.5 m piezometers at nests P7 to P10 and RA1 to RA4. Maximum change in head by piezometer length decreases with increasing depth.

ET forcing on the water table were still evident over the sample period. This is confirmed by correlation analysis between water table position and head change (Table 4-2). Correlation decreased with depth due to a dampening of precipitation and evapotranspiration forcing.

#### **Section 4.4 A groundwater flow reversal**

A groundwater flow reversal evolved during the evaporative draw-down of the 1998 season (see Figure 4-7 - Period 2) from July 8 to August 26, 1998. P, ET, R and  $\Delta S$  scaled to basin size for this event were 91, 160, 8 and -77 mm respectively. Figure 4-9 shows recharge-discharge plots, referenced to water table position at nest P10 for July 8 (189), July 16 (197), July 24 (205), August 15 (227), August 23 (235) and August 28, 1998 (240).

Precipitation during June and early July 1998 resulted in net recharge at P10 (Figure 4-9a) where surface heads were ~10.55 m and heads at depth were ~10.49 m. Over the next 8 days, water table position lowered and head values in shallow piezometers decreased to ~10.52 m (Figure 4-9b) on account of ET exceeding P (Figure 4-7). Head in deeper piezometers did not change over this time interval. By the next sampling day (July 24 - Figure 4-9c), water table position lowered to ~10.46 m. Deeper peats were over-pressured with respect to the water table and a reversal of groundwater flow occurred (Figure 4-9c). Measurements from the next two sample dates showed constant water table position at ~10.40 m and continued upward gradients (Figure 4-9 (d,e)). Head values in deeper piezometers decreased over the reversal period as discharge sustained surface heads (Figures 4-9 (c-e)). A large storm prior to the last sampling date (August 28) raised water table position and head in shallow piezometers to induce a reversal in gradients and yield recharge conditions through the profile (Figure 4-9f). A comparison of recharge-discharge plots for August 23 and August 28, 1998 show that the precipitation event caused head in deeper piezometers to increase marginally, but it was the dramatic increase in head between the water table and 0.75 m that terminated the reversal and restored original conditions. Recharge-discharge plots from nests P6 to P9 and RA1 to RA4 revealed the same patterns.

**Table 4-2. Correlation of head measurements by piezometer depth to water table position. Correlations for nests P7, P8 and P9 on the major axis are shown.**

**a. Correlation between water table and piezometers at nest P7.**

	WT	0.5 m	0.75 m	1.0 m	1.5 m	2.0 m	3.0 m	4.5 m
WT	1.00	—	—	—	—	—	—	—
0.5 m	0.80	1.00	—	—	—	—	—	—
0.75 m	0.81	0.86	1.00	—	—	—	—	—
1.0 m	0.71	0.75	0.73	1.00	—	—	—	—
1.5 m	0.70	0.74	0.80	0.96	1.00	—	—	—
2.0 m	0.73	0.83	0.84	0.96	0.98	1.00	—	—
3.0 m	0.82	0.91	0.82	0.89	0.89	0.94	1.00	—
4.5 m	0.76	0.87	0.76	0.94	0.89	0.92	0.90	1.00

**b. Correlation between water table and piezometers at nest P8.**

	WT	0.5 m	0.75 m	1.0 m	1.5 m	2.0 m	3.0 m	3.5 m
WT	1.00	—	—	—	—	—	—	—
0.5 m	0.80	1.00	—	—	—	—	—	—
0.75 m	0.75	0.93	1.00	—	—	—	—	—
1.0 m	0.71	0.89	0.99	1.00	—	—	—	—
1.5 m	0.71	0.89	0.98	0.99	1.00	—	—	—
2.0 m	0.68	0.90	0.95	0.94	0.96	1.00	—	—
3.0 m	0.65	0.86	0.94	0.94	0.96	0.98	1.00	—
3.5 m	0.65	0.80	0.88	0.88	0.90	0.96	0.96	1.00

**c. Correlation between water table and piezometers at nest P9.**

	WT	0.5 m	0.75 m	1.0 m	1.5 m	2.0 m	3.0 m	4.5 m
WT	1.00	—	—	—	—	—	—	—
0.5 m	0.83	1.00	—	—	—	—	—	—
0.75 m	0.68	0.89	1.00	—	—	—	—	—
1.0 m	0.73	0.93	0.98	1.00	—	—	—	—
1.5 m	0.65	0.87	0.97	0.99	1.00	—	—	—
2.0 m	0.61	0.85	0.95	0.97	0.99	1.00	—	—
3.0 m	0.74	0.90	0.97	0.96	0.93	0.90	1.00	—
4.5 m	0.72	0.91	0.97	0.96	0.93	0.92	0.99	1.00

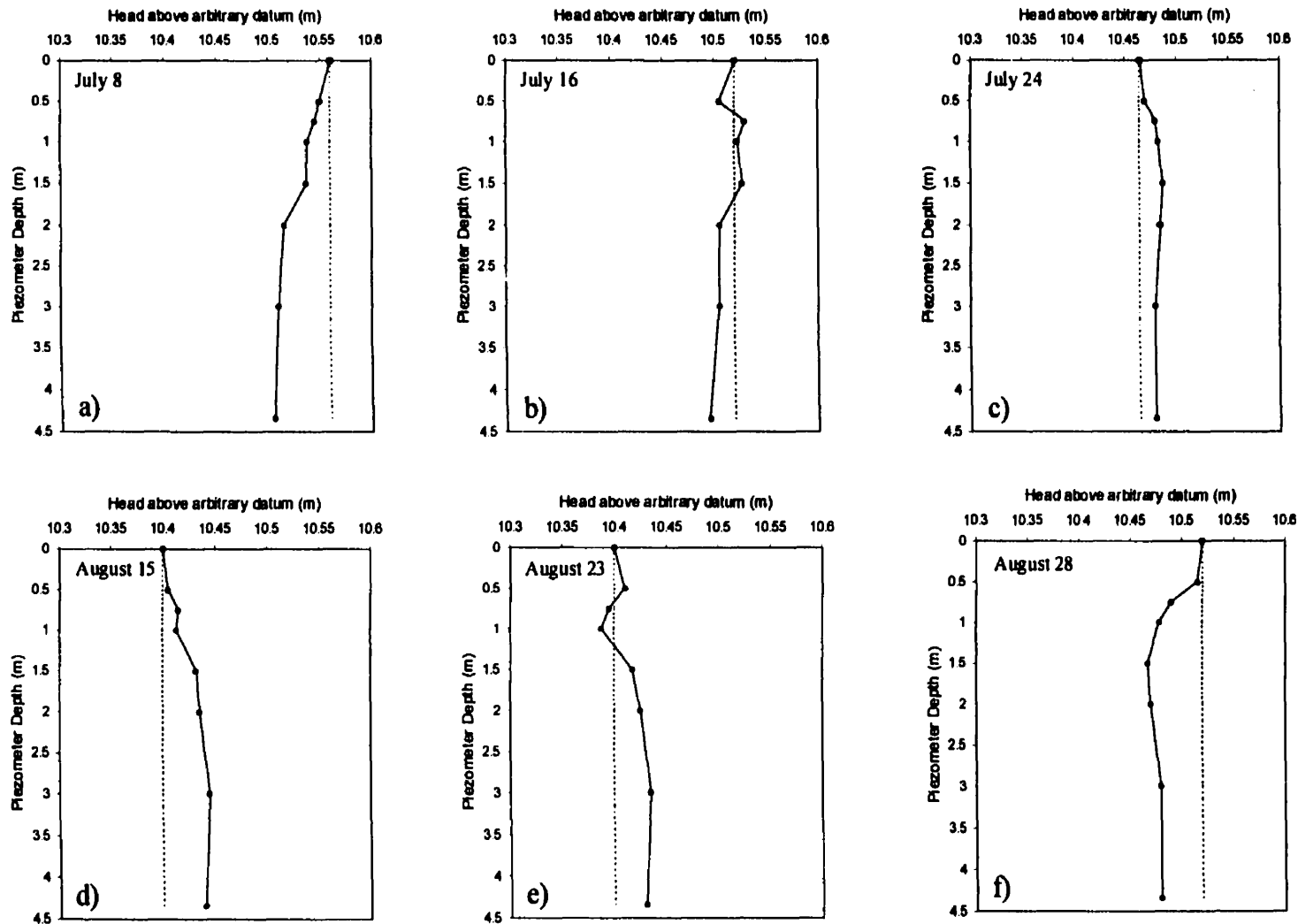


Figure 4-9. Summary of recharge-discharge plots over the period of the groundwater reversal as observed at P10. Head observations greater than the water table denote discharge whereas head values less than the water table denote recharge. Plots a) through f) depict conditions for July 8, July 16, July 24, August 15, August 23, and August 28, 1998 respectively.

Figure 4-10 (a,b) shows the initial conditions for the groundwater flow reversal. The evaporative draw-down decreased head in upper-most piezometers to induce discharge between July 19-23, 1998 (Julian days 200 to 204). Heads remain constant at the seepage face over the duration of the reversal (Figure 4-10c). Flownets for three sampling dates during and after the flow reversal are shown in Figure 4-11 to illustrate the changes in groundwater flow patterns through the event.

#### **Section 4.5 Changes in groundwater chemistry during the groundwater reversal**

Under reversal conditions, it was hypothesized that discharging waters from depth would cause an influx of lower concentrated DOC to surface waters and decrease concentrations of exportable DOC. Contrary to this, DOC concentrations were very conservative over the period of the flow reversal (Figure 4-12 a-d) and may have increased slightly at the point of groundwater convergence near P6 (Figure 4-12 d). However, the small increase of ~5 to 10 mg L<sup>-1</sup> cannot be separated from sampling noise. Field testing showed that multiple DOC samples taken from a single piezometer can vary by ±3 mg L<sup>-1</sup>.

Electrical conductivity increased in piezometers over the reversal period and then decreased after the reversal (Figure 4-13). The increase and decrease resulted from a discharge of more saline waters and subsequent recharge with less saline waters. As illustrated in Figure 4-14, changes in Na<sup>+</sup> concentration at piezometer nests were compared using sample dates June 23 (before reversal) and August 25, 1998 (during reversal). Sodium migration from the groundwater reversal was estimated assuming discharge to be vertical. The results from 29 migration estimates for piezometers between 0 to 2.0 m showed an average vertical migration of 0.153 m for a 25 day period, or 0.006 m day<sup>-1</sup> (see Appendix 3 for statistics and interpolation methods). Once recharge conditions were established after the reversal, downward migration was of similar magnitude to that observed during the reversal.

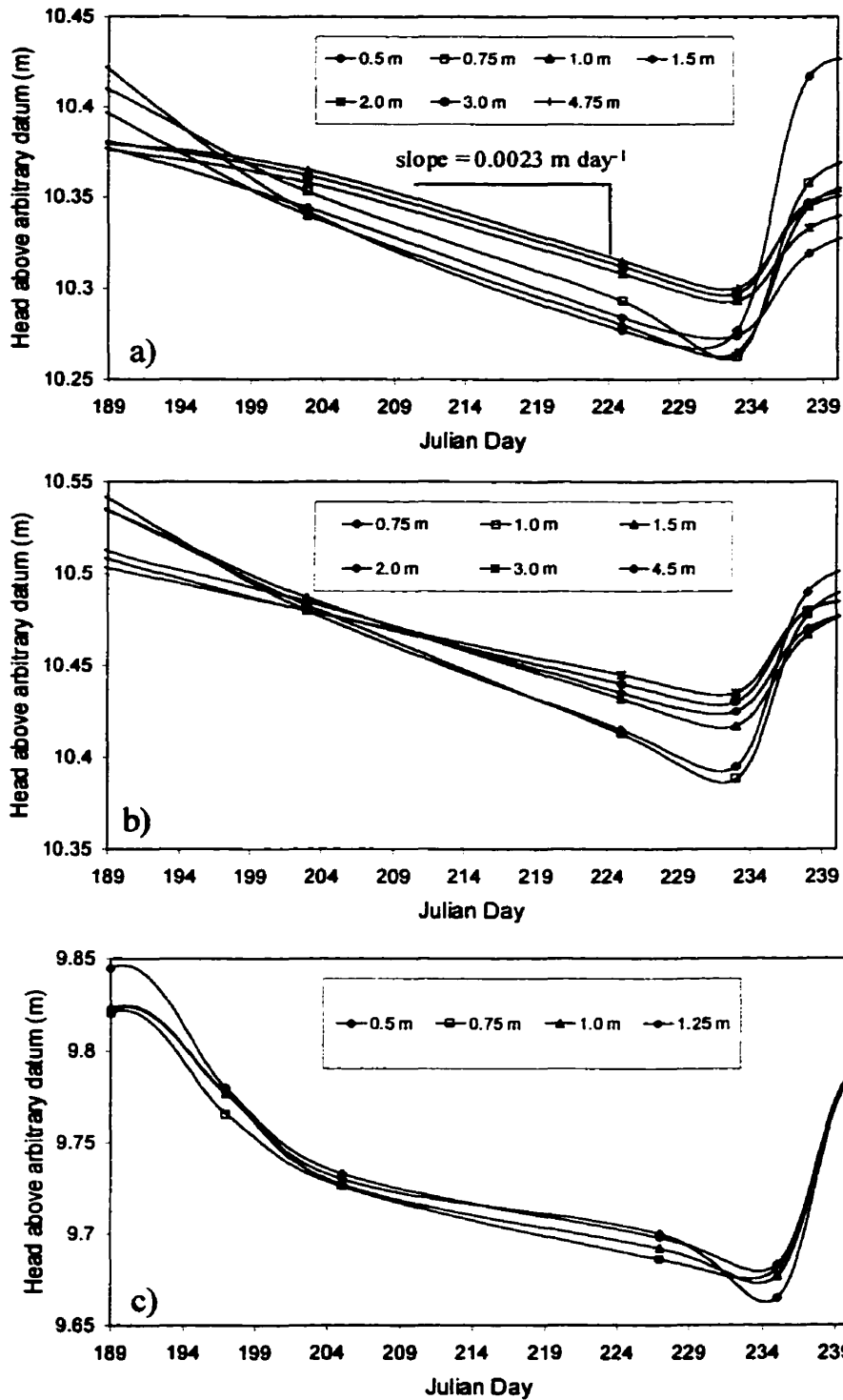


Figure 4-10. Plots a-b show head changes at nests RA2 and P10 over the reversal period respectively. ET causes shallow piezometers to 'cross' head values in deeper piezometers between Julian days 200 and 210 (July 19-29, 1998) and create an over-pressure in deeper peats. c. Changes in head at P2 over the reversal period. Horizontal flow was maintained at the peatland margins during the event.

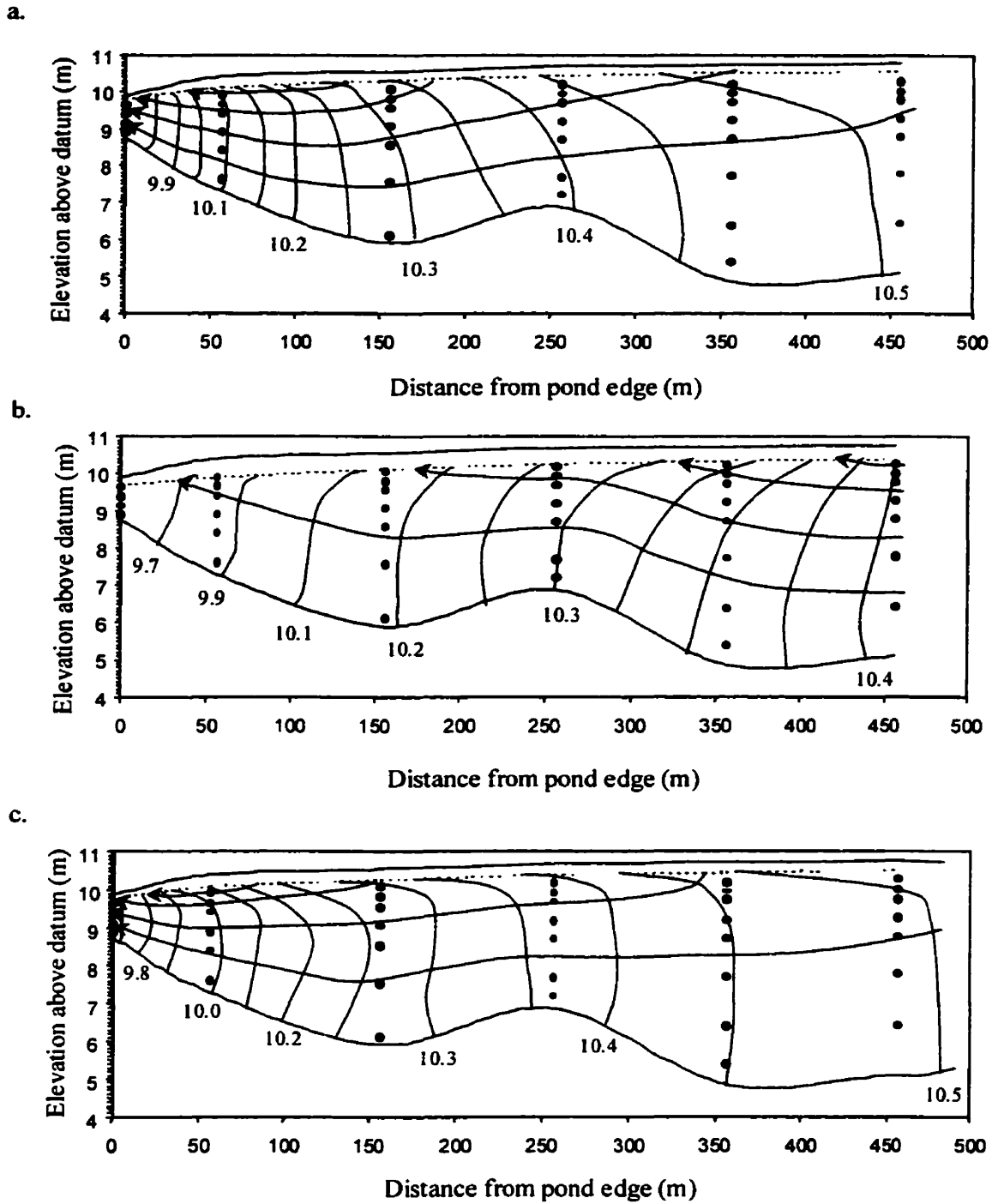


Figure 4-11. Changes in groundwater flow patterns over the course of the reversal as depicted by flownets across the major axis. Flownets for July 8, and August 26, 1998 (a and c) show recharge patterns whereas the flownet for August 23, 1998 (b) shows a discharge pattern. Equipotentials are labelled in metres above an arbitrary datum. Plot (c) is the flownet shown in Figure 4-1.

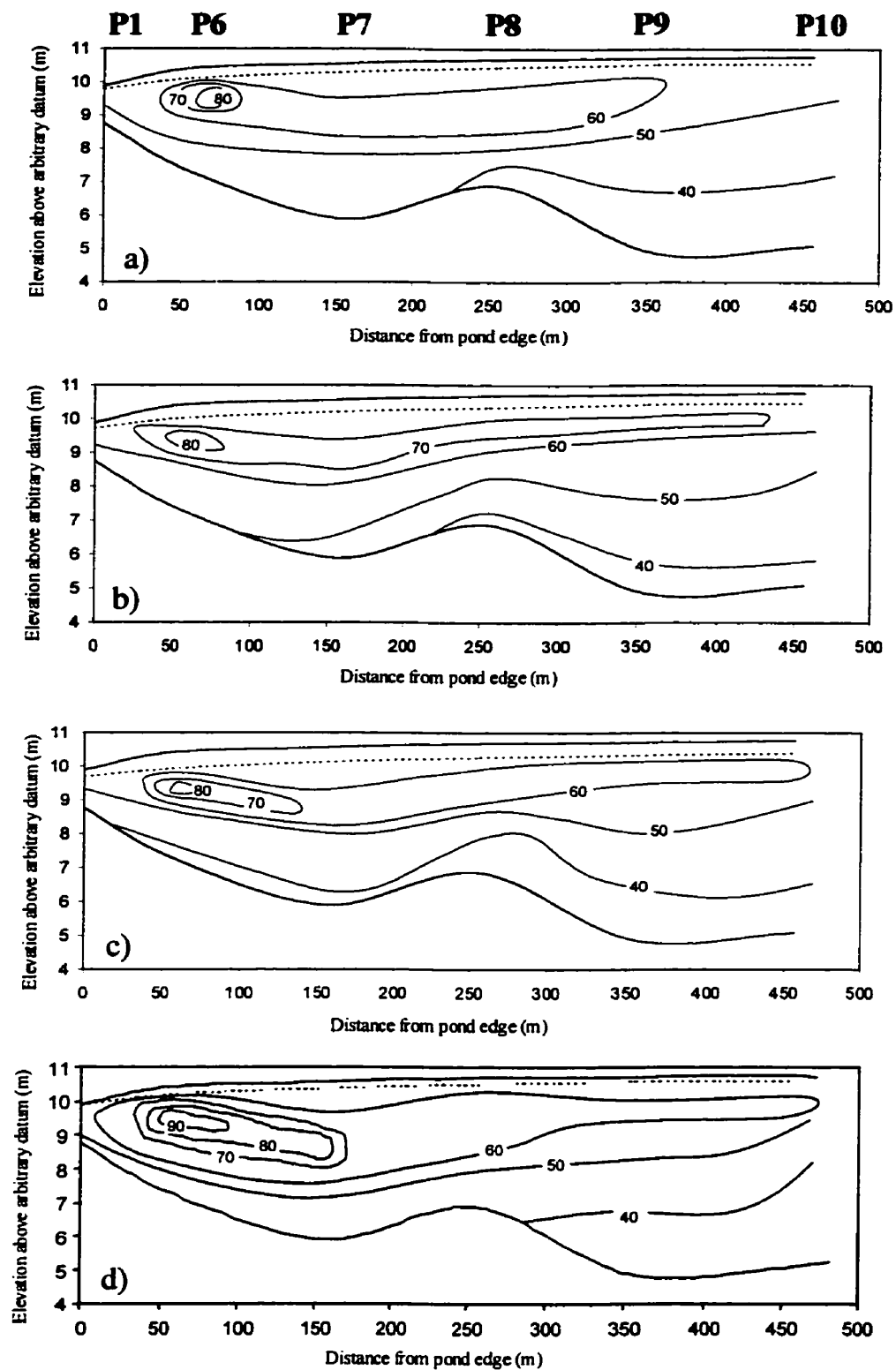


Figure 4-12. Changes in DOC concentrations over the period of groundwater reversal. Spatial changes for July 9, July 22, August 13, and August 26, 1998 are shown (a-d) respectively.

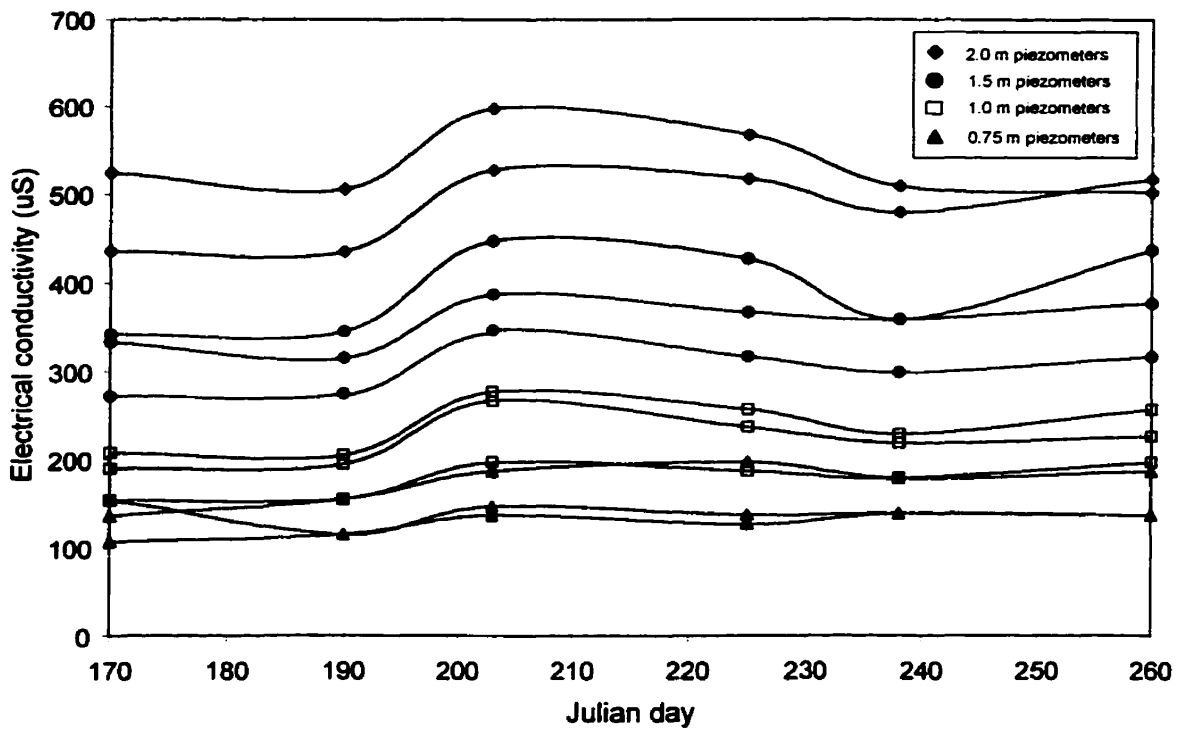


Figure 4-13. Changes in electrical conductivity from piezometers of depth 0.75, 1.0, 1.5 and 2.0 m at nests P8, P9 and P10.

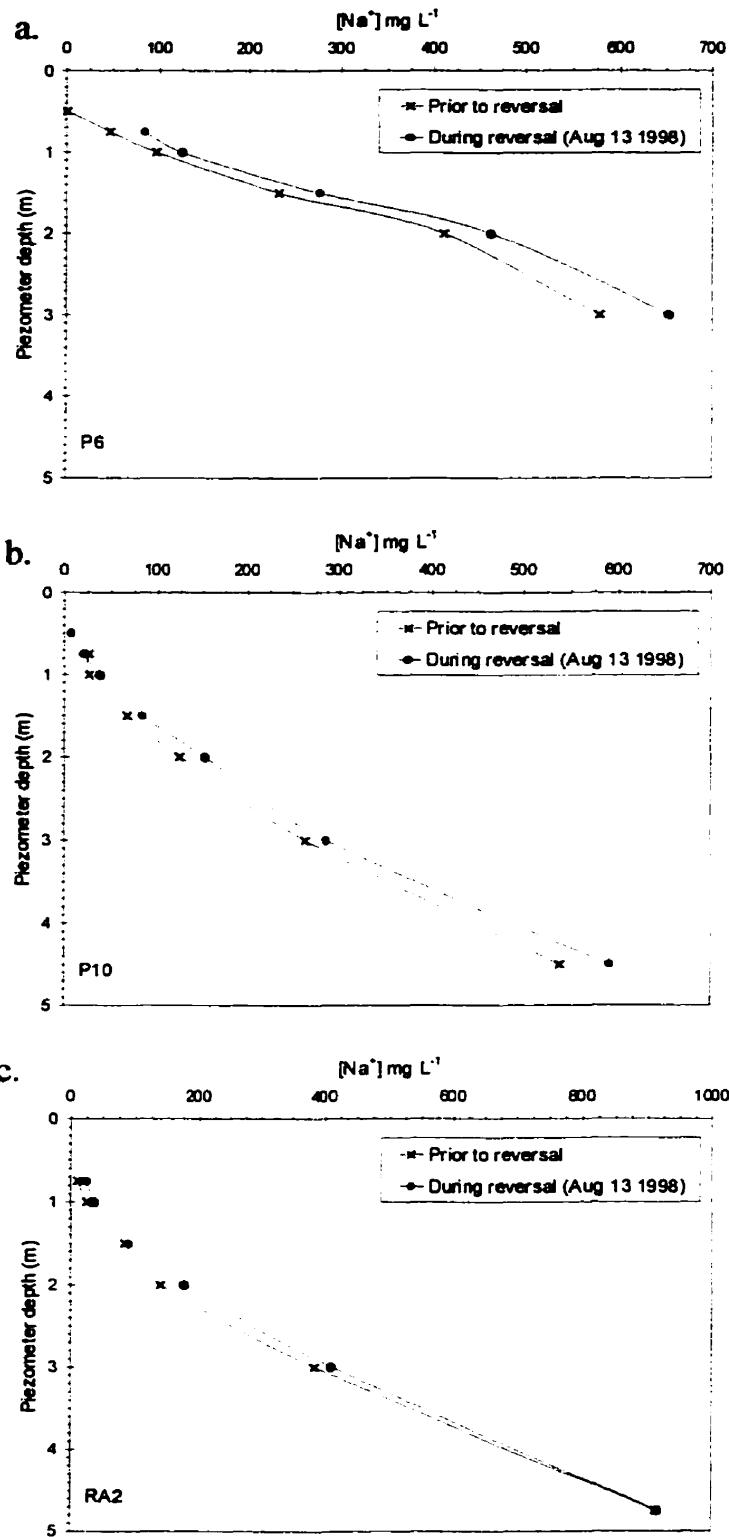


Figure 4-14. Changes in Na<sup>+</sup> concentration prior to and during the reversal. Plots a-c show changes for nests P6, P10 and RA2 respectively. Migration of Na<sup>+</sup> over the reversal was determined based on position change from a measured point prior to the reversal to a point during the reversal assuming the discharge component to be vertical.

## **Section 4.6 Discussion of groundwater flow patterns at the Mer Bleue bog**

### **Section 4.6.1 Groundwater flow patterns at the Mer Bleue bog**

#### **Annual patterns of groundwater flow**

The patterns of groundwater flow at the Mer Bleue bog are controlled by changes in precipitation and evapotranspiration. Atmospheric control is dampened with increasing peat depth (Figures 4-7 and 4-8). Recharge conditions were the dominant groundwater flow pattern as P exceeds ET on an annual basis, but discharge conditions due to an evaporative draw-down were found to occur at a monthly time scale (Figures 4-9 to 4-11). Atmospheric maintenance of hydrological conditions at the Mer Bleue bog occurs in the absence of regional groundwater flow.

Romanowicz et al. (1993) and Siegel et al. (1995) found that groundwater flow reversals occurred in Minnesota peatlands and speculated they were due to drought conditions. Evaporative stress resulted in discharge from underlying glacial tills and sand aquifers once water table was drawn-down considerably. Devito et al. (1997) found that subsurface flow within peat can reverse in hydrogeological settings isolated from regional groundwater flow. They also speculated flow reversals were a function of evaporative stress. The results presented in this chapter confirm the conjectures of Romanowicz et al. (1993), Siegel et al., (1995) and Devito et al. (1997) that evaporation is a major driving mechanism for reversals.

#### **Flow reversals at the Mer Bleue bog**

The 1998 groundwater reversal at the Mer Bleue bog was terminated by a large input of water during a storm. Prior to the precipitation event, water table position had decreased ~0.15 m over the reversal period to a depth ~0.4 m below the average peat surface (Figures 4-7 and 4-9), and energy transfer from over-pressured deep peats to surface peats occurred

until this precipitation event. Hydraulic potential in deep piezometers decreased linearly at  $\sim 0.0023 \text{ m day}^{-1}$  over the reversal (Figure 4-8a). Hydraulic potential in deep peats was within 0.03 m of the water table at the end of the reversal (Figure 4-9).

A reversal at the Mer Bleue bog will continue until hydraulic potential reaches hydrostatic equilibrium with depth under discharge conditions, or a precipitation event increases water table position to hydraulic potential greater than that at depth. Considering a situation where hydraulic potential is decreased until hydrostatic equilibrium occurs, suggests that the reversal at the Mer Bleue bog could have been sustained for 15 additional days provided there was no precipitation. In theory, the length of a reversal is controlled by the amount of time corresponding to conditions where  $ET \gg P$  (May, June, July August), but field measurements and climate normals suggest that a four month flow reversal in the Mer Bleue bog would be anomalous. Reversal conditions lasting only one to two months at a maximum are most probable.

The length of a reversal at the Mer Bleue bog is indirectly controlled by the initial hydraulic potential of the water table and deep peats. Higher potentials in deep peats will increase the elapsed time until hydrostatic equilibrium occurs under evaporative stress. This indirect control on flow reversal duration is important for reversals terminated in hydrostatic equilibrium, but unimportant for reversals terminated by precipitation and surface recharge events.

### **Long-term patterns of groundwater flow**

Diffusion of  $\text{Na}^+$  from the underlying marine clay provides a natural tracer to assess the recharge-discharge function of the Mer Bleue bog. However, evaluation of groundwater flow patterns can only be qualitative as diffusion models are dependent upon several assumptions. The major deficiencies with the diffusion methods are evident when considering the conservativeness of the *in situ* tracer, and when determining an appropriate time scale to compare observed and predicted  $\text{Na}^+$  profiles. Finding a conservative tracer requires consideration of the physical, biological and chemical processes that affect pore

water concentrations of the tracer in the peat profile. Isolation of an appropriate time scale for diffusion scenarios requires consideration of peatland growth and the balance between P and ET over millennia.

Are the  $\text{Na}^+$  concentrations observed in the peat profile a direct result of upward diffusion and recharge mixing only, and is  $\text{Na}^+$  a conservative tracer at the Mer Bleue bog? Physical additions of  $\text{Na}^+$  through deposition and regional groundwater flow can be considered negligible at the Mer Bleue bog. Concentrations of  $\text{Na}^+$  in precipitation in the St. Lawrence lowlands range from 0.1 to 0.3  $\text{mg L}^{-1}$  (Drever, 1997) and are too small to be a significant source of salinity at the surface boundary condition. It has already been established that there are no sources of deep groundwater across the peat-clay interface (see Section 4-1). Therefore, any sodium in the peat profile has to be the result of diffusion.

Are there chemical alterations to *in situ*  $\text{Na}^+$  that may affect the recharge-discharge analysis undertaken? The cation exchange capacity (CEC) of peat soils ranges from 100-200  $\text{meq}/100 \text{ g}$  (Lévesque et al., 1980). Of the many cations in peat pore waters,  $\text{Na}^+$  has the highest exchange capacity and can be considered the most chemically conservative cation *in situ*, but from this information alone it cannot be concluded that  $\text{Na}^+$  is truly conservative. However, calculations using concentrations of  $\text{Na}^+$ , average estimates of CEC and average values of peat properties, show that under complete exchange of  $\text{Na}^+$ , peat pore water concentrations can only change by 2-7%.  $\text{Na}^+$  conservation at the Mer Bleue bog is thus a function of the high  $\text{Na}^+$  concentrations of peat pore water (up to 1000  $\text{mg L}^{-1}$  - see Appendix 1). CEC will be most important near the peat surface where concentrations decrease and exchange importance increases, but  $\text{Na}^+$  is conservative through enough of the peat profile to assess the recharge-discharge function adequately. Modeling attempts with lower concentrated, less exchangeable and biologically scavenged cations (i.e. -  $\text{Ca}^{2+}$ ) were not successful.

Were the lengths of diffusion scenarios used in evaluation of peatland recharge-discharge function appropriate? Considering accumulation in peatlands to be 0.5  $\text{mm yr}^{-1}$  (Gorham, 1991), the peat depth at the Mer Bleue bog increased by  $\sim 1.0 \text{ m}$  over the 2000 year period. Assuming the difference between historical P and ET were the same as they are now,

the hydraulic gradients and groundwater flow patterns would be very similar to present day for a ~1.0 m change in peat depth. Further, diffusion of Na<sup>+</sup> from the marine clay at the Mer Bleue bog is a 'bottom-up' process and has occurred since bog development ~9000 years ago. Since the direction of diffusion is the same as bog growth and diffusion has occurred well beyond the 2 000 year standard, the scenarios used to evaluate the recharge-discharge patterns at the Mer Bleue bog are conservative. Despite the choice of a conservative time interval, the diffusion scenarios for all nests revealed net recharge conditions (Figure 4-5). It is believed that within the uncertainty associated with the choice of Na<sup>+</sup> as a tracer, small annual fluctuations in recharge-discharge patterns at the Mer Bleue bog (see Section 4.4) are masked by a long-term recharge signal.

### **Vertical hydraulic conductivity**

Results from Na<sup>+</sup> migration plots (Figure 4-14) and diffusion scenarios (Figure 4-5) provide two different estimates of vertical hydraulic conductivity. During the groundwater reversal, average Na<sup>+</sup> migration was 0.153 m over a 25 day period. Translating this migration rate to a flow and using vertical gradients measured during the reversal, integrated estimates of K<sub>v</sub> were calculated to be 10<sup>-6</sup> to 10<sup>-7</sup> m s<sup>-1</sup>. Estimates of K<sub>v</sub> were also estimated from diffusion model estimates in which the vertical change in position between observed and simulated Na<sup>+</sup> profiles were translated to a rate of net downward velocity. Comparing the rate of downward recharge to upward diffusion revealed that downward recharge was 1.5 to 4 times greater than the rate of diffusion for scenarios ranging from 750 to 8000 years. Calculating K<sub>v</sub> from discharge and estimates of hydraulic gradients yielded an integrated K<sub>v</sub> on the order of 10<sup>-7</sup> m s<sup>-1</sup>. These estimates are several orders of magnitude greater than calculations revealed for K<sub>v</sub> (see Table 3-1) and suggest that the physical exchanges of water due to changes in recharge-discharge function could be much greater than previously thought. However, the calculations are dependent upon the biological and chemical conservation of Na<sup>+</sup> in the peat profile.

### Section 4.6.2 Groundwater as a control on biogeochemistry

Siegel et al. (1995) found that flow reversals could evolve on monthly time scales, but these short events had no effect on peatland chemistry. However, they also found that flow reversals resulting from evaporative draw-downs and subsequent connection to regional groundwater flow altered peatland chemistry when reversal conditions continued for several years. If the Mer Bleue bog only experiences seasonal changes to recharge-discharge patterns, what role do flow reversals have in maintaining and/or changing peatland biogeochemistry?

If a chemical species in a peat profile at the Mer Bleue bog is not conservative, the concentration of the species will be a function of the rate of diffusion from the underlying marine clay up through the profile, the rate of recharge of meteoric water through the profile and any *in situ* biogeochemical modifications subjected upon the species. Evaluation of the recharge-discharge function of the Mer Bleue bog using a sodium tracer revealed that recharge conditions give observed  $\text{Na}^+$  concentrations that are much lower than expected based on seemingly realistic diffusion scenarios. This long-term geochemical signal is the result of persistent recharge conditions, and it follows that the recharge conditions would have shaped peatland biogeochemistry at the Mer Bleue bog. In this way, recharge conditions are a critical control in *maintaining* long-term peatland biogeochemical function.

This does not exclude reversals from playing an important role in spatially and temporally *altering* peatland biogeochemistry. Calculations suggest that  $\text{Na}^+$  concentrations increased ~20% at 2.0 m depths and ~70% near the peat surface over the reversal period. A sizable increase in  $\text{Na}^+$  concentrations may or may not impact peatland biogeochemistry, but considering that marine clay contains boron, calcium, chloride, iron, mercury, bicarbonate, potassium, magnesium and sulphate (Harte, 1988), there is a potential to alter redox equilibria, cation exchange equilibrium, pH control and heavy metal cycling in the peat profile over a flow reversal. Flow reversals may also mediate microbial activity and methylation reactions ( $\text{CH}_4$  or  $\text{CH}_3\text{-Hg}^+$ ), particularly if discharge conditions replenish limited intermediate species such as calcium, nitrate and sulphate. No measurements of

chemical changes due to the reversal were made in this study, and the arguments being made are conjectural only. However, hydro-chemical evidence suggests that alterations to peatland biogeochemistry can occur over short time periods (40 days) and that biogeochemical changes would be greatest near the peat surface where concentration gradients are steepest and close to an oxic interface.

### **Section 4.6.3 Groundwater and the carbon budget of a boreal peatland**

#### **DOC**

Almost all DOC export occurs through a high K layer at the peatland surface and DOC export was estimated to be 11% of the C-sink at the Mer Bleue bog (refer to Chapter 3 for more details). DOC concentrations were very conservative during the groundwater reversal (Figure 4-12) and a decrease in runoff at this time occurred due to water table draw-down (Chapter 3). This eliminates the importance of recharge-discharge patterns in changing DOC concentrations or DOC export from the peatland. However, the character of DOC varied considerably over the top 1.0 m of the peatland (Figure 4-2). If the reversal mixed DOC in a manner similar to  $\text{Na}^+$ , this could have considerable impact on carbon turnover and soil respiration. Increased drought decreased DOC yield from the peatland, but the decrease had no net effect on the C budget of the Mer Bleue bog.

#### **DIC and $\text{CH}_4$**

Dissolved carbon profiles for TC (total carbon), DOC, DIC and  $\text{CH}_4$  are shown in Figure 4-15. *In situ* DIC concentrations were lower than ambient  $\text{CO}_2$  at the peatland surface (Nigel Roulet, pers. comm.). Thus, degassing of DIC on the peatland is physically impossible and vertical transport of DIC during a flow reversal would have no effect on the carbon balance of the peatland. DIC loss can be attributed to hydrological transport, but export is confined to the peatland margins and controlled by gradients and hydraulic conductivity.

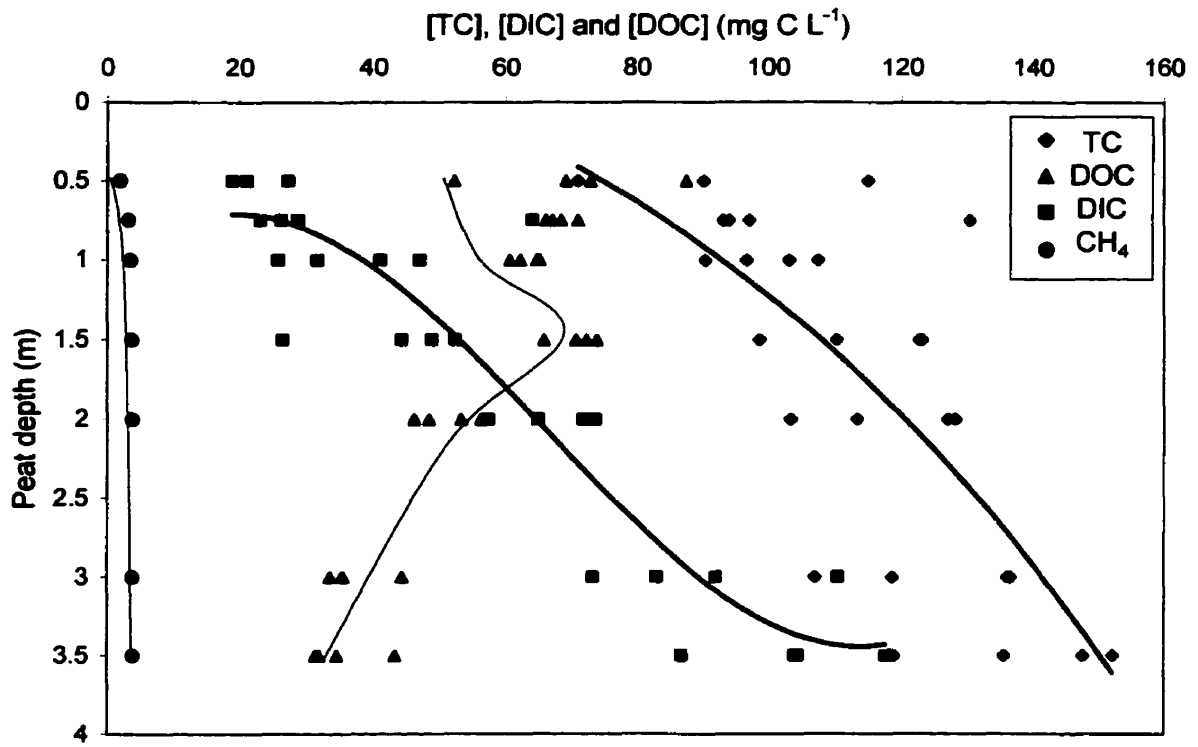


Figure 4-15. Representative dissolved carbon profiles for the Mer Bleue bog. The carbon profiles shown are from four sample dates for spring-summer 1999.

Since runoff ceased during the flow reversal, DIC flux was negligible at this time.

Romanowicz et al. (1993) and Siegel et al. (1995) have suggested that episodic emissions of CH<sub>4</sub> could have an important role in peatland carbon budgets. Did the groundwater flow reversal at the Mer Bleue bog induce degassing that effected the carbon budget of the peatland? Considering an average vertical migration for the reversal period to be 0.2 m, calculations with CH<sub>4</sub> concentrations of 2 mg L<sup>-1</sup>, observed hydraulic gradients, and K values ranging from 10<sup>-6</sup> to 10<sup>-7</sup> m s<sup>-1</sup> suggest that CH<sub>4</sub> degassing was at most 0.05 g C m<sup>-2</sup> for the forty day period. However, several studies attribute episodic emissions of CH<sub>4</sub> to anomalous continuities in peat structure or to macro-pore connectivity (Chason and Siegel, 1986; Siegel et al., 1995) and ebullition under super-saturated conditions. No measurements of CH<sub>4</sub> flux were made over the reversal, but assuming all stored CH<sub>4</sub> was released in an episodic event, the peatland would be a CH<sub>4</sub> source no greater than 5-10 g C m<sup>-2</sup>.

## **Chapter 5 - Summary and discussion**

The goals of this research were to gain insight into the role of dissolved carbon export in the contemporary carbon budget of a peatland, to isolate the controls on ground and surface water hydrology, and further delineate the links between groundwater and biogeochemistry in peatlands. The results addressing these goals can be found in Chapters 3 and 4 and the discussion section in each chapter attempted to clarify the results.

The purpose of this final chapter is to summarize the hydrological and biogeochemical findings from this study and propose some possible direction for future research. The chapter is divided into four sections. The first section summarizes the hydro-biogeochemical linkages at the Mer Bleue bog, whereas the second section raises important research questions concerning hydro-biogeochemical linkages that could be addressed at the Mer Bleue bog. The remaining sections focus on the contemporary carbon budgets of northern peatlands by considering hydrological and biogeochemical processes at larger scales.

### **Section 5.1 Linking hydrology and biogeochemistry at the Mer Bleue bog**

During the ice-free season, runoff at the Mer Bleue bog was generated by a groundwater seepage process at the peatland margin. Groundwater seepage was, in turn, controlled by the profile of hydraulic conductivity and gradients in the upper 0.25 m of the peat profile. As a result, flow was horizontal. Groundwater flow patterns on the peatland were controlled by changes in P and ET because this defined the hydraulic potential of surface boundary conditions. *In situ* Na<sup>+</sup> concentrations revealed that the peatland recharge-discharge function is transient on a monthly time scale, but showed a tendency for long-term recharge. Basin runoff generated from snow-melt events resulted from a fast flow process over frozen soil and ice.

The linkages between hydrological pathway and peatland biogeochemistry are shown in Figure 5-1 a. Event-based hydrology generated almost all annual runoff and biogeochemical flux from the Mer Bleue bog by fast flow over frozen peat (1) and acrotelmic discharge (2).

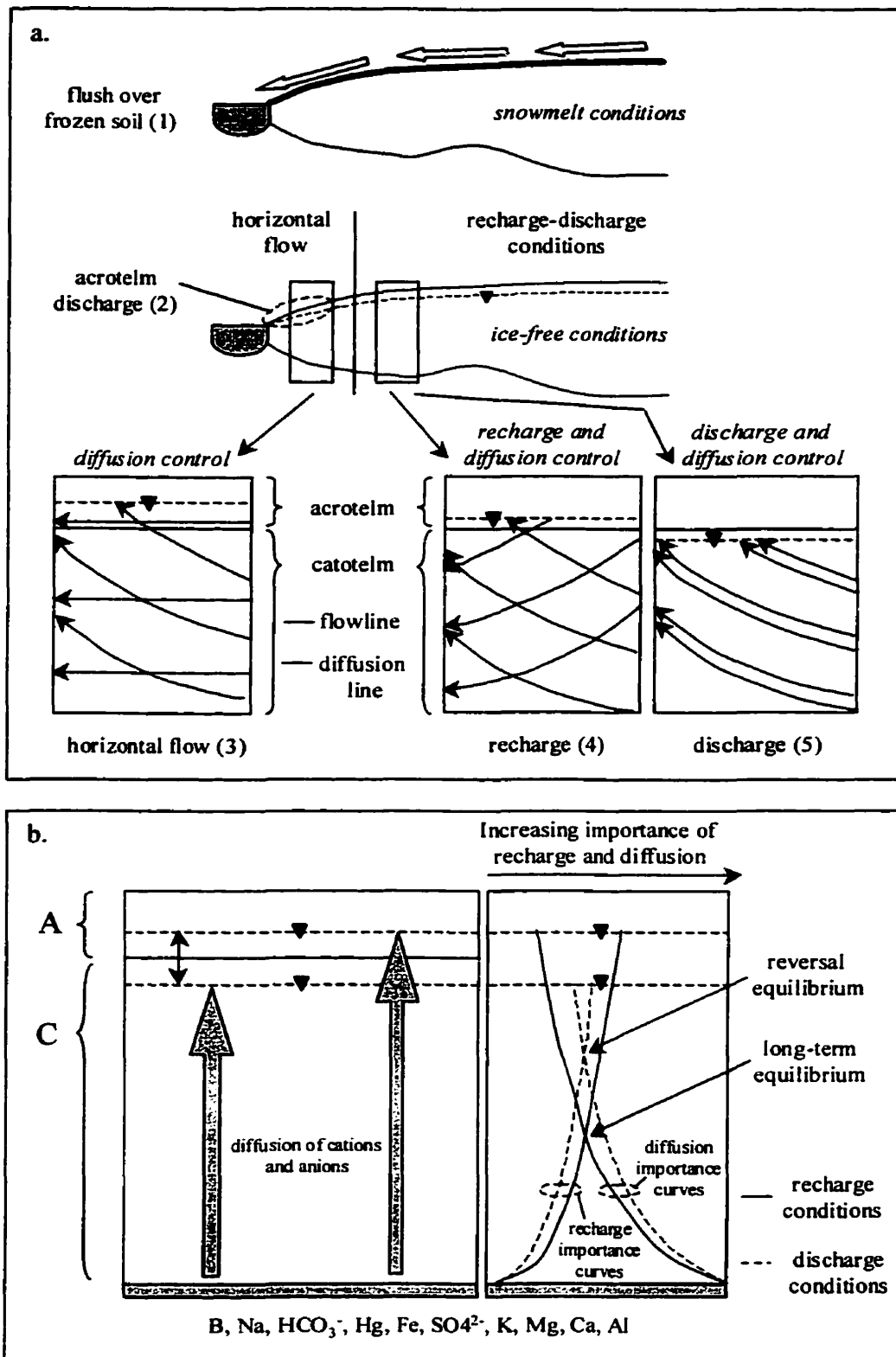


Figure 5-1. a. Summary of the five hydrological-biogeochemical linkages observed at the Mer Bleue. b. Conceptual diagram of the hydrological-biogeochemical interactions that occur during recharge and discharge conditions.

Evaluation of groundwater flow patterns in the catotelm showed that peatland biogeochemistry was maintained by horizontal flow and diffusion at the peatland margin (3) and by recharge and diffusion on the peatland itself (4). Seasonal flow reversals yielded discharge and diffusion controlled alterations in the peatland (5). Bracketed numbers refer to flow pathways illustrated in Figure 5-1a.

## Section 5.2 Groundwater and biogeochemistry

At one temporal extreme, rapid hydro-biogeochemical linkages are associated with signals that can be successfully measured. At the other extreme, hydro-biogeochemical equilibrium in peatlands at time-scales of millennia is appreciated in a holistic sense. However, establishing peatland hydro-biogeochemical linkages at annual to decadal time-scales is critical to our understanding of ecosystem function and response, but limited by the crude scales of measure in groundwater hydrology. Unfortunately, quantifying groundwater-biogeochemical linkages at these temporal scales will be critical for complete understanding of decomposition and microbial activity, the coupling of biogeochemical cycles and resulting feedbacks, *in situ* methylations, peatland succession and regeneration, and the role of climate variability in peatland function.

Figure 5-1b shows hydro-biogeochemical interactions that occur in peatlands under recharge and discharge conditions. Equilibrium between long-term recharge and diffusion supply substrates for *in situ* biogeochemical transformations and maintain redox and pH control through the peat profile. Under discharge conditions, equilibrium shifts toward the peat surface as the importance of recharge decreases and the importance of diffusion increases. In this situation, groundwater still provides a supply of substrate for biogeochemical transformations, but may directly stimulate biogeochemical processes under disequilibrium or indirectly inhibit processes due to redox-pH changes in the peat profile. Lower water table position during discharge conditions also yields an increased oxic zone near the peat surface. The model presented in Figure 5-1 is conceptual only. It will be a major challenge to establishing quantitative measurements and meaningful interpretations of such

complex hydro-biogeochemical linkages.

Can groundwater studies be scaled down to quantify hydro-biogeochemical linkages in peatlands? Will climate variability increase the frequency and intensity of draw-down events? What biogeochemical-hydrological feedbacks might be expected under climate change scenarios? These questions are important and warrant further attention, but it will be a challenge to find a system with a degree of hydrological control such that the required measurements could be made. The large size and no flow boundary make the Mer Bleue bog a unique system for hydrological studies, and the presence of *in situ* tracers allow for a physical measurement of groundwater change that can be linked to geochemistry. Further, the cation/anion rich pore waters would likely yield large and measurable redox-pH changes over flow reversals that could be linked to biological and chemical change *in situ*. Since the hydrology of Mer Bleue is well established, perhaps the peatland could serve as a site to establish the importance of groundwater in biogeochemical cycling and test new hypotheses?

### **Section 5.3 Dissolved carbon flux beyond the catchment**

Hydrological studies have been limited to small catchments to provide good control on water and mass balances. This study was no different. However, the scales of observation required to assess the magnitude of dissolved carbon flux from northern peatlands differs greatly from the scales of observation hydrologists find manageable. Several studies have illustrated empirical relationships between peatland development, shape, size and/or function (Verry et al., 1978; Verry et al, 1988; Gafni and Brooks, 1990; see Section 1.6.2 for a summary), but most peatlands are much larger than those found in small, relatively isolated catchments. How can catchment-scale hydrological processes be ‘scaled up’ or generalized to provide water yield and load data to biogeochemists and modellers at the scale of peatlands in the boreal and subarctic regions?

Using the results from this study as an example (see Figure 3-9), runoff and load estimates predicted from continuous measurements of water table should be representative of intensive hydrological records provided the catchment remains in steady state and that the

initial rating curves used to calculate runoff were of high quality. Built into these site specific empirical relationships are functions such as acrotelmic hydraulic conductivity, hydraulic gradients, catchment size, groundwater connectivity, hillslope connectivity and basin order. If water table-runoff data sets from many large peatlands are compiled, is it possible to yield empirical functions that could be used to predict water yield and chemical loads with confidence?

Though a daunting task, a generalization of peatland runoff processes in a statistical framework would likely produce surprising results for several reasons. Firstly, peatlands are often large relative to basin size. This would yield strong empirical relationships since runoff-water table signals for peatlands are unaffected by hillslope connection (i.e. - Mer Bleue bog). Peatlands are also autogenic landforms that develop with low hydraulic gradients and have a characteristic 'order of magnitude' difference in hydraulic conductivity between the acrotelm and catotelm. Thus, the processes of peatland development should give inter-peatland hydrological similarities that can be exploited. Lastly, a significant portion of northern peatlands are in regions where  $P \gg ET$  and a runoff-water table relationship could be invoked. The methodology would be less suitable for small catchments dominated by hillslopes, groundwater-dominated fens or peatlands in regions where  $P \approx ET$ . However, an approach such as this may aid hydrologists and biogeochemists when transcending scales to the boreal and sub-arctic regions.

One of the major challenges would be to find and assemble available data sets, assign meaningful inter-catchment variables, and extrapolate empirical relationships to predict water yield. The next major obstacle would be obtaining water table records from peatlands to serve as input for runoff calculations. Obtaining water table measurements from a strategic subset of northern peatlands is logistically possible and would require minimal maintenance after well installation. Water table records could also be predicted by land-atmosphere modeling schemes such as the Canadian Land Surface Scheme (CLASS) and local climate data (Letts et al., In press). Export scenarios based on DOC concentration and DOC:DIC ratio could be used to calculate load once runoff was determined.

## **Section 5.4 Contemporary carbon budgets beyond the catchment**

NEE at the Mer Bleue bog dominated the annual carbon budget, but the magnitude of the measured dissolved carbon flux could systematically force a pristine northern peatland from sink to source if NEE was small. Roulet (pers. comm.) hypothesizes that the large contemporary C sink at the Mer Bleue bog may be attributed to high N deposition and increased C fixation, but these findings are based on annual estimates from a single site. Which regions and what percentage of peatlands in Canada experience high N loading and low loading? Do peatlands in high N deposition regions have significantly greater NEE and vice-versa? In which regions and wetland types will dissolved carbon export systematically affect C budgets in northern peatlands? Are there spatial patterns to peatland C balance sensitivity when considering NEE or dissolved carbon export?

The areal extent of northern peatlands is too large and continuous records of NEE and dissolved carbon flux are too few to assess C sink-source role directly. Thus, ecosystem modelling appears to be the only practical approach to manage large-scale questions such as peatland trace gas biogeochemistry. A major problem is that NEE has been identified as the critical term in peatland C budgets and models, but continuous records of NEE are too few to calibrate ecological models for heterogeneous land covers. A monitoring strategy for NEE will be critical to quantifying the source-sink nature of northern peatlands, but such a strategy carries such a financial burden it may not be an option with present day technology.

As a precursor to intensive ecosystem modelling, it would be useful to perform a qualitative spatial analysis of the changes to peatland carbon balances considering regional patterns of NEE (PAR, temp), dissolved carbon flux (P-ET) and nitrogen deposition for boreal and subarctic regions. The analysis would be crude, but tools as simple as a geographical information system (GIS) may prove to be a suitable framework to isolate regional patterns of differential C sequestration. Not only would the analysis be a suitable start point to study the C source-sink patterns in northern peatlands, it may identify regions where measurements are needed to better understand NEE, biogeochemical coupling (N-deposition) and dissolved carbon flux in Northern peatlands.

# Appendix

## Appendix 1.

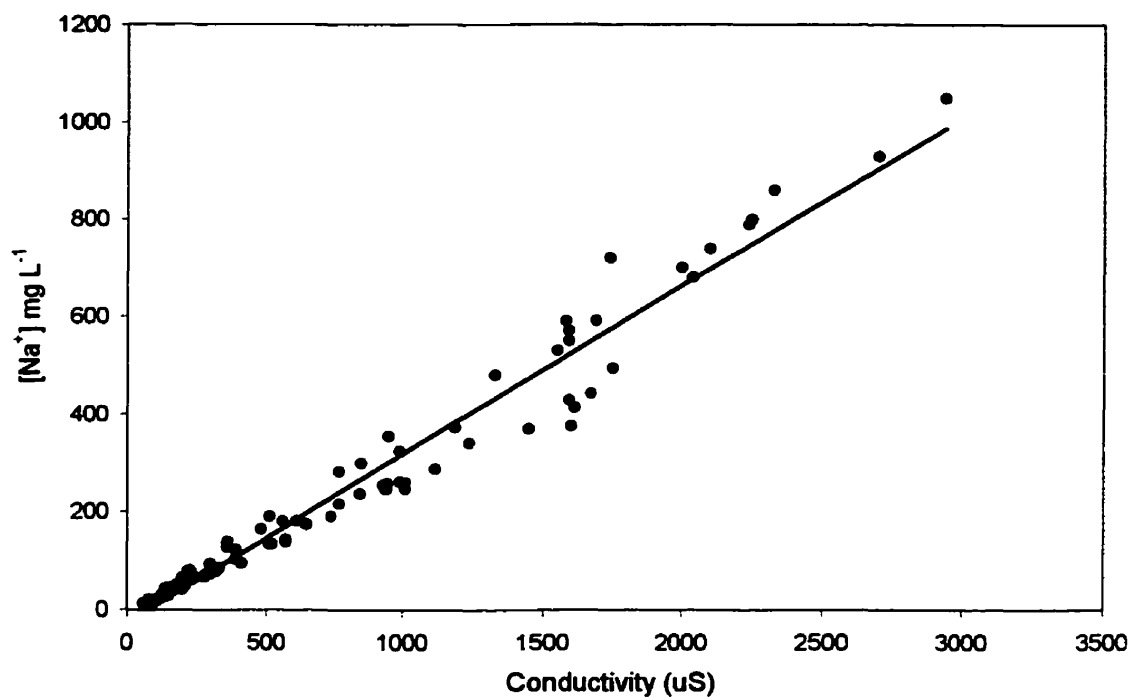


Figure A.1. Regression of Na<sup>+</sup> concentrations and electrical conductivity measurements from 84 piezometers on August 26, 1999.

Regression Statistics					
R Square	0.966				
Adjusted R Square	0.966				
Standard Error	46.533				
Observations	84				
ANOVA					
	<i>df</i>	<i>SS</i>	<i>MS</i>	<i>F</i>	<i>Significance F</i>
Regression	1	5079303.6	5079303.6	2345.7	0.00000
Residual	82	177559.4	2165.4		
Total	83	5256863.0			
	<i>Coefficients</i>	<i>Standard Error</i>	<i>t Stat</i>	<i>P-value</i>	
Intercept	-26.8	7.7	-3.5	0.00076	
X Variable 1	0.3	0.0	48.4	0.00000	

Table A.1. Regression statistics for data shown in Figure A.1.

## Appendix 2.

Table A.2. Summary of hydraulic conductivity calculations using bail tests after Hvorslev (1951) where  $K_h$  reported in m/s. Refer to Figure 2-2 for nest identification.

a)  $K_h$  measurements for peatland stations near the seep.

<i>Depth (m)</i>	<i>P1</i>	<i>P2</i>	<i>P3</i>	<i>P4</i>	<i>P5</i>	<i>P6</i>
0.25	1.84E-06	---	---	---	---	---
0.5	1.05E-08	5.76E-09	6.46E-08	9.13E-08	4.12E-07	2.97E-05
0.75	7.76E-07	2.39E-07	3.13E-07	6.24E-07	5.61E-08	4.40E-08
1	5.92E-07	1.41E-07	3.50E-06	1.39E-07	1.91E-07	7.50E-08
1.5	---	2.23E-07	6.32E-07	3.29E-07	8.47E-08	1.20E-07
2	---	---	---	1.34E-07	9.25E-07	1.10E-07
3	---	---	---	---	---	1.67E-06

b)  $K_h$  measurements for peatland stations of the major axis.

<i>Depth (m)</i>	<i>P6</i>	<i>P7</i>	<i>P8</i>	<i>P9</i>	<i>P10</i>
0.5	2.97E-05	1.11E-03	1.84E-08	4.80E-05	8.60E-07
0.75	4.40E-08	4.90E-08	4.92E-08	1.54E-07	2.32E-07
1	7.50E-08	7.38E-08	5.24E-07	1.52E-07	8.61E-08
1.5	1.20E-07	8.00E-08	1.23E-07	4.30E-07	2.90E-07
2	1.10E-07	4.11E-08	5.19E-08	9.50E-08	1.26E-07
3	1.67E-06	6.25E-06	2.10E-07	1.18E-06	4.64E-07
4.5	---	7.49E-08	1.33E-07	1.31E-06	1.05E-06

c)  $K_h$  measurements for peatland stations of the minor axis.

<i>Depth (m)</i>	<i>RA1</i>	<i>RA2</i>	<i>RA3</i>	<i>RA4</i>
0.5	8.70E-06	7.62E-05	2.23E-05	1.27E-05
0.75	1.60E-07	3.60E-08	1.47E-08	4.55E-08
1	9.48E-07	2.32E-07	2.10E-07	4.77E-08
1.5	3.87E-07	4.20E-07	1.44E-06	9.50E-06
2	8.82E-08	1.16E-07	2.40E-07	1.20E-07
3	7.00E-06	1.93E-06	2.64E-06	6.05E-07
4.5	8.75E-08	5.11E-09*	3.01E-09*	9.35E-09*

d)  $K_h$  measurements for mineral hillslope piezometers.

<i>Depth (m)</i>	<i>HS2</i>	<i>HS3</i>	<i>HS4</i>
0.25	5.54E-06	---	---
0.5	6.47E-08	4.70E-06	---
0.75	2.05E-05	1.73E-05	1.55E-05
1	7.25E-06	5.45E-10*	8.70E-05

\* denotes piezometer touching underlying marine clay.

### Appendix 3.

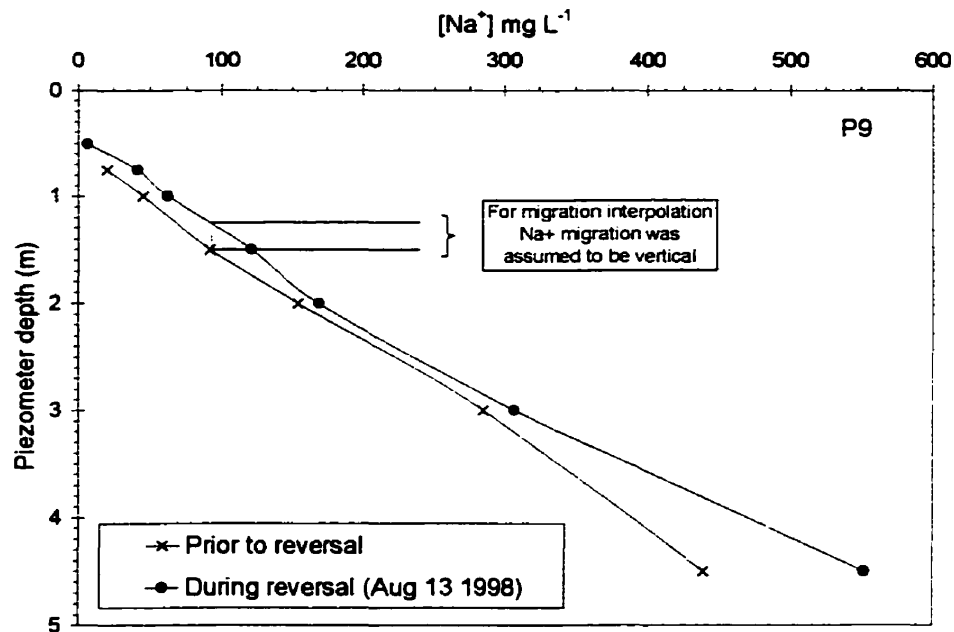


Figure A.2. Changes in  $Na^+$  concentration prior to and during the reversal at nest P9. Migration of  $Na^+$  over the reversal was determined based on position change from a measured point prior to the reversal to a point during the reversal assuming the discharge component to be vertical.

#### Descriptive Statistics

Mean	0.153
Standard Error	0.008
Standard Deviation	0.044
Variance	0.002
Kurtosis	-0.972
Skewness	0.296
Range	0.150
Minimum	0.080
Maximum	0.230
Count	29
Confidence Level ( 0.95 )	0.016

Table A.3. Descriptive statistics for 29 migration estimates for nests P6 to P10 and RA1 to RA4 between the peat surface and 2.0 m depths. Mean migration was 0.153 m over a 25 day period or  $\sim 0.006 m day^{-1}$ .

## References

- Baldwin, W.K.W. and T. Mosquin. 1969. Scientific and cultural studies of the Mer Bleue. *The Canadian Field Naturalist* 83: 4-6.
- Barnola, J.M., D. Raynaud, Y.S. Korotkevich and C. Lorius. 1987. Vostok ice core provides 160,000-year record of atmospheric CO<sub>2</sub>. *Nature* 329: 408-14.
- Bay, R.R. 1969. Runoff from small peatland watersheds. *Journal of Hydrology* 9: 90-102.
- Bear, J. 1972. *Dynamics of fluids in porous media*. Elsevier Publishing Company, New York, 764 pp.
- Belanger, J.R. and J.E. Harrison. 1977. Bedrock geology, drift thickness trend and bedrock topography, Ottawa-Hull, Ontario and Quebec. *Geological Survey of Canada Paper* 77-11.
- Bik, M.J.J., R. Herr and J. Salm. 1971. Saline groundwater, Central Research Forest, Ramsayville, Ontario. *Geological Survey of Canada, Report of Activities Paper* 71-1, A.
- Boelter, D.H. 1965. Hydraulic conductivity of peats. *Soil Science* 100: 227-31.
- Branfireun, B.A., A. Heyes and N.T. Roulet. 1996. The hydrology and methylmercury dynamics of a Precambrian Shield headwater peatland. *Water Resources Research* 32: 1785-1794.
- Bridgham, S.D., C.A. Johnston, J. Pastor and K. Updegraff. 1995. Potential feedbacks of Northern wetlands on climate change. *BioScience* 45: 262-74.
- Brooks, K.N. 1993. Surface Hydrology, Chapter 10. In *The patterned peatlands of Northern Minnesota*. H.E. Wright, Jr. (editor), University of Minnesota Press, pp. 153-162.
- Carroll, P.C. and P. Crill. 1997. Carbon balance of a temperate poor fen. *Global Biogeochemical Cycles* 11: 349-56.

Chapellez, J., J.M. Barnola, D. Raynaud, Y.S. Korotkevic and C. Lorius, C. 1990. Ice-core record of atmospheric methane over the past 160 000 years. *Nature* 345: 127-131.

Chapellez, J., T. Blunier, D. Raynaud, J.M. Barnola, J. Schwander and B. Stauffer. 1993. Synchronous changes in atmospheric CH<sub>4</sub> and Greenland climate between 40 and 8 kyr BP. *Nature* 366: 443-5.

Chason, D.B. and D.I. Siegel. 1986. Hydraulic conductivity and related physical properties of peat, Lost River Peatland, Northern Minnesota. *Soil Science* 142: 91-9.

Christopherson, R.W. 1998. *Elemental Geosystems*. 2<sup>nd</sup> Edition. Prentice-Hall, New Jersey, 534 pp.

Ciais, P., P.P. Tans, M. Tollier, J.W.C. White and R.J. Francey. 1995. A large northern hemisphere terrestrial CO<sub>2</sub> sink indicated by the <sup>13</sup>C/<sup>12</sup>C ratio of atmospheric CO<sub>2</sub>. *Science* 269: 1098-1102.

Clair, T.A. and J.M. Ehrman. 1996. Variations in discharge and dissolved organic carbon and nitrogen export from terrestrial basins with changes in climate: A neural network approach. *Limnol. Oceanog.* 41: 921-7.

Clymo, R.S. 1984. The limits to peat bog growth. *Phil. Trans. R. Soc. Lond. B* 303: 605-54.

Clymo, R.S. (1996). Assessing the accumulation of carbon in peatlands. In *Northern Peatlands in Global Climatic Change*. R. Laiho, J. Laine and H. Vasander (editors), The Academy of Finland, Helsinki, Vol. 1, pp. 207-212.

Collier, K.J., R.J. Jackson and M.J. Winterbourn. 1989. Dissolved organic carbon dynamics of developed and undeveloped wetland catchments in Westland, New Zealand. *Arch. Hydrobiol.* 117: 21-38.

Crank, J. 1975. *The mathematics of diffusion*. 2<sup>nd</sup> Edition. Clarendon Press, Oxford, 414 pp.

Dahm, C.N. 1980. Pathways and mechanisms for removal of dissolved organic carbon from leaf leachate in streams. *Can. J. Fish. Aquat. Sci.* 38: 68-76.

Dai, A. and I.Y. Fung. 1993. Can climate variability contribute to the "missing" CO<sub>2</sub> sink? *Global Biogeochemical Cycles* 7: 599-609.

Dalva, M. and T.R. Moore. 1991. Sources and sinks of dissolved organic carbon in a forested swamp catchment. *Biogeochemistry* 15: 1-19.

Devito, K.J. 1995. Sulphate mass balances of Precambrian Shield wetlands: the influence of catchment hydrogeology. *Can. J. Fish. Aquat. Sci.* 52: 1750-1760.

Devito, K.J., P.J. Dillon and B.D. Lazerte. 1989. Phosphorus and nitrogen retention in five Precambrian shield wetlands. *Biogeochemistry* 8: 185-204.

Devito, K.J., J.M. Waddington and B.A. Branfireun. 1997. Flow reversals in peatlands influenced by local groundwater systems. *Hydrological Processes* 11: 103-110.

Donahue, W.F., D.W. Schindler, S.J. Page and M.P. Stainton. 1998. Acid-induced changes in DOC quality in an experimental whole-lake manipulation. *Environ. Sci. Technol.* 32: 2954-60.

Dooge, J. 1975. The water balance of bogs and fens. In *Proceedings of the Minsk Symposium, June 1972*. IAHS, The UNESCO Press, Paris, pp. 233-71.

Drever, J.I. 1997. *The geochemistry of natural waters: Surface and groundwater environments*. 3<sup>rd</sup> Edition. Prentice-Hall, New Jersey, 436 pp.

Freeze, R.A and J.A. Cherry. 1979. *Groundwater*. Prentice-Hall, Englewood Cliffs, New Jersey, 604 pp.

Gadd, M.R. 1962. Surficial geology of Ottawa Map-Area, Ontario and Quebec 31 G/5. *Geological Survey of Canada, Department of Mines and Technical Surveys, Canada. Paper 62-16*.

Gafni, A. and K.N. Brooks. 1990. Hydraulic characteristics of four peatlands in Minnesota. *Can. J. Soil Sci.* 70: 239-53.

Gorham, E. 1991. Northern Peatlands: Role in the carbon cycle and probable responses to climatic warming. *Ecological Applications* 1: 182-95.

Gorham, E. 1995. The biogeochemistry of northern peatlands and its possible responses to global warming. In *Biotic feedbacks in the global climate system: Will the warming feed the warming?* G.M. Woodwell and F.T. Mackenzie (editors), Oxford University Press, New York, pp. 169-186.

Hare, F.K. and M.K. Thomas. 1979. *Climate Canada 2<sup>nd</sup> Edition*. John Wiley and Sons Canada Limited, Toronto, 230 pp.

Harte, J. 1988. *Consider a spherical cow: A course in environmental problem solving*. University Science Books, Mill Valley, California, 283 pp.

Hegerl, G.C. and U. Cubasch. 1996. Greenhouse gas induced climate change. *Environmental Science and Pollution Research* 3: 99-102.

Hill, A.R. 1991. A ground water nitrogen budget for a headwater swamp in an area of permanent ground water discharge. *Biogeochemistry* 14: 209-24.

Hobson, G.D. 1970. Bedrock features of the Mer Bleue area by seismic methods. *The Canadian Field Naturalist* 84: 35-38.

Houghton, J. 1997. *Global Warming: The Complete Briefing*. Second Edition. Cambridge University Press, New York, 251 pp.

Huber, S.A., A. Balz and F.H. Frimmel. 1994. Identification of diffuse and point sources of dissolved organic carbon (DOC) in a small stream (Alb, Southwest Germany), using gel filtration chromatography with high-sensitivity DOC-detection. *Fresenius J. Anal. Chem.* 350: 496-503.

Hvorslev, M.J. 1951. Time lag and soil permeability in groundwater observations. *U.S. Army Corps Engrs. Waterways Exp. Sta. Bull.* 36, Vicksburg, Miss.

Ingram, H.A.P. (1982). Size and shape in raised mire ecosystems: a geophysical model. *Nature* 297: 300-303.

Ingram, H.A.P. and O.M. Bragg. 1984. The diplotelmic mire: Some hydrological consequences reviewed. In *Proceedings of the 7<sup>th</sup> International Peat Congress, Dublin, Vol. 1*, pp. 220-34.

Ingram, H.A.P., D.W. Rycroft, and D.J.A. Williams. 1974. Anomalous transmission of water through certain peats. *Journal of Hydrology* 22: 213-18.

IPCC. 1996. *Climate change 1995: Impacts, Adaptions and Mitigation of Climate Change: Scientific-Technical Analyses*. Cambridge University Press, New York, 878 pp.

Jardine, P.M., N.L. Weber and J.F. McCarthy. 1989. Mechanisms of dissolved organic carbon adsorption on soil. *Soil Sci. Soc. Amer. J.* 53: 1378-85.

LaBaugh, J.W. 1986. Wetland ecosystem studies from a hydrologic perspective. *Water Resources Bulletin* 22: 1-9.

Lafleur, P.M. and N.T. Roulet. 1992. A comparison of evaporation rates for mineral poor and mineral rich fens of the Hudson Bay Lowlands. *Aquatic Botany* 44: 59-69.

Letts, M.G., N.T. Roulet, S.T. Comer, M.R. Skarupa and D.L. Versegby. In press. Parameterization of peatland hydraulic properties for the Canadian Land Surface Scheme. *Atmosphere-Ocean*.

Lévesque, M., H. Morita, M. Schnitzer and S.P. Mathur. 1980. The physical, chemical, and morphological features of some Quebec and Ontario peats. *Research Branch, Agriculture Canada*. 70 pp.

Malcolm, R.L. 1993. Concentration and composition of dissolved organic carbon in soils, streams, and groundwaters. *Special Publications of the Royal Society of Chemistry* 135: 19-31.

Maltby, E. and P. Immirzi. 1993. Carbon dynamics in peatlands and other wetland soils: Regional and global perspectives. *Chemosphere* 27: 999-1023.

McGuire, A.D., J.M. Melillo, D.W. Kicklighter, Y. Pan, X. Xiao, J. Helfrich, B. Moore III, C.J. Vorosmarty and A.L. Schloss. 1997. Equilibrium responses of global net primary production and carbon storage to doubled atmospheric carbon dioxide: Sensitivity to changes in vegetation nitrogen concentration. *Global Biogeochemical Cycles* 11: 173-89.

McKnight, D., E.M. Thurman, R.L. Wershaw and H. Hemond. 1985. Biogeochemistry of aquatic humic substances in Thoreau's Bog, Concord, Massachusetts. *Ecology* 66: 1339-52.

McNamara, J.P., D.I. Siegel, P.H. Glaser and R.M. Beck. 1992. Hydrogeologic controls on peatland development in the Malloryville Wetland, New York (USA). *Journal of Hydrology* 140: 279-96.

Moore, T.R. 1987. Patterns of dissolved organic matter in subarctic peatlands. *Earth Surface Processes and Landforms* 12: 387-97.

Moore, T.R. 1989. Dynamics of dissolved organic carbon in forested and disturbed catchments, Westland, New Zealand 1. Maimai. *Water Resources Research* 25: 1321-30.

Moore, T.R., 1997. Dissolved organic carbon: sources, sinks and fluxes and role in the soil carbon cycle. In *Soil Processes and the Carbon Cycle, Advances in Soil Science*. R. Lal, J.M. Kimble, R.F. Follett and B.A. Stewart (editors), CRC Press, Boca Raton. pp. 281-292.

Moore, T.R., W. DeSouza and J.-F. Koprivnjak. 1992. Controls on the sorption of dissolved organic carbon by soils. *Soil Science* 154: 120-9.

Moore, T.R. and R.J. Jackson. 1989. Dynamics of dissolved organic carbon in forested and disturbed catchments, Westland, New Zealand 2. Larry River. *Water Resources Research* 25: 1331-9.

Mott, R.J. and M. Camfield. 1969. Palynological studies in the Ottawa area. *Geological Survey of Canada, Paper 69-38*.

Mulholland, P.J. 1981. Organic carbon flow in a swamp-stream ecosystem. *Ecological Monographs* 51: 307-22.

Munro, D.S. 1979. Daytime energy exchange and evaporation from a wooded swamp. *Water Resources Research* 15: 1259-65.

Naiman, R.J. 1982. Characteristics of sediment and organic carbon export from pristine boreal forest watersheds. *Can. J. Fish. Aquat. Sci.* 39: 1699-1718.

National Capital Commission Review. 1997. Mer Bleue Conservation Area: Information Sheet on RAMSAR Wetlands. <http://www.wetlands.ca/wetcentre/wetcanada>.

National Wetlands Working Group. 1988. *Wetlands of Canada*. Ecological Land Classification Series, No. 24. Sustainable Development Branch, Environment Canada, Ottawa, Ontario, and Polyscience Publications Inc., Montreal, Quebec. 452 pp.

Oke, T.R. 1987. *Boundary layer climates*. 2<sup>nd</sup> Edition. Methuen, New York, 435 pp.

Overpeck, J., K. Hughen, D. Hardy, R. Bradley, R. Case, M. Douglas, B. Finney, K. Gajewski, G. Jacoby, A. Jennings, S. Lamoureux, A. Lasca, G. MacDonald, J. Moore, M. Retelle, S. Smith, A. Wolfe and G. Zielinski. 1997. Arctic environmental change of the last four centuries. *Science* 278: 1251-6.

Price, J.S. 1991. Evaporation from a blanket bog in a foggy coastal environment. *Boundary-Layer Meteorology* 57: 391-406.

Qualls, R.G. and B.L. Haines. 1991. Geochemistry of dissolved organic nutrients in the water percolating through a forest ecosystem. *Soil Sci. Soc. Am. J.* 55: 1112-23.

Randerson, J.T., M.V. Thompson, T.J. Conway, I.Y. Fung and C.B. Fung. 1997. The contribution of terrestrial sources and sinks to trends in the seasonal cycle of atmospheric carbon dioxide. *Global Biogeochemical Cycles* 11: 535-60.

Richard, S.H., N.R. Gadd and J.S. Vincent. 1987. Surficial geology and the Ice Age in the National Capital Region. *Energy, Mines and Resources Canada*.

Romanowicz, E.A., D.I. Siegel and P.H. Glaser. 1993. Hydraulic reversals and episodic emissions during drought cycles in mires. *Geology* 21: 231-34.

Roulet, N.T., A. Jano, C.A. Kelly, L.F. Klinger, T.R. Moore, R. Protz, J.A. Ritter and W.R. Rouse. 1994. Role of the Hudson Bay lowlands as a source of atmospheric methane. *Journal of Geophysical Research* 99 (D1): 1439-54.

Roulet, N.T., S.C. Munro, and L. Mortsch. 1997. Wetlands. In *Surface Climates of Canada*, T. Oke, W.R. Rouse, and W. Bailey (editors), McGill-Queen's Press, Montreal, pp. 149-171.

Roulet, N.T. and Woo, M-K. 1986. Wetland and lake evaporation in the low arctic. *Arctic and Alpine Research* 18: 195-200.

Rouse, W.R., P.F. Mills and R.B. Stewart. 1977. Evaporation in high latitudes. *Water Resources Research* 13: 909-14.

Schiff, S.L., R. Aravena, S.E. Trumbore, M.J. Hinton, R. Elgood and P.J. Dillon. 1997. Export of DOC from forested catchments on the Precambrian shield of Central Ontario: Clues from  $^{13}\text{C}$  and  $^{14}\text{C}$ . *Biogeochemistry* 36: 43-65.

Schimel, D.S. 1995. Terrestrial ecosystems and the carbon cycle. *Global Change Biology* 1: 77-91.

Schimel, D.S., B.H. Braswell, R. McKeown, D.S. Ojima, W.J. Parton and W. Pulliam. 1996. Climate and nitrogen controls on the geography and timescales of terrestrial biogeochemical cycling. *Global Biogeochemical Cycles* 10: 677-92.

Schindler, D.W. and S.E. Bayley. 1993. The biosphere as an increasing sink for atmospheric carbon: estimates from increased nitrogen deposition. *Global Biogeochemical Cycles* 7: 717-33.

Schindler, D.W. and P.J. Curtis. 1997. The role of DOC in protecting freshwaters subjected to climatic warming and acidification from UV exposure. *Biogeochemistry* 36: 1-8.

Schulthess, C.P. and C.P. Huang. 1991. Humic and fulvic acid adsorption by silicon and aluminum oxide surfaces on clay minerals. *Soil Sci. Soc. Amer. J.* 55: 34-42.

Scott, M.J., N.M. Jones, C. Woof and E. Tipping. 1998. Concentrations and fluxes of dissolved organic carbon in drainage water from an upland peat system. *Environment International* 24: 537-46.

Shurpali, N.J., S.B. Verma, J. Kim and T.J. Arkebauer. 1995. Carbon dioxide exchange in a peatland ecosystem. *Journal of Geophysical Research* 100 (D7): 14319-26.

Siegel, D.I. 1987. A review of the recharge-discharge function of wetlands. In *Proceedings of the International Symposium on Ecology and Management of Wetlands*. Croom Helm Ltd., Beckenham, Kent, UK. pp. 56-66.

Siegel, D.I. 1988. The recharge-discharge function of wetlands near Juneau, Alaska: Part II. Geochemical Investigations. *Ground Water* 26: 580-6.

Siegel, D.I. 1993. Groundwater Hydrology. Chapter 11, In *The Patterned Peatlands of Northern Minnesota*. H.E. Wright, Jr. (editor), University of Minnesota Press, pp. 163-172.

Siegel, D.I., A.S. Reeve, P.H. Glaser and E.A. Romanowicz. 1995. Climate-driven flushing of pore water in peatlands. *Nature* 374: 531-3.

Siegenthaler, U. and J.L. Sarmiento. 1993. Atmospheric carbon dioxide and the ocean. *Nature* 365: 119-125.

Tans, P.P., I.Y. Fung and T. Takahashi. 1990. Observational constraints on the global atmospheric CO<sub>2</sub> budget. *Science* 247: 1431-38.

Thomson, D.J. 1995. The seasons, global temperature and precession. *Science* 268: 59-68.

Thurman, E.N. 1985. *Organic Geochemistry of Natural Waters*. Martinus Nijhoff / Dr W. Junk Publishers, Boston, 497 pp.

Urban, N.R., S.E. Bayley and S.J. Eisenreich. 1989. Export of dissolved organic carbon and acidity from peatlands. *Water Resources Research* 25: 1619-28.

Verry, E.S. and D.H. Boelter. 1978. Peatland hydrology. In *Wetland functions and values: The state of our understanding*. American Water Resource Association. Minneapolis, Minnesota, pp. 389-402.

Verry, E.S., K.N. Brooks and P.K. Barten. 1988. Streamflow response from an ombrotrophic mire. In *Proceedings of the International Symposium on the hydrology of wetlands in temperate and cold regions, Joensuu, Finland*. Vol. 1, pp. 52-59.

Waddington, J.M. and N.T. Roulet. 1996. Atmosphere-wetland carbon exchanges: Scale dependency of CO<sub>2</sub> and CH<sub>4</sub> exchange on the developmental topography of a peatland. *Global Biogeochemical Cycles* 10: 233-45.

Waddington, J.M. and N.T. Roulet. 1997. Groundwater flow and dissolved organic carbon movement in a boreal peatland. *Journal of Hydrology* 191: 122-38.

Whiting, G.J. 1994. CO<sub>2</sub> exchange in the Hudson Bay lowlands: Community characteristics and multi-spectral reflectance properties. *Journal of Geophysical Research* 99(D1): 1519-28.

Williamson, C.E., R.S. Stemberger, D.P. Morris, T.M. Frost, S.G. Paulsen. 1996. Ultraviolet radiation in North American lakes: attenuation estimates from DOC measurements and implications for plankton communities. *Limnol. Oceanog.* 41: 1024-34.